NASA TECHNICAL MEMORANDUM

NASA TM X-2525

NASA TM X-2525

ATLAS-CENTAUR AC-17 PERFORMANCE FOR APPLICATIONS TECHNOLOGY SATELLITE ATS-D MISSION

Lewis Research Center
Cleveland, Ohio 44135

NATIONAL AERONAUTICS AND SPACE ADMINISTRATION • WASHINGTON, D. C. • MAY 1972

1. Report No.	2. Government Accession No.	3. Recipient's Catalog No.
NASA TM X-2525		

4. Title and Subtitle	5. Report Date
ATLAS-CENTAUR AC-17 PERFORMANCE FOR APPLICATIONS TECHNOLOGY SATELLITE ATS-D MISSION	May 1972
	6. Performing Organization Code

7. Author(s)	8. Performing Organization Report No.
Lewis Research Center	E-6510
	10. Work Unit No. 491-02
9. Performing Organization Name and Address	11. Contract or Grant No.
Lewis Research Center National Aeronautics and Space Administration Cleveland, Ohio 44135	13. Type of Report and Period Covered Technical Memorandum
12. Sponsoring Agency Name and Address	14. Sponsoring Agency Code
National Aeronautics and Space Administration Washington, D.C. 20546	

15. Supplementary Notes

16. Abstract

The Atlas-Centaur launch vehicle (AC-17) with Applications Technology Satellite-D (ATS-D) was launched from Cape Kennedy in August 1968. Mission objectives were not achieved because the Centaur main engine failed to start for the second powered phase. This report contains an evaluation of the performance of the Atlas-Centaur systems, from lift-off through the Centaur restart attempt. It includes a brief analysis of the Centaur failure.

17. Key Words (Suggested by Author(s))	18. Distribution Statement
Atlas applications Centaur applications Launch vehicle Applications technology satellite	Unclassified - unlimited

19. Security Classif. (of this report)	20. Security Classif. (of this page)	21. No. of Pages	22. Price*
Unclassified	Unclassified	148	$3.00

* For sale by the National Technical Information Service, Springfield, Virginia 22151

ATLAS-CENTAUR AC-17 PERFORMANCE FOR APPLICATIONS TECHNOLOGY SATELLITE ATS-D MISSION

Lewis Research Center

I. SUMMARY

The Atlas-Centaur launch vehicle AC-17 with the Applications Technology Satellite-D (ATS-D) spacecraft was launched from Eastern Test Range Complex 36A at 1733:02 hours eastern standard time on August 10, 1968. Mission objectives were not achieved because the Centaur main engines failed to restart.

The Atlas and Centaur stages performed satisfactorily in placing the Centaur/ATS-D into the desired elliptical parking orbit. After a 61-minute coast in this orbit, Centaur main engine restart was initiated to place the ATS-D in a highly elliptical transfer orbit with apogee near synchronous altitude. However, the Centaur main engines failed to restart and the Centaur/ATS-D remained in the initial parking orbit. The orbit degenerated with time and eventually the Centaur/ATS-D re-entered the atmosphere in October 1969.

Post-flight analyses indicated that the Centaur main engines did not restart because the propellant boost pumps failed to operate. Subsequently, a comprehensive investigation and test program was conducted to determine the cause of the failure. Results of this program determined that the hydrogen peroxide froze in the supply line that is common to both boost pumps. The most probable cause for the freezing was cryogenic oxidizer (liquid oxygen) leaking onto the surface of the common hydrogen peroxide supply line.

This report contains an evaluation of the Atlas-Centaur system performance in support of the ATS-D mission.

II. INTRODUCTION

by Roy K. Hackbarth

The primary purpose of the Applications Technology Satellite-D (ATS-D) mission was to demonstrate precision spacecraft stabilization in synchronous orbit by use of gravity gradient techniques. The objectives of the Atlas-Centaur launch vehicle AC-17 were to inject the ATS-D into the proper elliptical transfer orbit (apogee near synchronous altitude), to aline the ATS-D to the required apogee motor firing vector, to initiate spacecraft separation, and to perform a post-separation maneuver to ensure adequate orbital separation from ATS-D.

This was the fourth in a planned series of five ATS missions. The launch vehicles for this series were the responsibility of the Lewis Research Center. Atlas-Agena vehicles launched the first three ATS spacecraft, and Atlas-Centaur vehicles were designated for the last two. ATS-1 was successfully placed into orbit in December 1966. ATS-B, launched in April 1967, did not attain the proper orbit due to failure of the Agena engine to start for its second powered phase. ATS-3 was successfully placed into orbit in November 1967. ATS-D was launched in August 1968.

The flight plan was designed to use an indirect (parking orbit) mode of ascent to place the ATS-D into a highly elliptical transfer orbit that matches the capability of the ATS-D apogee motor to reduce orbit inclination and circularize the orbit near synchronous altitude. The Atlas stage and Centaur first powered phase are used to place the Centaur/ATS-D into an elliptical parking orbit. After a 61-minute coast, the Centaur main engine is restarted to accelerate the Centaur/ATS-D into a synchronous transfer orbit. After main engine second cutoff, the Centaur orients the ATS-D to the desired apogee motor firing vector and separates the ATS-D from Centaur. The Centaur then performs a maneuver to establish and maintain proper separation distance from ATS-D. After separation from Centaur, the ATS-D coasts for 5.5 hours to the apogee of the transfer orbit, which is near synchronous altitude. The ATS-D apogee motor is then fired to accomplish a final plane change and accelerate the ATS-D into the desired nearly circular, synchronous, equatorial orbit.

The AC-17 flight was the eighth operational Centaur flown and the first to be used for a mission other than a lunar mission. The configuration of AC-17 was changed, compared to the previous Atlas-Centaur launch vehicle (AC-15), to accommodate requirements peculiar to the payload and the mission trajectory and to incorporate design improvements planned for all post-Surveyor vehicles. Configuration changes to

accommodate the payload include a new payload transition adapter, redistribution of conditioned air, and revised harnesses for payload functions. Configuration changes to accommodate trajectory requirements were primarily for a 61-minute Centaur coast period (the previous maximum coast was 22 min). These changes include addition of a second hydrogen peroxide bottle, a higher capacity Centaur main battery, and numerous modifications to assure that equipment and engine temperatures were the proper values for Centaur restart after the extended coast period. The design improvement changes included provisions for Centaur to supply the Atlas booster pitch program, increased flexibility in guidance equations, and an improved Centaur flight control system.

This report presents an evaluation of the Atlas-Centaur system performance in support of the ATS-D mission.

III. LAUNCH VEHICLE DESCRIPTION

by Eugene E. Coffey and Roy K. Hackbarth

The Atlas-Centaur is a two-stage launch vehicle consisting of an Atlas first stage and a Centaur second stage connected by an interstage adapter. Both stages are 3.05 meters (10 ft) in diameter, and the composite vehicle is 35.6 meters (117 ft) in length. The vehicle weight at lift-off is approximately 146 732 kilograms (323 489 lbm). The basic structure of the Atlas and the Centaur stages utilizes thin-wall, pressure-stabilized main propellant tank sections of monocoque construction. Figure III-1 shows the Atlas-Centaur lifting off with the ATS-D spacecraft.

The first stage SLV-3C Atlas (fig. III-2) is 21.03 meters (69 ft) long. It is powered by a propulsion system consisting of a booster engine having two thrust chambers and with a total sea-level thrust of 1494×10^3 newtons (336×10^3 lbf), a sustainer engine with a sea-level thrust of 258×10^3 newtons (58×10^3 lbf), and two vernier engines with sea-level thrust of 2980 newtons (670 lbf) each. All engines use liquid oxygen and RP-1 (kerosene) as propellants and are ignited prior to lift-off. The booster engine thrust chambers are gimbaled for pitch, yaw, and roll control during the booster engine phase of the flight. This phase is completed at booster engine cutoff, which occurs when the vehicle acceleration reaches about 5.7 g's. The booster engine section is jettisoned about 3 seconds later.

The sustainer engine and the vernier engines continue to thrust for the Atlas sustainer phase of the flight. During this phase the sustainer engine is gimbaled for pitch and yaw control, while the vernier engines are gimbaled for roll control only. The sustainer and vernier engines provide thrust until propellant depletion. The Atlas is severed from the Centaur by the firing of a shaped charge system located on the forward end of the interstage adapter. The firing of a retrorocket system then separates the Atlas/interstage adapter from the Centaur.

The Centaur second stage (fig. III-3) is about 9.1 meters (30 ft) long. It is a high-performance stage with a design specific impulse of approximately 442 seconds. The Centaur is powered by two main engines which use liquid hydrogen and liquid oxygen as propellants and which generate a total thrust of approximately 133×10^3 newtons (30 000 lbf). These engines are gimbaled to provide pitch, yaw, and roll control during Centaur powered flight. Fourteen hydrogen peroxide engines, mounted on the aft periphery of the oxidizer tank, operate during nonpowered phases of flight to provide various thrust levels for attitude control, for propellant settling and retention, and for vehicle reorientation.

The cylindrical section of the Centaur hydrogen tank is insulated with four jettisonable fiber-glass panels whose primary function is to reduce liquid-hydrogen boiloff. A fiber-glass nose fairing is used to provide an aerodynamic shield for the spacecraft, for the Centaur guidance equipment, and for the Centaur electronic equipment during ascent. The insulation panels and the nose fairing are jettisoned during the Atlas sustainer phase. The Applications Technology Satellite (ATS-D) spacecraft is shown in figure III-4.

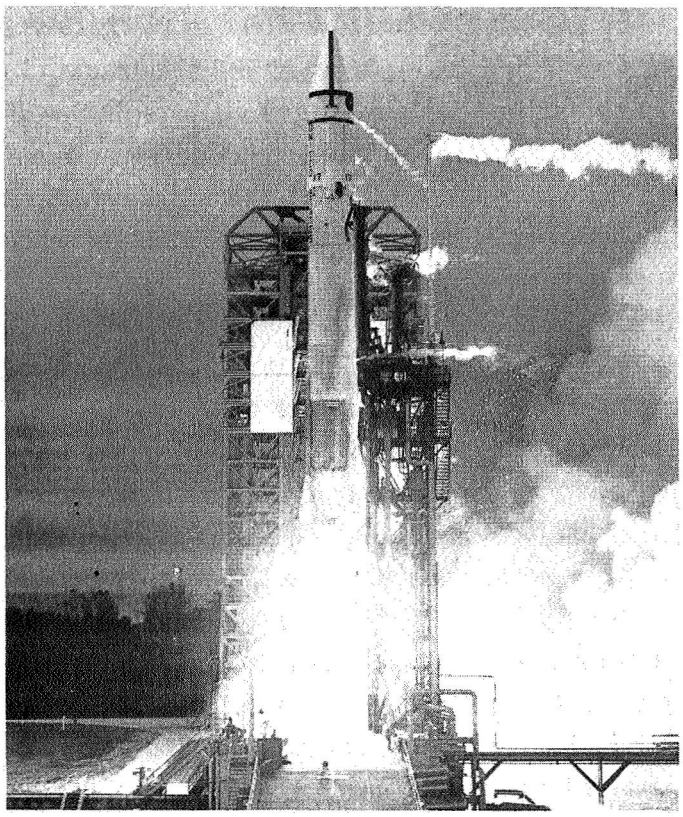

Figure III-1. - Atlas-Centaur lift-off with ATS-D.

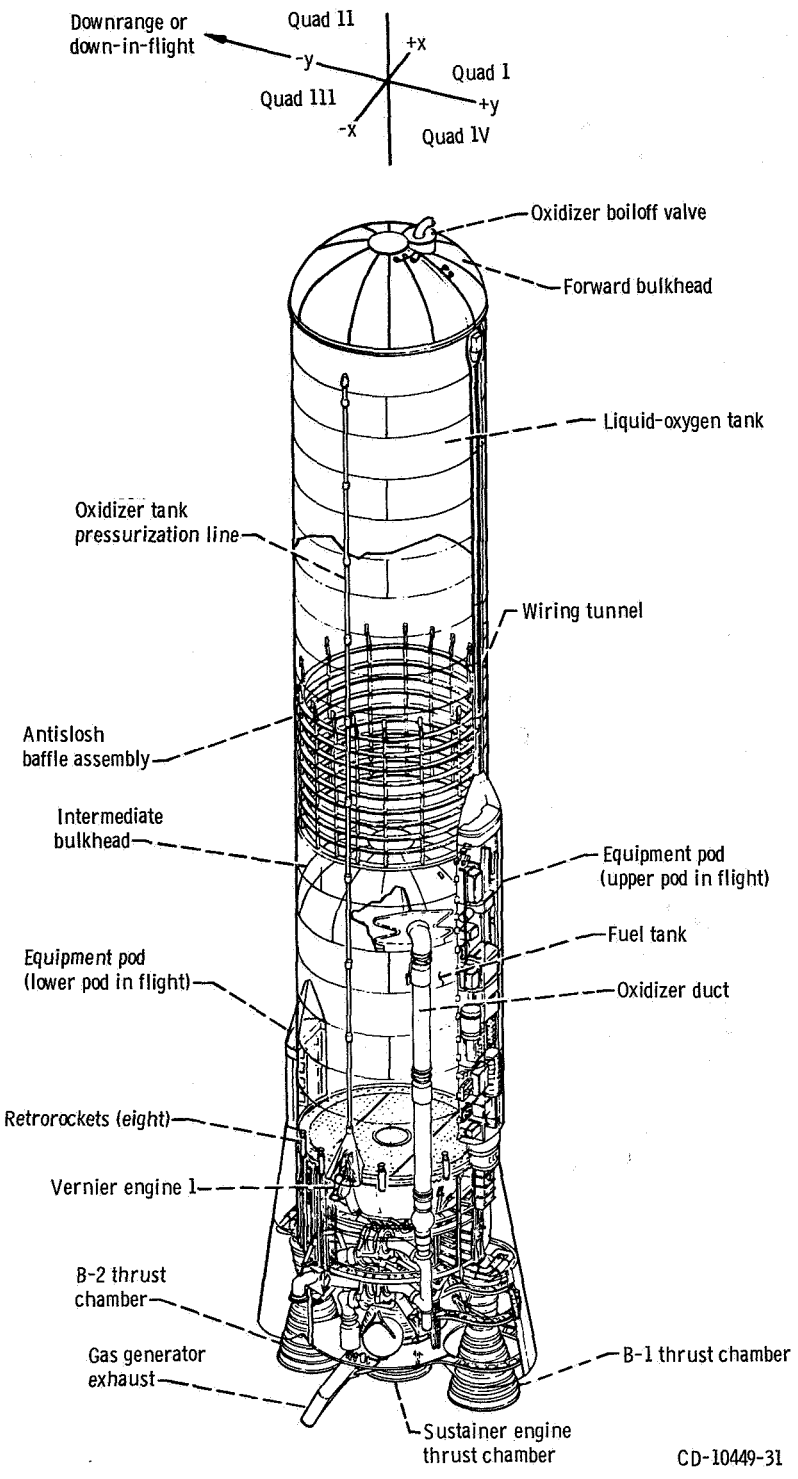

Figure III-2. - General arrangement of Atlas launch vehicle, AC-17.

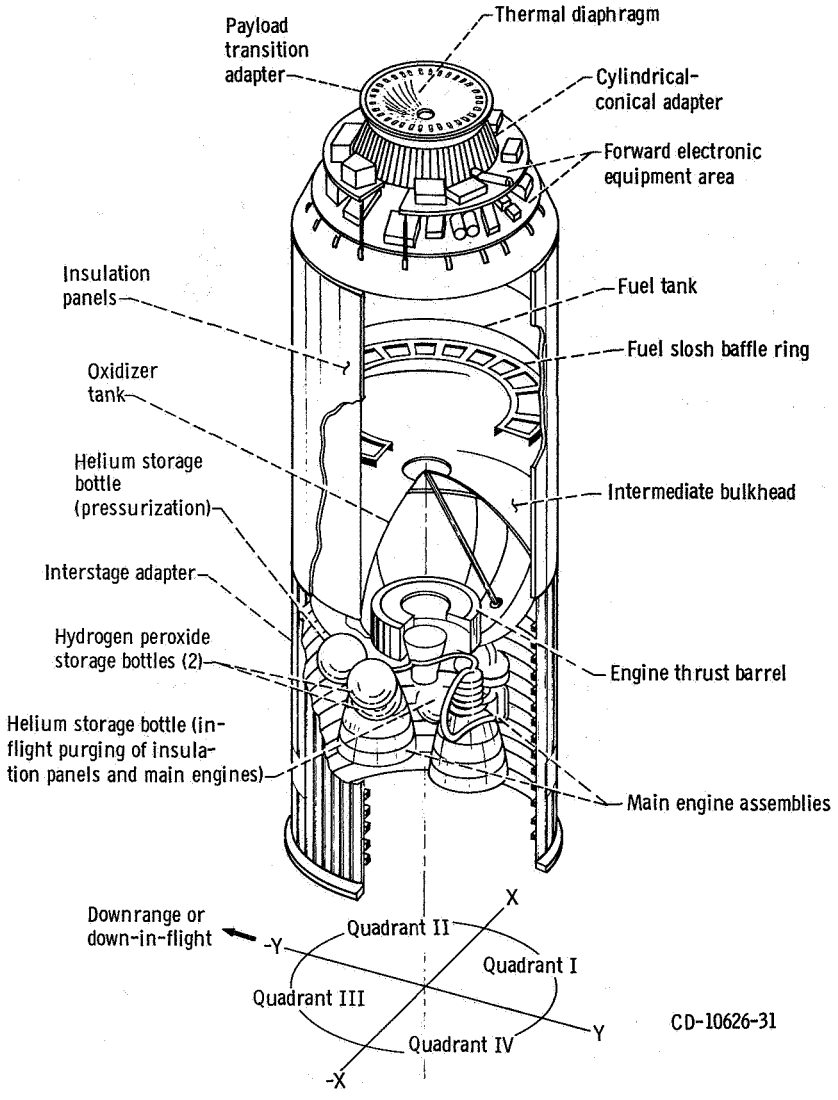

Figure III-3. - General arrangement of Centaur vehicle, AC-17.

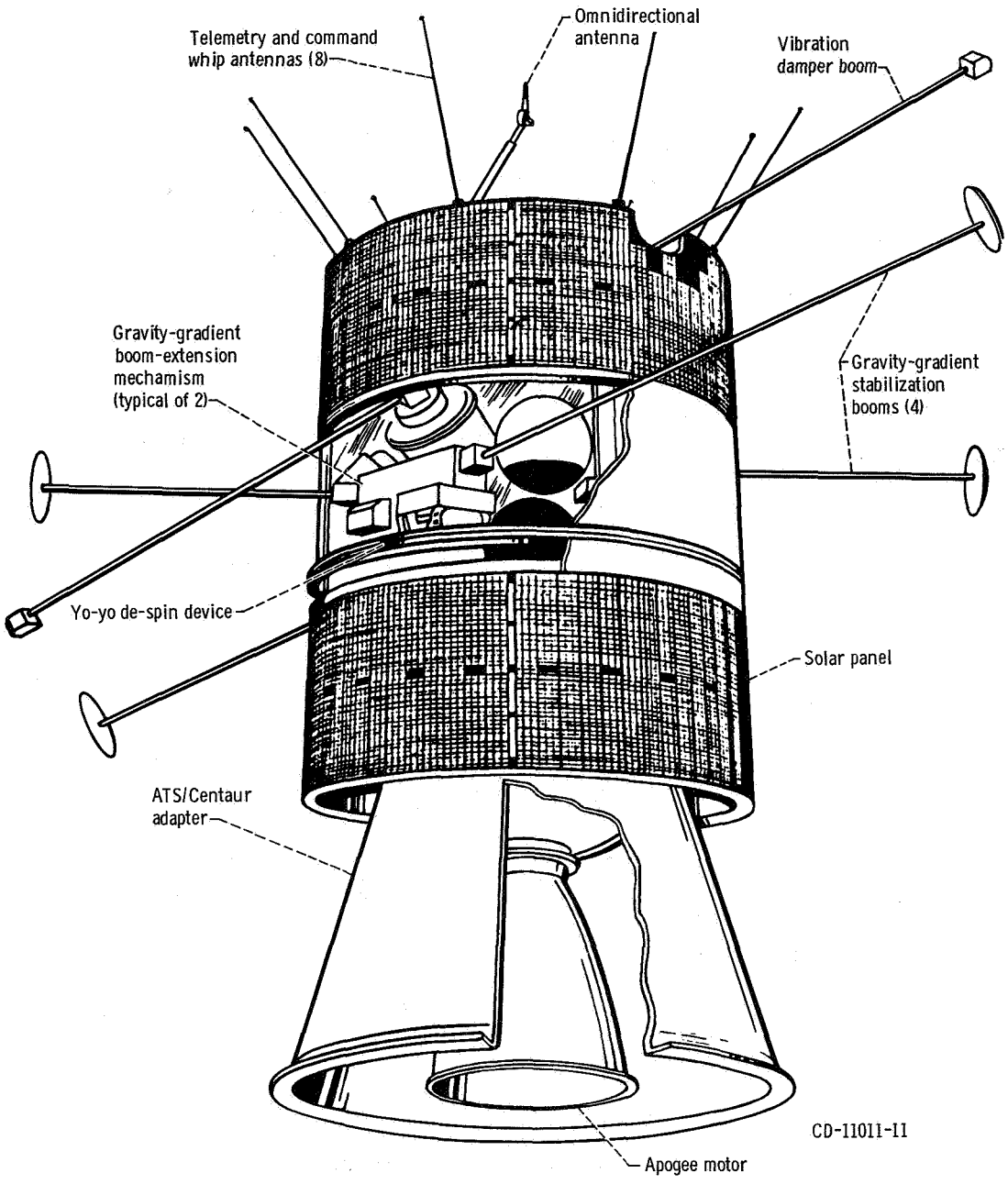

Figure III-4. - Configuration of Applications Technology Satellite, AST-D. (Spacecraft booms shown partially extended for illustrative purposes only; normal extension occurs after separation of adapter and apogee motor.)

IV. MISSION PERFORMANCE

by William A. Groesbeck

The Atlas-Centaur launch vehicle AC-17 with Applications Technology Satellite (ATS-D) was successfully launched from Eastern Test Range Complex 36A on August 10, 1968, at 1733:02 hours eastern standard time. However, the mission objective to inject the ATS-D spacecraft into a precise transfer ellipse, using an indirect (Centaur two powered phase) mode of ascent, was not accomplished. Launch vehicle performance through the Atlas boost phase, the Centaur main engine first firing, and the 61.2-minute coast was normal; but the Centaur main engine failed to restart for the Centaur main engine second firing. Freezing of hydrogen peroxide in the supply line blocked the flow of hydrogen peroxide to the boost pump catalyst beds, and as a result the liquid-oxygen and liquid-hydrogen boost pumps failed to operate.

ATLAS FLIGHT PHASE

Ignition and thrust buildup of the Atlas engines were normal. The vehicle lifted off (T + 0 sec) with a combined vehicle weight of 146 732 kg (323 489 lbm) and a thrust-weight ratio of 1.212. Two seconds after lift-off, the vehicle initiated a programmed roll from the launch pad azimuth of 105° to the required flight azimuth of 97°. This flight azimuth was attained at T + 15 seconds. At T + 15 seconds, the vehicle began a programmed pitchover maneuver which lasted through booster engine cutoff. The Centaur inertial guidance system was functioning during this phase, but steering commands were not admitted to the Atlas flight control system until after booster engine staging. For this programmed period of flight, guidance was accomplished by pitch and yaw programs which were selected and stored in the Centaur computer during launch countdown. The programs were selected on the basis of trajectory requirements and predicted structural loading determined from prelaunch upper-wind soundings. AC-17 was the first flight in which the entire pitch program was provided by Centaur.

Vehicle acceleration during the boost phase was according to the mission plan. Centaur guidance issued the booster engine cutoff signal when the vehicle acceleration reached 5.74 g's (specification, 5.7 ± 0.113 g's). About 3 seconds later, at T + 155.1 seconds, the Atlas programmer issued the staging command to separate the booster engine section from the vehicle. Staging transients were small; and the maximum vehicle

angular rate in pitch, yaw, or roll did not exceed 2.8 degrees per second. Vehicle steering by the inertial guidance system was initiated about 4 seconds after Atlas booster engine staging. At the start of guidance steering, the vehicle was slightly off the required steering vector by about 4^{o} nose low in pitch and 0.5^{o} nose right in yaw. The guidance system steered the vehicle to the proper vector and issued commands to continue the pitch-over maneuver during the Atlas sustainer flight phase.

Insulation panels were jettisoned during the sustainer flight phase at T + 196.8 seconds. All four panels were severed by the shaped charges and fell away from the vehicle. The nose fairing was jettisoned at T + 233.5 seconds. Vehicle angular rates resulting from the jettisoning of the insulation panels and nose fairing were insignificant.

Sustainer and vernier engine system performance was satisfactory throughout the flight. Sustainer engine cutoff was initiated by liquid-oxygen depletion at T + 246.2 seconds. Maximum vehicle acceleration just prior to sustainer engine cutoff was 1.78 g's. Coincident with sustainer engine cutoff, the guidance steering commands to the Atlas flight control system were disabled and the Centaur main engines were driven toward center (null) to maintain clearance between the engines and the interstage adapter during Atlas/Centaur separation.

The Atlas staging command was issued by the flight programmer at T + 248.2 seconds. A shaped-charge firing cut the interstage adapter to separate the two stages. Eight retrorockets on the Atlas then fired to move the Atlas stage away from the Centaur. The transients during separation were small, and the maximum angular rate imparted to the vehicle did not exceed 0.7 degree per second.

CENTAUR FLIGHT PHASE

Centaur Main Engine First Firing

The main engine start sequence for the Centaur stage was initiated prior to sustainer engine cutoff. The propellant boost pump started at T + 213.7 seconds. To prevent boost pump cavitation during the near-zero-gravity period from sustainer engine cutoff until main engine start at T + 257.7 seconds, the required net positive suction pressure was assured by pressure pulsing the propellant tanks with helium. Eight seconds prior to main engine start, the Centaur programmer issued prestart commands for engine firing. Centaur main engines were gimbaled to zero, and engine prestart valves were opened to flow liquid hydrogen through the lines to chill the engine turbopumps. Chilldown of the turbopumps ensured against cavitation during pump acceleration and made possible a uniform and rapid thrust buildup after engine ignition. At T + 257.7 seconds the ignition command was issued by the flight programmer, and engine thrust increased to full flight levels.

Guidance steering for the Centaur stage was enabled at T + 261.7 seconds. The total residual angular rates and disturbing torques induced during the Atlas/Centaur staging interval resulted in only a slight vehicle drift off the steering vector. This attitude drift error was corrected within 1 second after start of guidance steering. Engine performance throughout the first powered phase was normal.

At T + 536.2 seconds, two of the four 222-newton (50-lbf) thrust hydrogen peroxide engines were fired for 2.5 seconds, two of the four 13.5-newton (3-lbf) thrust hydrogen peroxide engines were fired for 10 seconds, and all attitude control engines were fired for 10 seconds. This firing thermally conditioned these engines, thereby providing additional assurance for their proper operation after the long coast phase (61.2 min). The remaining hydrogen peroxide engines were not fired at this time since they were programmed to fire during the coast period for propellant settling and retention. Main engine shutdown was commanded by Centaur guidance at T + 595.8 seconds. Orbital insertion occurred at an altitude of about 186 kilometers (100.9 n mi).

Centaur main engine cutoff occurred 8.8 seconds later than expected. This additional firing time was necessary to compensate for an apparent lower thrust level. The propellant utilization system performed satisfactorily and accurately controlled the fuel and oxidizer flow rates to the engines.

CENTAUR COAST PHASE

At main engine first cutoff, the Centaur/ATS-D began a 61.2-minute orbital coast. The hydrogen peroxide thrusters provided attitude control throughout the coast period. During the first 51 minutes, the inertial guidance system provided attitude error information to the flight control system to aline the Centaur roll axis with the flightpath velocity vector. During the last 10 minutes, the inertial guidance system issued small incremental attitude changes to reorient the Centaur/ATS-D to the desired attitude for Centaur second powered phase.

The coast-phase control mode sequence consisted of firing two of the four 222-newton (50-lbf) thrust engines at main engine cutoff for the first 76 seconds of coast. This thrust level provided a vehicle acceleration of 7×10^{-3} g's to settle the residual propellants and to suppress any disturbances of the liquids induced by main engine cutoff transients. After 76 seconds the 222-newton (50-lbf) thrust engines were commanded off, and two of the 13.3-newton (3-lbf) thrust engines were commanded on to provide a continuous, low-level acceleration of 4×10^{-4} g's.

Forty seconds prior to main engine restart, the thrust level was increased to 444 newtons (100 lbf) by again firing two of the 222-newton (50-lbf) thrust hydrogen peroxide engines. At the same time the two 13.3-newton (3-lbf) thrust engines were commanded off. The increased thrust level gave additional assurance of settled propellants prior to

the main engine second start sequence. Eight seconds later, commands were given to start the propellant boost pumps, but they failed to start. Apparent freezing of the hydrogen peroxide in the common supply line to the boost pump catalyst beds blocked the flow and prevented their operation. As a result the engines did not restart, and the vehicle with ATS-D attached remained in the parking orbit.

V. TRAJECTORY AND PERFORMANCE

by John J. Nieberding

MISSION PLAN

The AC-17 mission plan required the Atlas-Centaur launch vehicle to inject the ATS-D spacecraft into a highly elliptical transfer orbit (apogee near synchronous altitude) from which ATS-D achieves near-synchronous circular orbit by firing its fixed-impulse apogee motor. The Atlas first places the Centaur/ATS-D on a suborbital coast ellipse through two powered phases - a booster phase and a sustainer phase. After the Atlas' powered phases are complete, the Centaur/ATS-D separates from Atlas, and the Centaur first powered phase places the Centaur/ATS-D into an elliptical parking orbit. This orbit has an apogee altitude of 768 kilometers (415 n mi), a perigee altitude of 186 kilometers (100 n mi), and an orbital inclination of 29.12°. After injection into this parking orbit, the Centaur/ATS-D coasts (for about 61.2 min) until its crosses the equator for the second time. At this time, the Centaur second powered phase accelerates the Centaur/ATS-D from the parking orbit into a highly elliptical transfer orbit with an apogee altitude of about 35 882 kilometers (19 375 n mi) and a perigee altitude of about 664 kilometers (358 n mi) and reduces the orbital inclination from 29.12° to 16.15°.

After Centaur main engine second cutoff, the Centaur executes a turning maneuver, mostly out of the orbital plane, of approximately 180°. This maneuver orients the spacecraft to the inertial attitude required at apogee of the transfer orbit. After this reorientation, the spacecraft separates from the Centaur. The Centaur then performs a post-separation maneuver by turning approximately 90° and then thrusting towards earth by means of the hydrogen peroxide engines and the discharging of residual propellants.

The spacecraft coasts in the transfer orbit for about 5.5 hours (1/2 orbit) in a spin stabilization mode. This stabilization maintains the inertial attitude provided by the Centaur at separation. Upon reaching the first apogee of the transfer orbit, while crossing the equator, the spacecraft motor fires to accomplish the orbital plane change of 17.59° and to accelerate the spacecraft into the desired nearly circular final orbit. This orbit is inclined 1.44° to the equator. At spacecraft motor burnout, the spacecraft is at about 103° West longitude and 0.09° North latitude. From this position, it drifts at the rate of about 1° per day eastward until it reaches the desired final longitude, where it is commanded by ground control to assume a nearly stationary position. Figure V-1 illustrates the mission profile.

TRAJECTORY RESULTS

Lift-Off Through Atlas Booster Phase

Wind conditions as measured by a weather balloon sent aloft near the time of lift-off are presented in figures V-2 and V-3. These wind conditions required the use of pitch program Code PP31 and yaw program Code YP6 to minimize the launch vehicle angle of attack, and hence aerodynamic structural loading, throughout the booster phase of flight.

Radar tracking and Centaur guidance data indicated that the AC-17 flightpath during the Atlas booster phase was very close to the predicted path. The transonic region, or the timespan when the vehicle passes through Mach 1, occurred from about T + 60 to T + 65 seconds. During this period the axial load factor (thrust acceleration in g's) was nearly constant (fig. V-4), an indication that the vehicle is passing through a period of high aerodynamic drag. Maximum dynamic pressure occurred at about T + 83 seconds. Atlas booster engine cutoff (BECO) occurred at T + 152.0 seconds (see table V-1) when the vehicle axial load factor reached 5.74 g's. (The axial load factor at BECO is designed to be 5.7±0.113 g's.) This cutoff was 0.8 second earlier than predicted. At BECO, the altitude was about 0.82 kilometer (0.44 n mi) higher than predicted, while the inertial velocity was about 16.5 kilometers per hour (15 ft/sec) higher than predicted (figs. V-4 and V-5). These deviations are well within tolerances.

Atlas Sustainer Phase

An abrupt decrease in acceleration occurred at booster engine cutoff (T + 152.0 sec). This decrease is shown in figure V-5 and also in figure V-4, where a change in slope indicates a change in acceleration. A small but abrupt increase in acceleration occurred at T + 155.1 seconds when the booster engine section, weighing 3392 kilograms (7478 lbm), was jettisoned. (Atlas and Centaur weight summaries are presented in tables V-2 and V-3.) Following booster jettison, the constantly decreasing propellant weight caused the axial acceleration to increase smoothly, except for small perturbations, until sustainer and vernier engine cutoff at T + 246.2 seconds. These perturbations were caused by jettisoning the 526-kilogram (1160-lbm) insulation panels at T + 196.8 seconds and the 979-kilogram (2158-lbm) nose fairing at T + 233.5 seconds. Sustainer engine cutoff (SECO) occurred 1.6 seconds earlier than predicted. At SECO, the altitude was only 0.21 kilometer (0.14 n mi) higher than expected (figs. V-6 and V-7); the inertial velocity was about 11.5 kilometers per hour (10 ft/sec) high. The axial acceleration at sustainer and vernier engine cutoff dropped abruptly to zero, indicating the loss of all thrust.

Centaur Main Engine Firing Phase

Atlas/Centaur separation was timed to occur 1.9 seconds after SECO, and Centaur main engine first start (MES-1) was timed to occur 11.5 seconds after SECO. Since SECO was early, these two events were also early. The increase in acceleration and velocity at Centaur main engine start, T + 257.7 seconds, can be seen in figures V-4 and V-5, respectively.

During the Centaur powered phase, the axial acceleration and relative velocity increased uniformly until Centaur main engine first cutoff (MECO-1) at T + 595.8 seconds. During this period, however, the acceleration was lower than predicted because of an apparent lower-than-expected Centaur thrust. This effect can be seen in figure V-5 where the velocities are lower than expected throughout the Centaur phase until the proper cutoff velocity had been achieved. Because of the low velocity profile, main engine cutoff occurred 8.8 seconds later than predicted (see fig. V-4). Based on a trajectory derived from post-flight Centaur guidance data, altitude at main engine cutoff was 40 meters (141 ft) higher than predicted and velocity was 1.4 kilometers per hour (1.2 ft/sec) high. After MECO-1, two 222-newton (50-lbf) thrust hydrogen peroxide engines fired for 76 seconds to settle the Centaur propellants. The actual and predicted parking orbit parameters at this epoch are compared in table V-4. Since the Centaur main engines failed to restart, the Centaur/spacecraft combination remained essentially in this parking orbit.

TABLE V-1. - COMPARISON OF PREDICTED AND ACTUAL EVENT TIMES, AC-17

Event	Programmer time, sec	Predicted time[a], sec	Actual time, sec
Lift-off	----------	T + 0.0	T + 0.0
Booster engine cutoff	BECO	T + 152.8	T + 152.0
Booster engine section jettison	BECO + 3.1	T + 155.9	T + 155.1
Insulation panel jettison	BECO + 45	T + 197.8	T + 196.8
Nose fairing jettison	BECO + 82	T + 234.8	T + 233.5
Sustainer engine cutoff; start Centaur programmer	SECO	T + 247.8	T + 246.2
Atlas/Centaur separation (retrorocket fire)	SECO + 2.0	T + 249.7	T + 248.2
Centaur main engine first start	SECO + 11.5	T + 259.3	T + 257.7
Centaur main engine first cutoff; start propellant settling engines	MECO-1	T + 587.0	T + 595.8
Stop propellant settling engines; start propellant retention engines	MECO-1 + 76	T + 663.9	T + 671.8
Start reorientation for Centaur second start	MES-2 - 600	T + 3662.0	T + 3665.1
Stop propellant retention engines; start propellant settling engines	MES-2 - 40	T + 4222.0	T + 4225.1
Centaur main engine second start; stop propellant settling engines	MES-2	T + 4262.0	T + 4265.1
Centaur main engine second cutoff; start propellant settling engines; start alining Centaur roll axis to spacecraft separation vector	MECO-2	T + 4365.4	(b)
Stop propellant settling engines	MECO-2 + 5.0	T + 4370.4	(b)
Separate spacecraft	MECO-2 + 135.0	T + 4500.4	(b)
Start alining Centaur roll axis to local vertical	MECO-2 + 140.0	T + 4505.4	(b)
Start propellant settling engines	MECO-2 + 197.0	T + 4562.4	(b)
Stop propellant settling engines; start propellant retention engines	MECO-2 + 246.0	T + 4611.4	(b)
Stop propellant retention engines; start Centaur main engine blowdown	MECO-2 + 570.0	T + 4935.4	(b)
Stop Centaur main engine blowdown	MECO-2 + 2298.0	T + 6663.4	(b)
Electrical system cutoff	MECO-2 + 2300.0	T + 6665.4	(b)

[a]Based on post-flight predicted trajectory.

[b]Subsequent events were precluded by failure to achieve a successful Centaur main engine second firing.

TABLE V-2. - ATLAS WEIGHT SUMMARY, AC-17

Component	Weight	
	kg	lbm
Booster jettison weight:		
Booster dry weight	2 863	6 311
Booster residuals	472	1 041
Unburned lubrication oil	17	38
Total	3 352	7 390
Sustainer jettison weight:		
Sustainer dry weight	2 707	5 968
Sustainer residuals	443	1 076
Interstage adapter	476	1 049
Unburned lubrication oil	7	15
Total	3 683	8 115
Flight expendables:		
Main impulse RP-1	37 341	82 323
Main impulse oxygen	83 807	184 763
Helium-panel purge	2	5
Oxygen vent loss (boost phase)	141	311
Lubrication oil	84	185
Oxygen vent loss (sustainer phase)	81	178
Total	121 456	267 765
Ground expendables:		
Fuel	242	533
Oxidizer	819	1 805
Lubrication oil	1	3
Exterior ice	24	54
Liquid nitrogen in helium shrouds	113	250
Pre-ignition gaseous oxygen loss	204	450
Total	1 403	3 095
Total tanked weight	129 894	286 368
Minus ground expendables	-1 403	-3 095
Total Atlas weight at lift-off	128 491	283 273

TABLE V-3. - CENTAUR WEIGHT SUMMARY, AC-17

Component	Weight	
	kg	lbm
Basic hardware:		
Body	502	1 106
Propulsion group	529	1 166
Guidance group	154	339
Fluid systems group	130	286
Electrical group	127	281
Separation group	36	79
Flight instrumentation	161	356
Miscellaneous equipment	79	175
Total	1 718	3 788
Jettisonable hardware:		
Nose fairing	979	2 158
Insulation panels	526	1 160
Ablated ice	23	50
Total	1 528	3 368
Centaur residuals at MECO-1 (after thrust decay):		
Liquid-hydrogen residual	643	1 417
Liquid-oxygen residual	2 966	6 540
Gaseous hydrogen	18	39
Gaseous oxygen	27	60
Hydrogen peroxide	198	437
Helium	4	9
Ice	5	12
Total	3 861	8 514
Centaur expendables through MES-2:		
First-powered-phase main impulse hydrogen	1 666	3 673
First-powered-phase main impulse oxygen	8 485	18 706
Gas boiloff on ground, hydrogen	4	8
Gas boiloff on ground, oxygen	0	0
In-flight chill hydrogen	42	93
In-flight chill oxygen	50	111
Booster-phase vent hydrogen	24	53
Booster-phase vent oxygen	30	66
Sustainer-phase vent hydrogen	14	30
Sustainer-phase vent oxygen	27	60
Engine shutdown loss hydrogen	3	6
Engine shutdown loss oxygen	6	13
Parking orbit vent hydrogen	39	87
Parking orbit vent oxygen	0	0
Parking orbit leakage hydrogen	1	2
Parking orbit leakage oxygen	2	5
Hydrogen peroxide	133	293
Helium	2	5
Total	10 528	23 211
Total tanked weight	17 447	38 465
Minus ground vent	-4	-8
Total Centaur weight at lift-off	17 443	38 457
Spacecraft weight	798	1 759
Total Atlas/Centaur/spacecraft lift-off weight	146 732	323 489

TABLE V-4. - PARKING ORBIT PARAMETERS, AC-17

Parameter	Units	Predicted[a]	Actual[b]
Epoch[c]	sec	T + 663.9	T + 671.8
Perigee altitude	km	185.90	185.99
	n mi	100.38	100.43
Apogee altitude	km	767.97	766.89
	n mi	414.67	414.09
Semimajor axis	km	6855.12	6854.60
	n mi	3701.47	3701.19
Eccentricity	----	0.042455	0.042372
Inclination	deg	29.119	29.141
Period	min	94.141	94.131
Energy, C_3	$(km/sec)^2$	-58.147	-58.151
	$(ft/sec)^2$	-6.258889×10^8	-6.25930×10^8

[a]Based on best preflight trajectory.

[b]Data based on trajectory reconstructed from Centaur guidance telemetry; data does not reflect guidance hardware errors.

[c]Parking orbit defined at MECO-1 + 76 sec, at termination of firing of two 222-N (50-lbf) thrust engines.

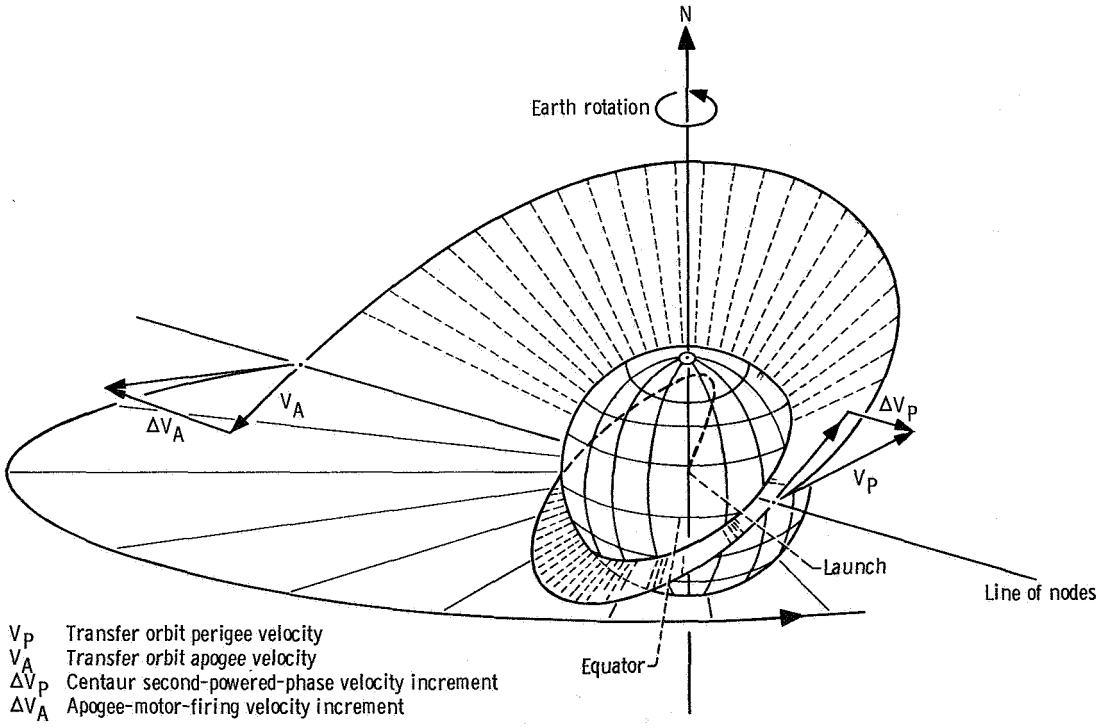

Figure V-1. - ATS-D mission ascent profile.

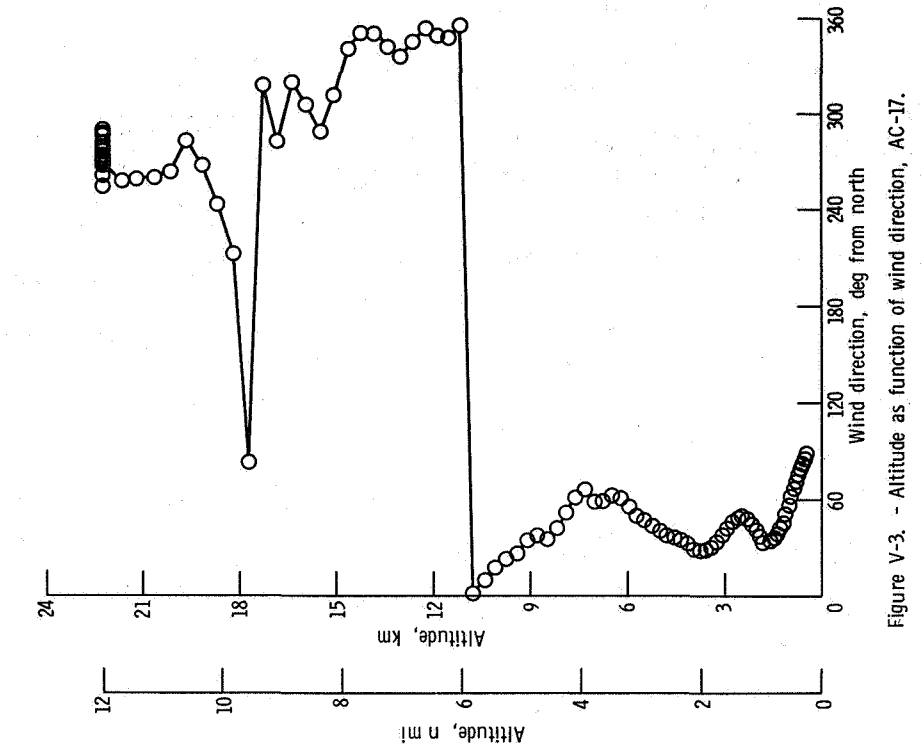

Figure V-3. - Altitude as function of wind direction, AC-17.

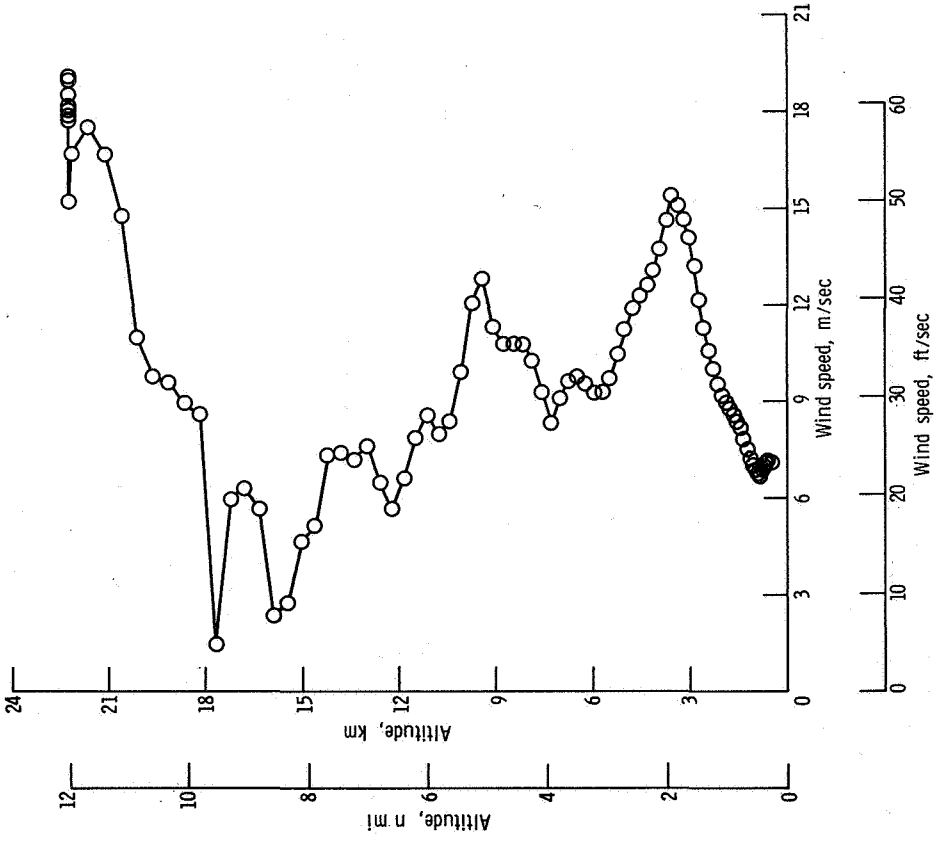

Figure V-2. - Altitude as function of wind speed, AC-17.

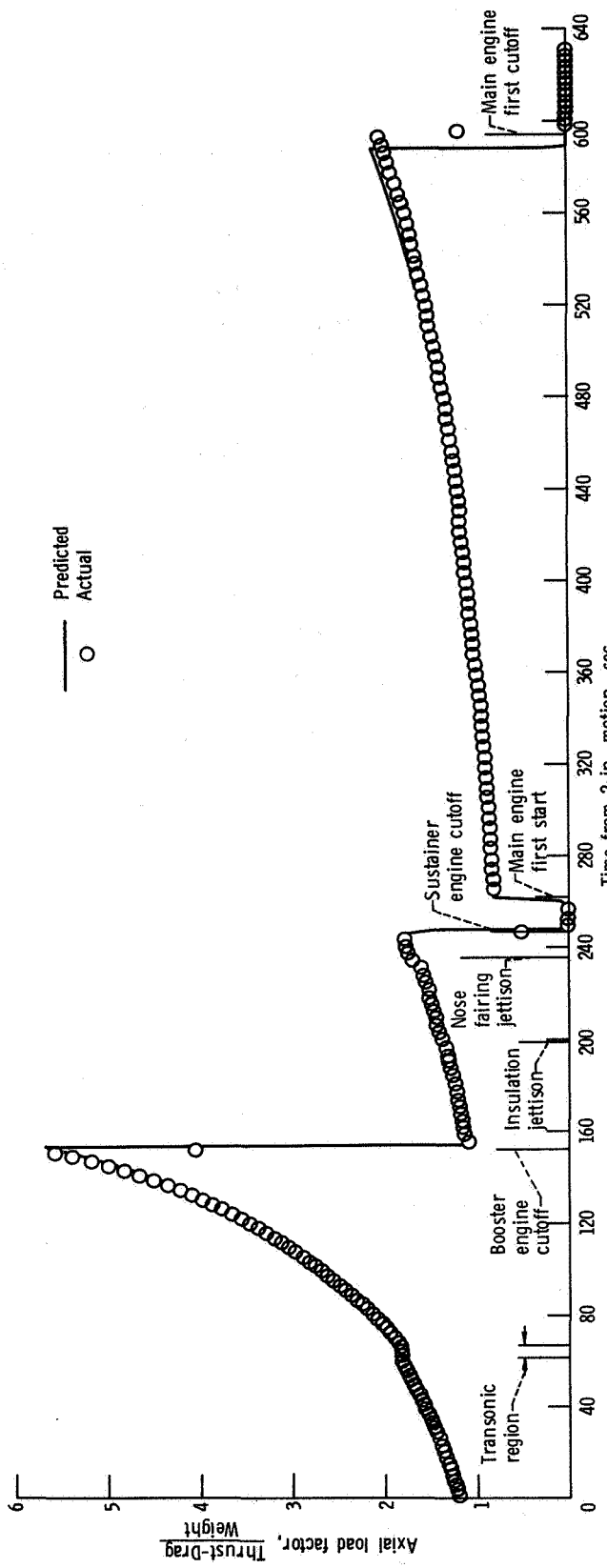

Figure V-4. - Axial load factor as function of time, AC-17.

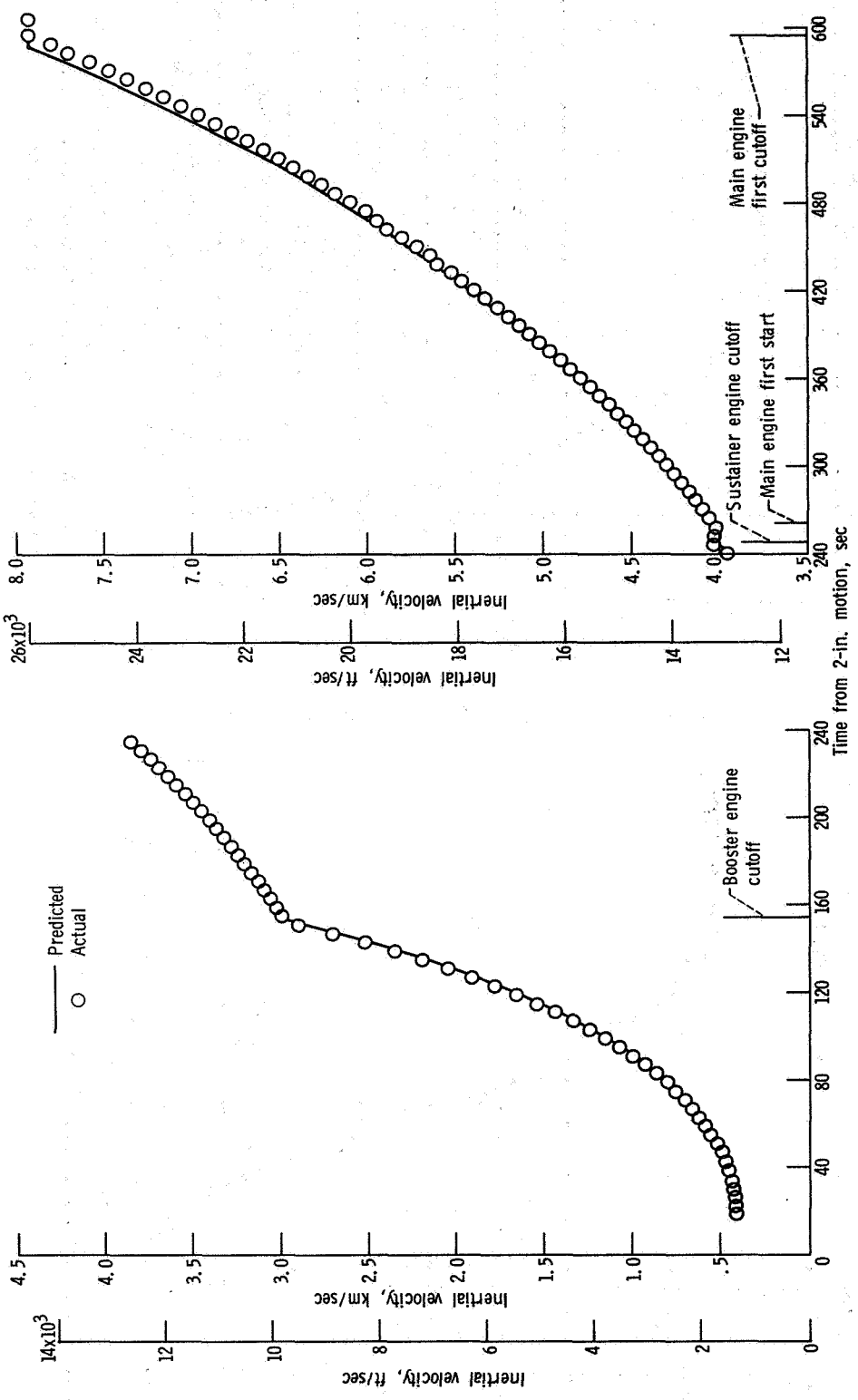

Figure V-5. - Inertial velocity as function of time, AC-17.

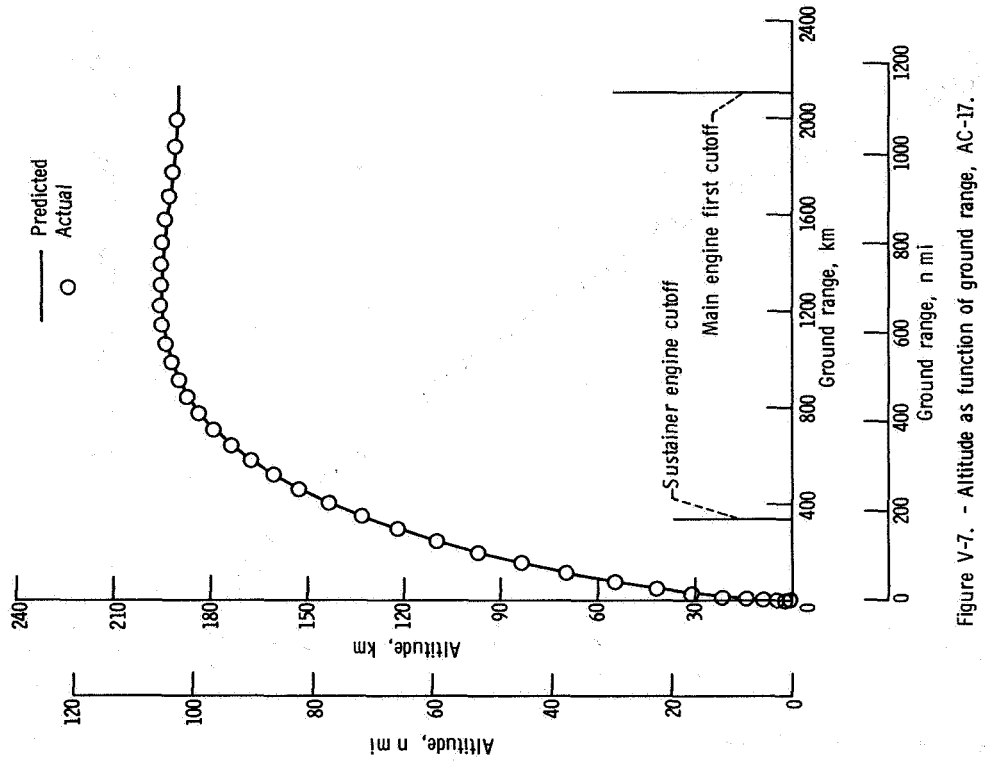

Figure V-7. - Altitude as function of ground range, AC-17.

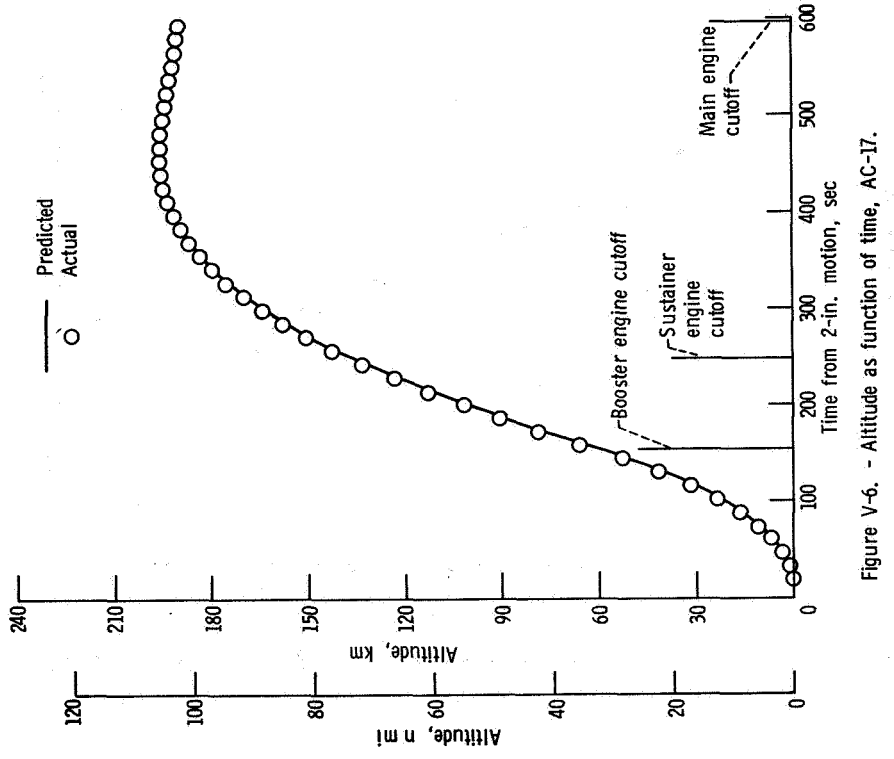

Figure V-6. - Altitude as function of time, AC-17.

VI. LAUNCH VEHICLE SYSTEM ANALYSIS

PROPULSION SYSTEMS

by Charles H. Kerrigan and Donald B. Zelten

Atlas Engines

System description. - The Atlas engine system (fig. VI-1) consists of a booster engine, a sustainer engine, two vernier engines, an engine start tank system, and an electrical control system. The engines use liquid oxygen and RP-1 (kerosene) for propellants. During engine start, electrically fired pyrotechnic igniters are used to ignite the gas generator propellants for driving the turbopumps; and hypergolic igniters are used to ignite the propellants in the thrust chambers of the booster, sustainer, and vernier engines. The pneumatic control of the engine system is discussed in the section PNEUMATIC SYSTEMS that follows.

The booster engine, rated at 1494×10^3 newtons (336×10^3 lbf) thrust at sea level, consists of two gimbaled thrust chambers, propellant valves, two oxidizer and two fuel turbopumps driven by one gas generator, a lubricating oil system, and a heat exchanger. The sustainer engine, rated at 258×10^3 newtons (58×10^3 lbf) thrust at sea level, consists of a thrust chamber, propellant valves, one oxidizer and one fuel turbopump driven by a gas generator, and a lubricating oil system. The entire sustainer engine system gimbals. Each vernier engine is rated at 2.98×10^3 newtons (670 lbf) thrust at sea level, and propellants are supplied from the sustainer turbopump. The vernier engines gimbal for roll control.

The engine start tank system consists of two spherical helium-pressurized propellant tanks, one for liquid oxygen and one for RP-1 (kerosene), each approximately 51 centimeters (20 in.) in diameter. This system supplies starting propellants (oxidizer and fuel) for the gas generators and the vernier engines, and fuel only for the booster and sustainer engines for a period of approximately 2 seconds; thereafter the turbopumps provide the propellants to sustain the engines.

System performance. - The performance of the Atlas propulsion system was satisfactory. During the engine start phase, valve opening times and starting sequence events were within tolerances. The flight performance of the engines was evaluated by comparing measured parameters with the expected values. These are tabulated in table VI-1. Booster engine cutoff occurred at T + 152 seconds when the axial acceleration reached

5.74 g's. Sustainer engine cutoff and vernier engine cutoff were due to liquid-oxygen depletion, the planned shutdown mode, and occurred at T + 246.2 seconds. Transients were normal during shutdown of all engines.

Centaur Main Engines

System description. - The Centaur main engine system consists of two engines (identified as C-1 and C-2). Each engine is gimbal mounted and has its own oxidizer and fuel turbopump, thrust chamber, solenoid control valves, propellant valves, and spark igniter system (fig. VI-2). The engines are capable of making multiple starts after long coast periods in space. Propellants are liquid oxygen and liquid hydrogen. The rated thrust of each engine is 66 700 newtons (15 000 lbf) at an altitude of 61 000 meters (200 000 ft).

These engines operate by the "topping cycle" principle: pumped fuel, after circulating through the thrust chamber tubes, is expanded through a turbine which drives the propellant pumps. This routing of fuel through the thrust chamber tubes serves the dual purpose of cooling the thrust chamber walls and of adding energy to the fuel (hydrogen) prior to expansion through the turbine. After passing through the turbine, the fuel is injected into the combustion chamber. The pumped oxidizer is supplied directly to the combustion chamber after passing through the propellant utilization (mixture ratio control) valve.

Pneumatically operated valves start and stop propellant flow to the engines. Helium pressure to these valves is supplied through engine-mounted solenoid valves which are controlled by electrical signals from the vehicle control system. Opening of the oxidizer and fuel pump inlet valves allows the turbopumps to be prechilled for a predetermined time period prior to propellant ignition. Oxidizer passes through the oxidizer pump and into the combustion chamber; fuel flows through the fuel pump and is discharged through two separate cooldown valves. Ignition is accomplished by means of a spark igniter recessed in the propellant injector face. The thrust level is maintained by regulating the amount of fuel bypassed around the turbine as a function of combustion chamber pressure.

To protect the main engines from excessive heating caused by impingement of exhaust products from the hydrogen peroxide engines, the main engines are shielded in five locations: the fuel and oxidizer pump housings, the propellant utilization valve, the fuel pump discharge line, and the thrust chamber jacket inlet line.

System performance - main engine first powered phase. - The main engine prestart signal was issued, as programmed, 8 seconds prior to the engine start signal. During this period the turbopumps were prechilled. Turbopump surface temperature data indicated the prechill was satisfactory. Propellant pressures and temperatures at the pump inlets were satisfactory during the prestart period. Main engine first start was

commanded at T + 257.7 seconds. The start transients were normal. Steady-state operating performance of the engines was evaluated by comparing measured parameters with expected values. These data are tabulated in table VI-2. The values for the chamber pressures were lower than expected; however, the other internal parameters for the engines indicated normal levels. Low chamber pressure values have been recorded during a number of previous flights. The cause is not known. The signal for main engine cutoff was generated by the guidance system computer and occurred at T + 595.8 seconds. Engine shutdown sequences were normal.

System performance - main engine second powered phase. - The coast period between main engine powered phases was 61.2 minutes, as compared to a maximum coast duration of approximately 22 minutes for previous two-powered-phase missions. The turbopump prechill period was increased to 29 seconds for the main engine second start sequence. The increased prechill duration was provided to overcome probable greater heat inputs to the turbopump and propellant supply system resulting from the longer coast phase (table VI-3).

Main engine second start was commanded at T + 4265.1 seconds. The C-1 engine attained a momentary ignition as indicated by fuel turbine inlet temperature data; however, the C-2 engine did not ignite. Also, liquid hydrogen was gasified by the residual heat in the thrust chamber jackets sufficiently to momentarily accelerate both turbopumps to steady-state speed levels. Momentary pumping was also obtained by the fuel pumps as evidenced by a rise in fuel pump discharge pressure. Main engine thrust chamber pressures reached a maximum value of approximately 10 percent of steady-state levels. The failure of the main engine to start and operate normally is attributed to insufficient propellant inlet pressure, which resulted from failure of the boost pumps to operate.

Following the attempted main engine start, propellants continued to be expelled from the propellant tanks through the engines. The oxidizer system remained in the identical configuration as during the prestart sequence; that is, some liquid oxygen flows through the oxidizer pump and then overboard through the thrust chamber injector. The fuel system flowed propellant overboard through both the thrust chamber and the pump interstage cooldown valves (fig. VI-2). This occurred because the command for main engine start is executed by opening the main fuel shutoff valve (thereby allowing flow to the thrust chamber) and by closing the discharge cooldown valve completely and the interstage cooldown valve only partially. During a normal engine start, however, the interstage cooldown valve would close as fuel pump discharge pressure increased. The engine valves remained in this abnormal configuration until the termination of data acquisition.

Centaur Boost Pumps

System description. - A single boost pump is used in each propellant tank to supply propellants to the main engine pumps at the required inlet pressures. Each boost pump is a mixed-flow centrifugal type and is powered by a hot-gas-driven turbine. The hot gas consists of superheated steam and oxygen from the catalytic decomposition of 90-percent-concentration hydrogen peroxide. Constant power is maintained on each turbine by metering the hydrogen peroxide through fixed-area orifices upstream of the catalyst bed. A speed control system is provided on each turbine to prevent overspeeding if the pump is inadvertently unloaded. The complete boost pump and hydrogen peroxide supply systems are shown in figures VI-3 to VI-5, and VI-11.

The speed control system consists of a speed sensor, an electronics assembly, and a normally open solenoid valve in the hydrogen peroxide supply line upstream of the catalyst bed. When a predetermined speed is exceeded, two series-redundant relays within the electronics assembly close, and power is applied to the solenoid valve. (Both relays must be closed to complete the circuit and apply power to the valve solenoid.) The valve closes and stops the flow of hydrogen peroxide to the catalyst bed. When the turbine speed has decayed to another predetermined speed, one (or both) of the relays open and power is removed from the valve solenoid. The valve opens and hydrogen peroxide flow to the catalyst bed is resumed.

The configuration of the boost pumps and turbine drives on AC-17 was similar to those on AC-15, the preceding two-powered-phase vehicle. The only differences were thermal modifications to the AC-17 overspeed control system on both the liquid-oxygen and liquid-hydrogen turbines. These thermal modifications were designed to reduce the temperature of the electronic control equipment during the 61-minute coast period and consisted of the following:

(1) A rectangular hole was added in the cover over the valve distribution box.

(2) The top of the overspeed valve distribution box was painted white.

(3) The top surface of the signal conditioning unit was painted white.

(4) Silicone grease was added between the cover and the sides of the distribution box to improve conductive contact.

System performance. - Performance of each boost pump was satisfactory for the first operating period. The boost pumps were started 44.0 seconds prior to main engine first start and continued to operate until main engine cutoff at T + 595.8 seconds. The turbine inlet pressure delay times (time from boost pump start signal to time of first indication of turbine inlet pressure rise) were less than 1 second for both turbines. A comparison of expected and actual steady-state performance data for the boost pump is shown in table VI-4. The steady-state turbine speeds were higher than the expected values by 600 and 1350 rpm for the liquid-oxygen and liquid-hydrogen boost pumps, respectively. Higher-than-expected turbine speeds were also noted on previous Centaur flights

and are attributed to the inability to precisely duplicate the flight conditions during prelaunch ground tests (turbine exhaust backpressure, hydrogen peroxide flow rate to the turbines, liquid propellant flow rates through the pumps, etc.).

Temperature data for the boost pump turbine bearings and the hydrogen boost pump overspeed sensor are shown in figure VI-6. Figures VI-7 and VI-8 show the pressure rise across the boost pumps, and figures VI-9 and VI-10 show the turbine speeds. The only anomaly observed during the first operating period was a relatively long time period required for the liquid-oxygen-boost-pump turbine speed to decay to zero after boost pump cutoff. On previous two-powered-phase vehicles, this time period varied from 54 to 76 seconds. As seen on figure VI-10, the time required before turbine rotation reached zero was approximately 90 seconds. The exact reason for the long decay time is not known; however, internal friction between rotating parts, turbine drive temperature, liquid level above the pump inlet, and net positive suction pressure at the pump inlet can affect the turbine speed decay time. This anomaly is not considered to be related in any way with failure of the boost pumps to start prior to the planned Centaur main engine second firing.

The command to start the boost pumps for the main engine second firing was sent by the programmer at the scheduled time (28 sec prior to main engine second start). Boost pump operation for the scheduled second firing did not occur, and as a result the main engines did not start. Boost pump turbine speeds and turbine inlet pressures remained at zero throughout the scheduled second operating period. Measurements of pressure rise across the boost pumps also verified that no pump rotation occurred. The liquid-hydrogen and liquid-oxygen boost pump turbine bearing temperatures and the liquid-hydrogen boost pump over-speed sensor temperature were within expected ranges. There was, however, no evidence of hydrogen peroxide flow to the boost pump turbine catalyst beds. The reason for the failure of the hydrogen peroxide to reach the catalyst beds is discussed in the following section - Hydrogen Peroxide Engine and Supply System.

Hydrogen Peroxide Engine and Supply System

System description. - The hydrogen peroxide engine and supply system (figs. VI-11 and VI-12) consists of 14 thruster engines, two supply bottles, and interconnecting tubing to the thruster engines and boost pump turbines. The thruster engines are used during the nonpowered phases of flight. Four 222-newton (50-lbf) thrust engines and four 13.3-newton (3-lbf) thrust engines are used primarily for propellant settling and retention and for the post-spacecraft-separation maneuvers. Two clusters, each of which consists of two 15.6-newton (3.5-lbf) thrust engines and one 26.7-newton (6-lbf) thrust engine, are used for attitude control (see table VI-12, GUIDANCE AND FLIGHT CONTROL SYSTEMS section for modes of operation). Propellant is supplied to the engines from the two

positive-expulsion, bladder-type storage tanks which are pressurized with helium to an absolute pressure of about 210 N/cm^2 (305 psi) by the pneumatic system. The hydrogen peroxide is decomposed in the engine catalyst beds, and the hot decomposition gases are expanded through nozzles to provide thrust. Hydrogen peroxide is also used to drive the boost pump turbines. All the hydrogen peroxide supply lines are equipped with heaters to maintain line temperatures between 278 K (40° F) and 322 K (120° F).

System configuration changes compared to previous two-powered-phase configurations were made on AC-17 because of ATS mission requirements (i.e., the extended coast period which necessitated additional hydrogen peroxide storage capacity and increased thermal protection for system components). Hydrogen peroxide storage capacity was increased by adding a second bottle. This in turn resulted in plumbing changes. In addition, the bottles were covered with aluminized Mylar insulation to ensure that the hydrogen peroxide would not get too cold during the long coast period. To thermally condition the engines, a programmed firing was made during the main engine first powered phase of the hydrogen peroxide engines that were not programmed to fire during the subsequent coast period. The V1 and V3 engines were fired for 2.5 seconds; and all the A engines, both P engines, and the S1 and S3 engines were fired for 10 seconds.

System performance. - The hydrogen peroxide supply system performed satisfactorily through Centaur first powered phase and the early portion of the coast phase. Subsequent to T + 800 seconds, several minor anomalies in temperature data occurred; however, the hydrogen peroxide engines operated satisfactorily during the 61.2-minute coast phase. At the end of the coast phase, a failure occurred when the boost pump failed to operate for the Centaur main engine second powered phase.

A comprehensive post-flight investigation was performed to determine the cause of the failure. System design, preflight history, and all flight data were analyzed in detail. An extensive series of tests were conducted both at General Dynamics' Convair Aerospace Division and at Lewis Research Center. These tests ranged from individual component tests to complete boost pump hydrogen peroxide supply system tests. Testing was performed at various environmental conditions including simulated space and zero gravity. All potential failure modes were simulated and tested.

It is concluded, from the evaluation of the data obtained during the investigation, that the most probable cause of the AC-17 failure was a cryogenic leak. This leak caused the hydrogen peroxide to freeze in the boost pump supply line, thereby preventing hydrogen peroxide flow to the boost pump catalyst beds. Consequently, the boost pumps did not operate for Centaur main engine second start. Other credible failure modes investigated are presented in the appendix.

The location of flight instrumentation for the system is shown in figure VI-12. The temperature data from this instrumentation with other vehicle data support the cryogenic leak theory. Although all the temperature data were not as predicted in preflight analysis, subsequent evaluation has shown that the data were not abnormal except possibly

for measurements CP344T and CP14T. Immediately after lift-off, all temperatures decreased due to termination of the warm gas conditioning supply to the thrust section. Figure VI-13 shows that at boost pump first start, temperatures at measurements CP344T and CP345T increased abruptly as the relatively warmer hydrogen peroxide from the supply bottle flowed through the lines. During boost pump operation these two line temperatures stabilized at values near the temperature of the hydrogen peroxide in the supply bottle. At main engine first cutoff the flow of hydrogen peroxide was terminated; and at the same time the 222-newton (50-lbf) thrust engines were fired in the V-half-on mode for 76 seconds. At this time the sharp increase in temperature at measurement CP344T is attributed to exhaust impingement from these engines. The increase in temperature at measurement CP345T after main engine first cutoff, and the increase in temperature at measurement CP738T between T + 280 and T + 620 seconds are attributed to solar heating. The large decrease in temperature at measurement CP344T during the absence of telemetry coverage between T + 805 and T + 1205 seconds was not considered normal. It is assumed that this decrease was partially caused by cryogenic leakage. The leakage probably was impinging not on the line at the measurement location but rather on the line upstream, and thereby cooling the residual hydrogen peroxide in the line. The movement of the residual peroxide to the measurement location resulted in the temperature decrease. Erratic changes in temperature data at measurement CP344T during the period between T + 1200 and T + 2200 seconds is further evidence of cool hydrogen peroxide moving back and forth ("slugging") in the line. The cessation of the perturbations at T + 2200 seconds indicates that the "slugging" had stopped. The 222-newton (50-lbf) engines are fired again in the V-half-on mode for 40 seconds prior to main engine second start. The sharp rise in temperature at measurement CP344T at this time is because of exhaust impingement from these engines. The subsequent decrease in temperature starting at the time planned for main engine second start is attributed to cooling from the hydrogen plume from the main engines. This cooling continued until T + 5000 seconds, when the liquid-hydrogen tank was depleted. The temperature at measurement CP345T increased, after the attempted main engine second start, because it was not exposed to the hydrogen plume and it was being heated by solar radiation.

At T + 536 seconds, the temperature at measurements CP14T, CP40T, and CP731T increased because of the flow of the warmer hydrogen peroxide through the lines when the engines were fired for thermal conditioning (fig. VI-13). At T + 1200 seconds, the temperatures at measurements CP14T and CP40T both show a decreasing trend. The same amount of hydrogen peroxide is flowing in each of these lines, but the measurements are located on the Centaur vehicle 180^{o} opposite each other. Since the vehicle is rolling very slowly, study of the space environment indicates that when the temperature at measurement CP40T is decreasing, the temperature at measurement CP14T should be increasing and vice versa. Therefore, the temperature at measurement CP14T should be increasing after T + 1200 seconds. The cooling trend is not attributed to external

cooling in the area of the measurement but rather to cooling of the hydrogen peroxide upstream in the line near the supply bottle. Cooling in this area correlates with a cryogenic leak. After main engine second start attempt, temperatures at measurements CP14T, CP40T, and CP730T all showed a cooling trend until the time when the liquid-hydrogen tank was depleted. This was caused by the hydrogen plume coming from the nonoperating Centaur main engines. It is assumed that due to the tumbling motion of the vehicle after main engine second start, measurement CP731T was not exposed to the hydrogen plume and therefore showed an increase due to the effects of solar radiation.

Figure VI-13 shows the temperature of both hydrogen peroxide bottles and that of the manifold line between the two bottles. A check valve in the manifold line allowed flow only from the boost pump bottle to the attitude control bottle and only after the attitude control bottle was depleted. The sharp rise in temperature at measurement CP756T about 20 seconds prior to the attempted main engine second start is a definite indication of depletion of the attitude control bottle and flow from the boost pump bottle through the manifold line. Depletion of the attitude control bottle near this time period was expected. The subsequent decrease in temperature at measurement CP756T occurred when flow through the line stopped at the time of the attempted main engine second start.

The common hydrogen peroxide supply lines (P/N 55-24160-10 and -14) are in close proximity to several potential leak sources in the liquid-oxygen system. A localized leak from one of these sources could freeze the hydrogen peroxide and plug the line and, at the same time, not be definitely detected by the available instrumentation. It was pointed out previously, however, that there actually was some unusual behavior of two temperature measurements, CP14T and CP344T.

Flight data also recorded a disturbing torque on the vehicle during the coast period. This disturbance began sometime during the period when no flight data were obtained, between T + 805 and T + 1205 seconds. When data were reacquired at T + 1205 seconds, the guidance and flight control data showed an unexplained increase in axial thrust of about 4.5 newtons (1 lbf) and a change in the disturbing torques on the vehicle. Although there were some variations in magnitude and direction, this disturbance remained on the vehicle for the remainder of the coast period. An analysis was made to determine the liquid-oxygen leak rate required to produce the disturbance seen on the vehicle. The analysis showed the leak rate to be from 23 to 45 grams per second (0.05 to 0.10 lbm/sec), dependent upon the exact location and direction of the leak.

Ground testing was performed in which a leak was simulated by spraying liquid nitrogen, at a rate of 16 grams per second (0.036 lbm/sec), on a line filled with hydrogen peroxide. The results of this test showed that the hydrogen peroxide in the line froze solid in just a few minutes.

Other information in support of cryogenic leak failure theory is that a potential source of leakage was found on AC-19 and AC-20 launch vehicles (which were being preflight tested while the investigation was in progress). Leakage was detected on AC-19 at

the liquid-oxygen sump-to-tank flange and on both AC-19 and AC-20 at the instrumentation boss on the liquid-oxygen supply duct. A leak originating from either of these areas would explain the disturbing forces acting on the vehicle during the coast period, the unexplained changes in temperature measurements CP14T and CP344T, and also freezing of the hydrogen peroxide supply line.

TABLE VI-1. - ATLAS PROPULSION SYSTEM PERFORMANCE, AC-17

Performance parameter	Units	Expected operating range	Flight values at -		
			T + 10 sec	Booster engine cutoff	Sustainer and vernier engine cutoff
Booster engine thrust chamber 1 (B-1) pressure, absolute	N/cm^2	386 to 410	394	394	------
	psi	560 to 595	571	571	------
Booster engine thrust chamber 2 (B-2) pressure, absolute	N/cm^2	386 to 410	395	395	------
	psi	560 to 595	573	573	------
Booster engine gas generator chamber pressure, absolute	N/cm^2	351 to 382	380	380	------
	psi	510 to 555	551	551	------
Booster engine thrust chamber 1 (B-1) turbopump speed	rpm	6225 to 6405	[a]6427	[a]6408	------
Booster engine thrust chamber 2 (B-2) turbopump speed	rpm	6165 to 6345	6334	6309	------
Sustainer engine thrust chamber pressure, absolute	N/cm^2	469 to 493	472	472	472
	psi	680 to 715	685	685	685
Sustainer engine gas generator discharge pressure absolute	N/cm^2	407 to 473	430	430	430
	psi	590 to 686	624	624	624
Sustainer engine turbopump speed	rpm	10 025 to 10 445	10 376	10 400	10 376
Vernier engine 1 thrust chamber pressure, absolute	N/cm^2	172 to 183	179	177	183
	psi	250 to 265	260	256	266
Vernier engine 2 thrust chamber pressure, absolute	N/cm^2	172 to 183	177	174	177
	psi	250 to 265	256	252	256
Duration of booster engine firing	sec	152.8	------	152.0	------
Duration of sustainer engine firing	sec	247.8	------	------	246.2
Duration of vernier engine firing	sec	247.8	------	------	246.2

[a]Higher than expected, but satisfactory when allowing for instrumentation system accuracy.

TABLE VI-2. - CENTAUR MAIN ENGINE FIRST FIRING STEADY-STATE OPERATING DATA, AC-17

Parameter	Units	Expected value	Flight values at-							
			MES-1[a] + 90 sec		MES-1[b] + 142 sec		MES-1[c] + 212 sec		MES-1[c] + 218 sec	
			C-1	C-2	C-1	C-2	C-1	C-2	C-1	C-2
Fuel pump inlet total pressure, absolute	N/cm^2	17.2 to 24.0	21.1	21.1	21.6	21.1	20.9	20.6	19.5	19.0
	psi	24.9 to 35.3	30.6	30.6	31.3	30.6	30.3	29.8	28.3	27.6
Fuel pump inlet temperature	K	20.3 to 21.9	21.7	21.6	21.6	21.6	21.5	21.4	21.4	21.4
	^oR	36.5 to 39.5	39.1	39.0	38.9	38.9	38.7	38.5	38.6	38.5
Oxidizer pump inlet total pressure, absolute	N/cm^2	35.5 to 53.8	43.2	43.6	41.2	42.0	42.6	43.0	43.2	44.1
	psi	51.5 to 78.0	62.6	63.2	59.7	61.0	61.9	62.4	62.7	64.0
Oxidizer pump inlet temperature	K	95.6 to 101.6	98.7	98.7	98.6	98.6	98.5	98.5	98.5	98.5
	^oR	172.0 to 183.0	177.9	177.8	177.7	177.6	177.2	177.2	177.2	177.2
Oxidizer pump speed	rpm	12 163±347	11 950	12 010	11 790	11 810	11 860	11 980	12 080	12 110
Fuel venturi upstream pressure, absolute	N/cm^2	[d]508±17	500	513	493	501	500	509	508	526
	psi	[d]737±25	725	744	715	726	725	738	737	762
Fuel turbine inlet temperature	K	[d]217±12	214	212	234	232	214	215	195	195
	^oR	[d]390±22	386	383	421	418	385	387	352	352
Oxidizer injector differential pressure	N/cm^2	[d]31.7±6.9	27.7	27.7	30.2	29.6	28.2	26.0	26.2	24.0
	psi	[d]46±10	40.1	40.2	43.8	42.9	40.8	37.7	38.0	34.7
Engine chamber pressure, absolute	N/cm^2	[d]270.8±3.7	265	268	265	267	265	267	263	267
	psi	[d]392.4±5.4	384	386	384	387	384	387	382	387
Fuel pump discharge pressure, absolute	N/cm^2	[e]676	660	667	640	646	651	646	671	678
	psi	[e]981	959	967	929	936	944	936	974	982
Oxidizer pump discharge pressure, absolute	N/cm^2	[e]408	403	399	389	389	396	405	414	416
	psi	[e]591	584	579	564	564	575	588	600	604

[a]Main engine first start (MES-1) + 90 seconds is normally selected as time to check engine performance. This time is selected because it is the latest time during the engine first firing that the propellant utilization valve is guaranteed to be in null position.

[b]MES-1 + 142 seconds represents a time when the propellant utilization valves were commanded to the oxidizer-rich stop.

[c]MES-1 + 212 and MES-1 + 218 seconds represent high and low values obtained while propellant utilization valves were controlling.

[d]Expected value with nominal inlet conditions and nulled propellant utilization valve angles.

[e]Nominal design value.

TABLE VI-3. - CENTAUR MAIN ENGINE TEMPERATURE DATA

DURING COAST PHASE, AC-17

Parameter	Units	Flight values at-					
		Main engine first cutoff		Main engine first cutoff + 76 sec		Main engine second cutoff - 50 sec	
		C-1	C-2	C-1	C-2	C-1	C-2
Fuel pump housing temperature	K	31	39	62	63	159	156
	°R	56	70	111	114	287	281
Oxidizer pump housing temperature	K	102	102	143	133	197	202
	°R	183	183	257	240	355	363
Fuel turbine inlet temperature	K	182	182	195	193	166	166
	°R	327	327	350	347	299	299
Thrust chamber skin temperature	K	133	127	187	200	206	208
	°R	239	228	337	360	372	374
Engine bell station 518 temperature	K	84	84	217	226	204	258
	°R	151	151	391	407	367	465
Engine bell station 507 temperature	K	101	101	230	226	204	195
	°R	181	181	415	407	367	351
Engine bell station 500 temperature	K	80	83	235	230	243	280
	°R	144	151	423	415	419	504
Fuel pump discharge line temperature	K	<33	(a)	192	(a)	210	(a)
	°R	<60		345		378	
Fuel pump housing second stage temperature	K	<33	(a)	87	(a)	160	(a)
	°R	<60		158		288	
Fuel jacket inlet line temperature	K	54	(a)	136	(a)	219	(a)
	°R	97		245		394	

[a]Not applicable.

TABLE VI-4. - COMPARISON OF EXPECTED AND ACTUAL BOOST PUMP STEADY-STATE PERFORMANCE DATA FOR CENTAUR FIRST FIRING, AC-17

Performance parameter	Units	Expected (a)	Actual
Liquid-oxygen boost pump turbine inlet pressure, absolute	N/cm^2	66.0	65.8
	psi	95.9	95.5
Liquid-hydrogen boost pump turbine inlet pressure, absolute	N/cm^2	67.2	66.5
	psi	97.5	96.5
Liquid-oxygen boost pump turbine speed	rpm	33 500	34 100
Liquid-hydrogen boost pump turbine speed	rpm	40 400	41 750
Liquid-oxygen boost pump pressure rise	N/cm^2	19.3	19.8
	psi	28.0	28.8
Liquid-hydrogen boost pump pressure rise	N/cm^2	7.7	7.4
	psi	11.2	10.8

[a]Values obtained from prelaunch component acceptance test.

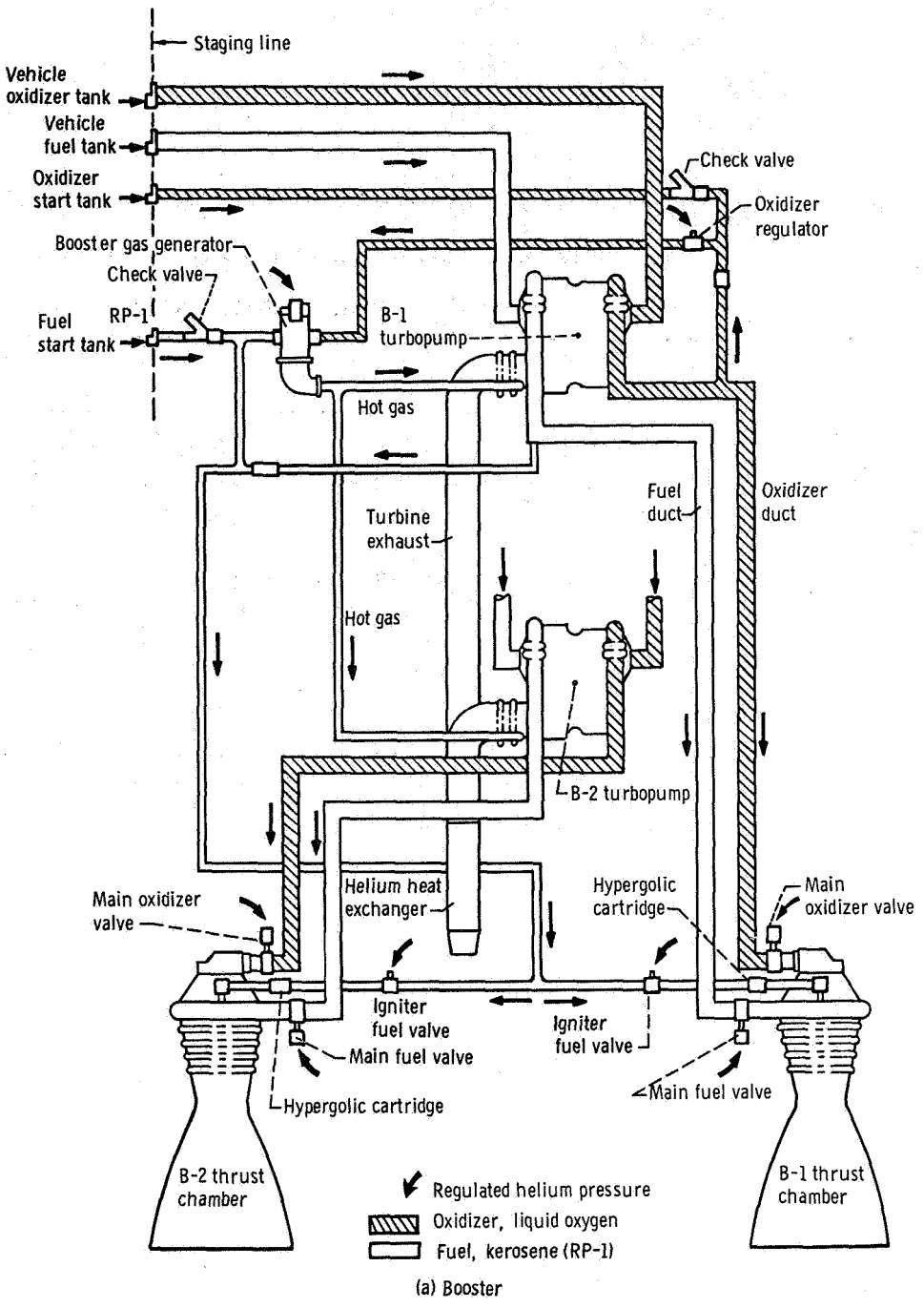

(a) Booster

Figure VI-1. - Atlas propulsion system, AC-17.

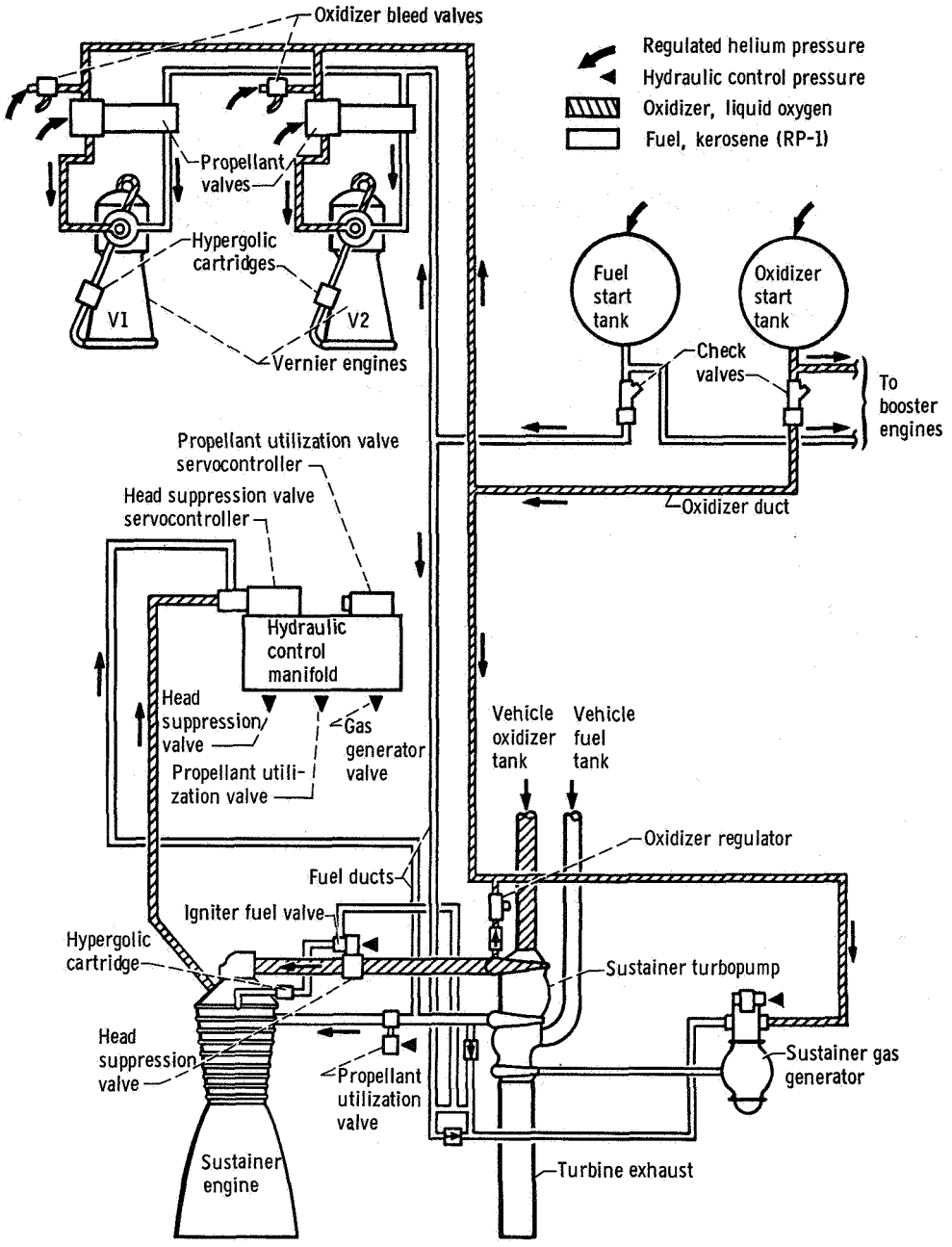

(b) Sustainer and vernier.

Figure VI-1. - Concluded.

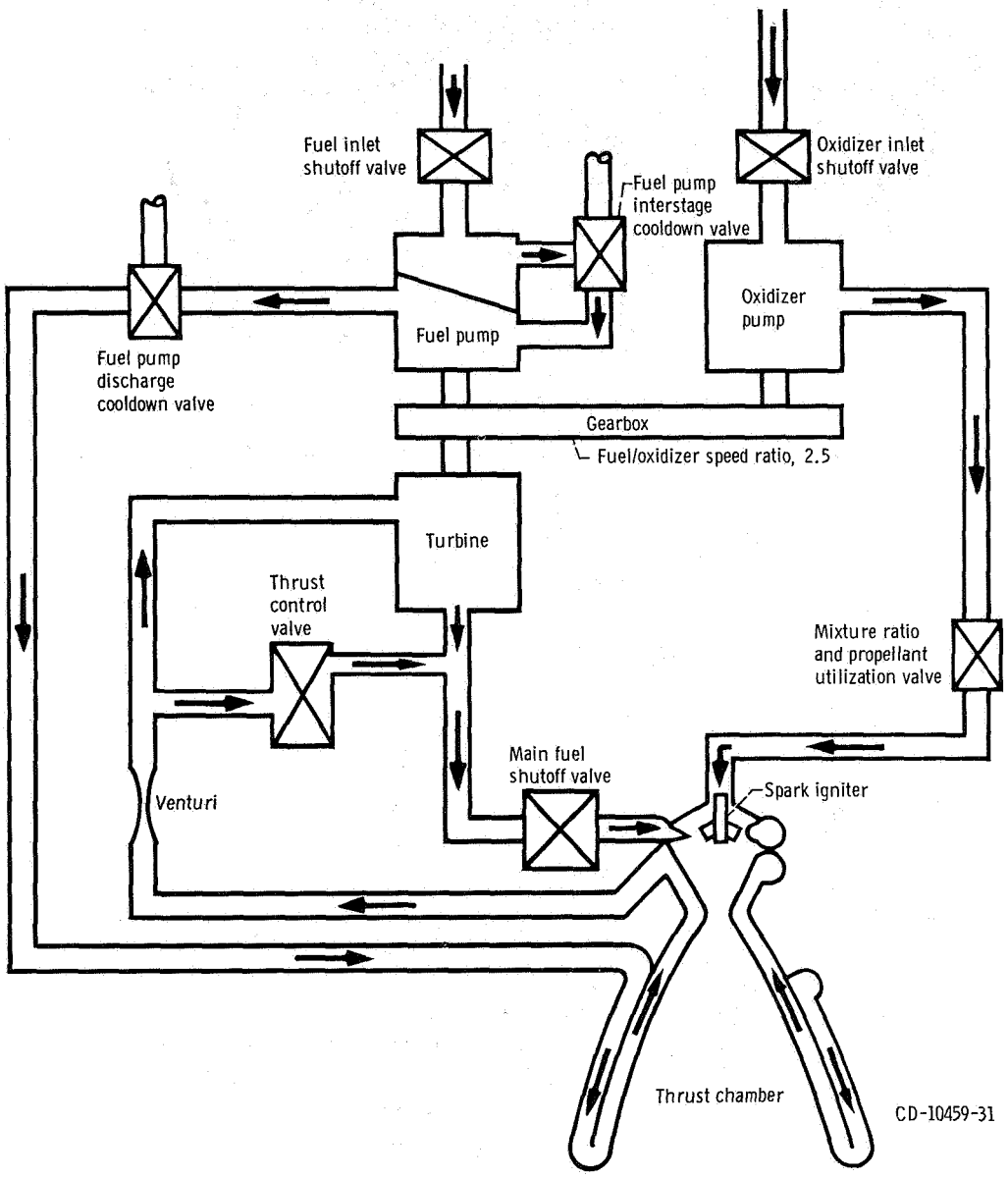

Figure VI-2. - Schematic drawing of Centaur main engine, AC-17.

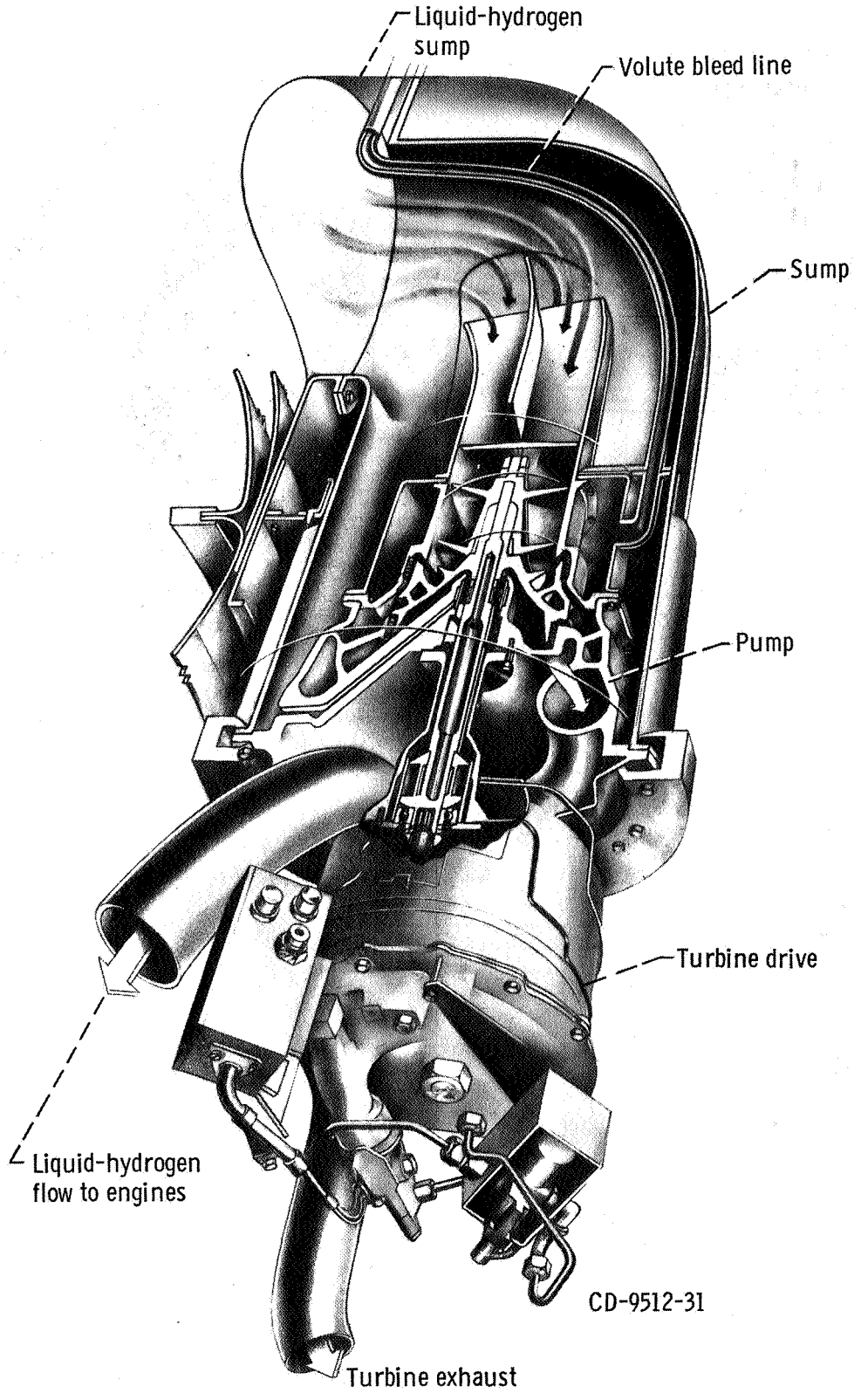

Figure VI-3. - Centaur liquid-hydrogen boost pump and turbine cutaway, AC-17.

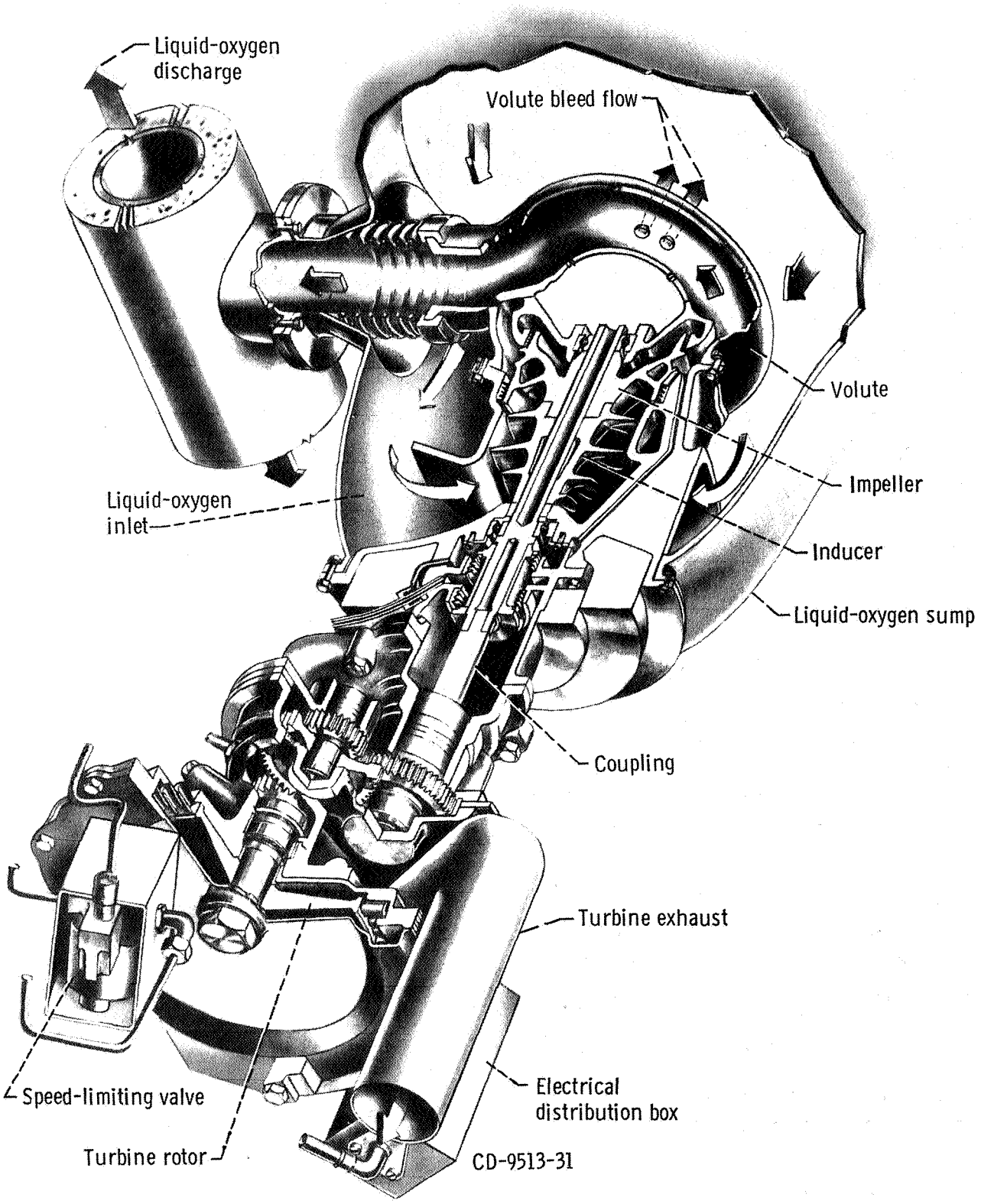

Figure VI-4. - Centaur liquid-oxygen boost pump and turbine cutaway, AC-17.

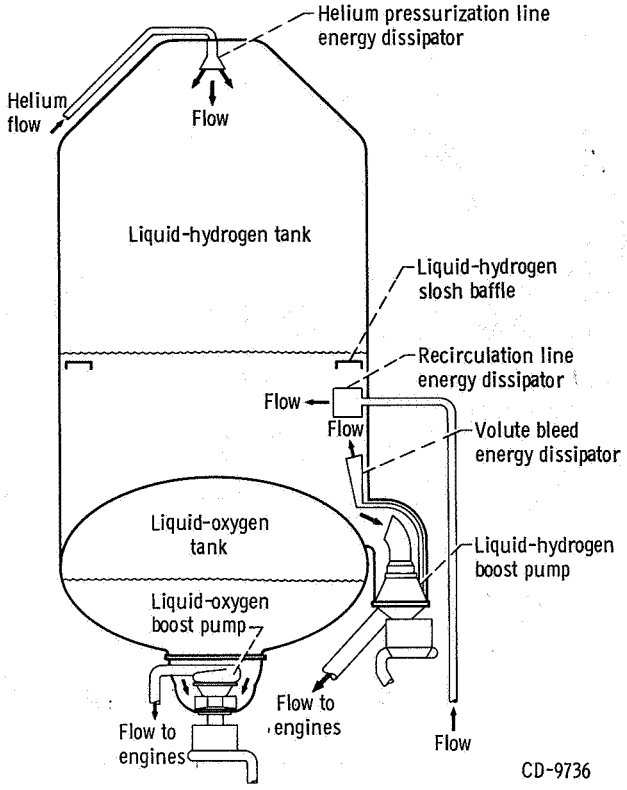

Figure VI-5. - Location of Centaur liquid-hydrogen and liquid-oxygen boost pumps, AC-17.

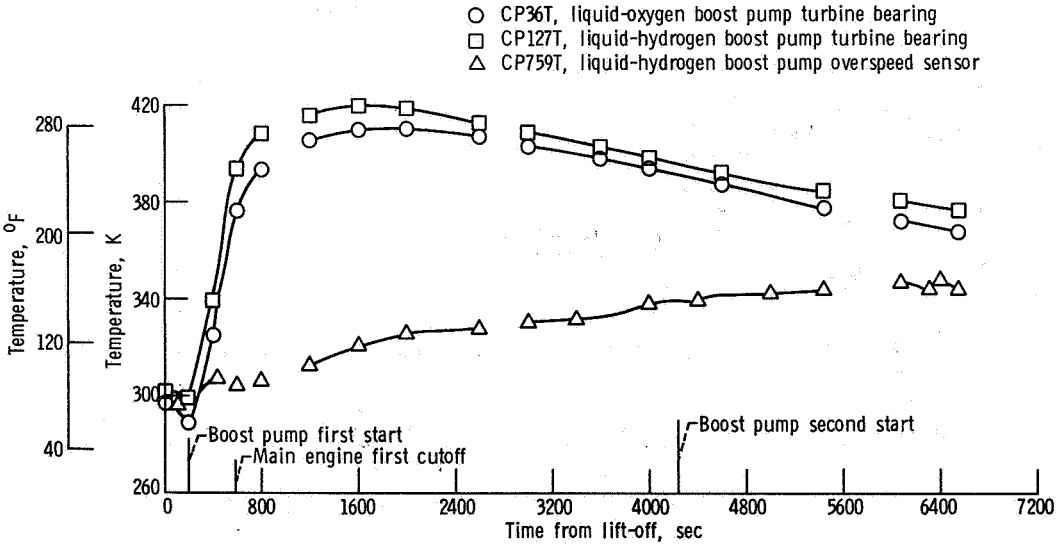

Figure VI-6. - Boost pump temperature, AC-17.

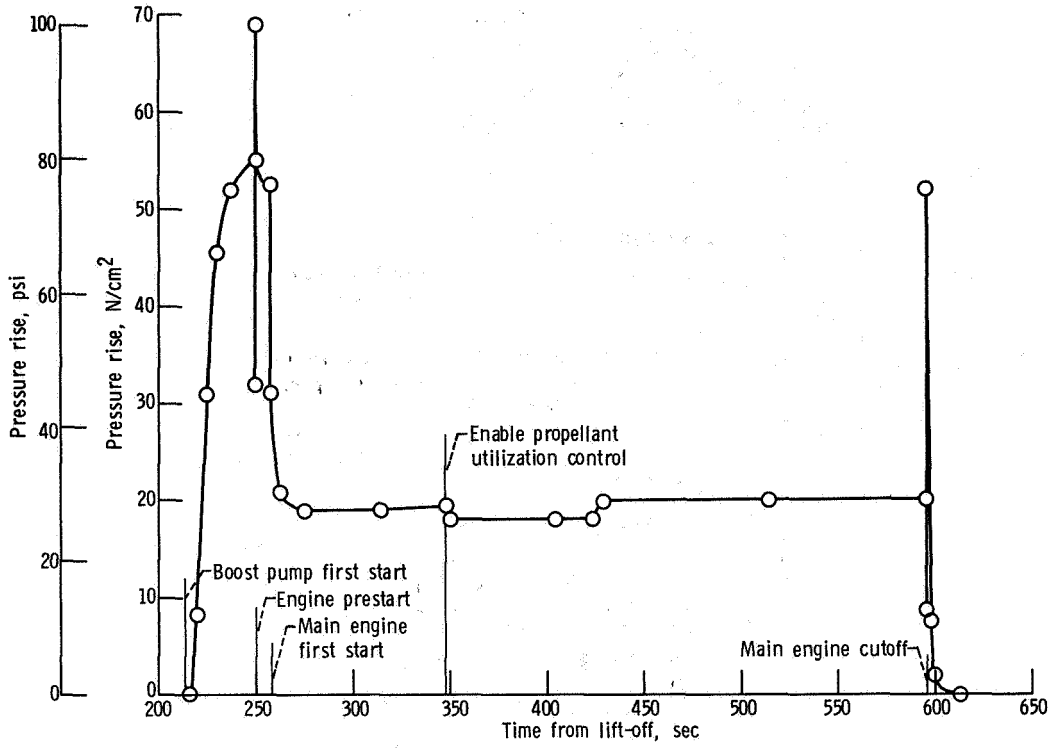

Figure VI-7. - Liquid-oxygen boost pump pressure rise, AC-17.

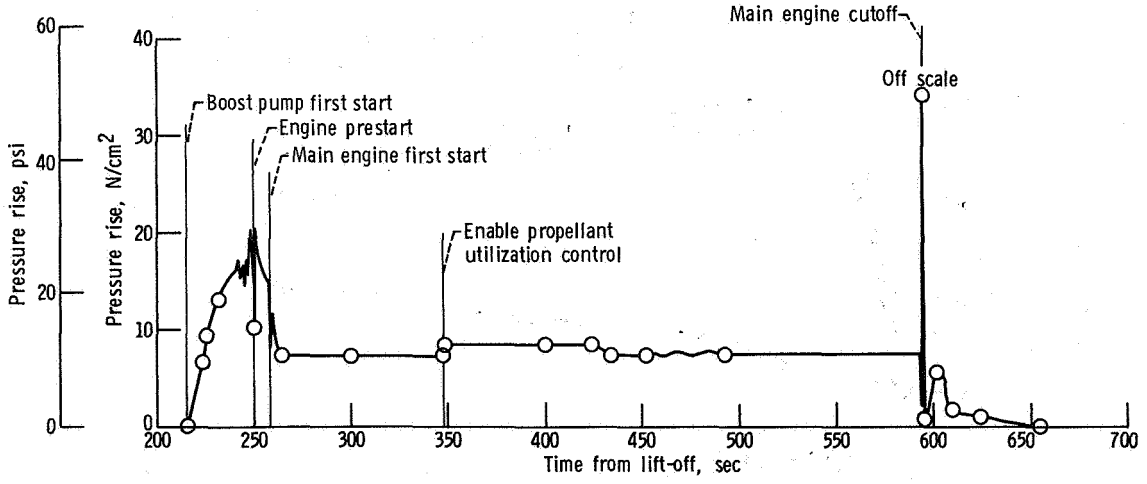

Figure VI-8. - Liquid-hydrogen boost pump pressure rise, AC-17.

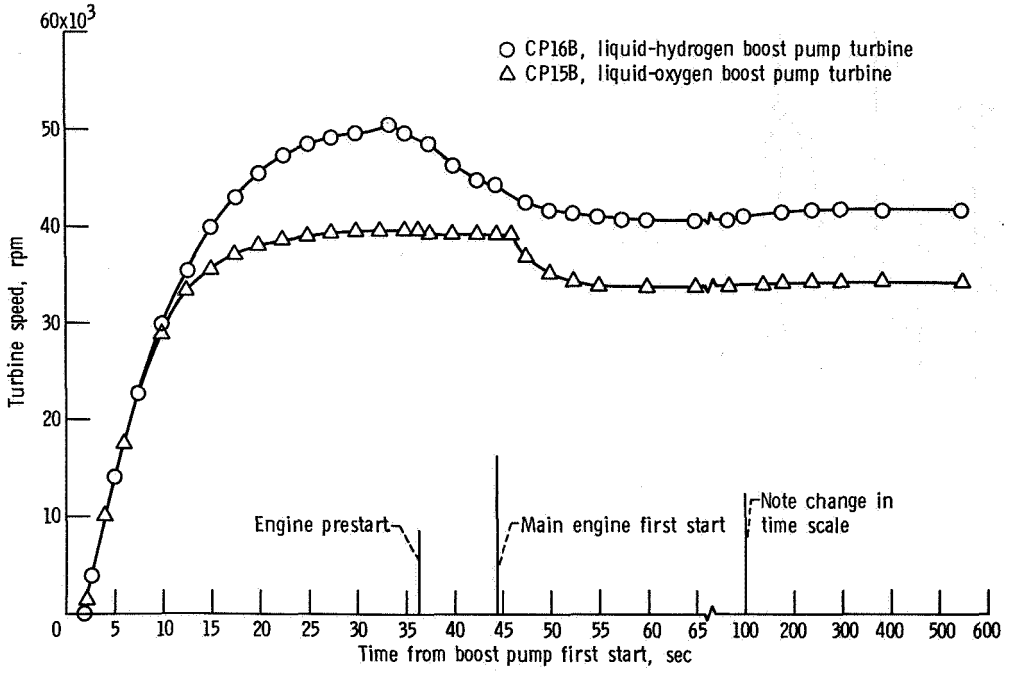

Figure VI-9. - Boost pump turbine speed for 600 seconds after boost pump first start, AC-17.

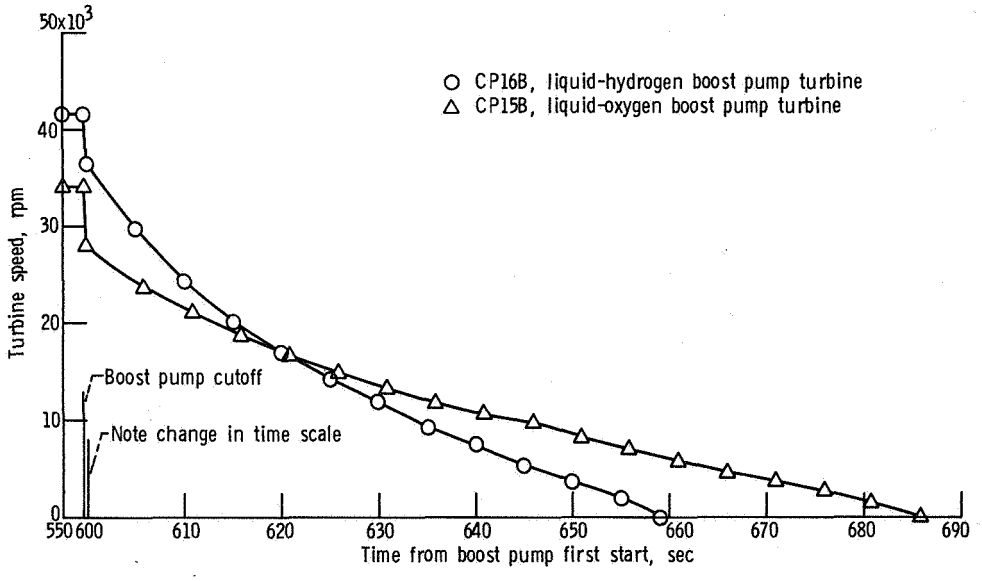

Figure VI-10. - Boost pump turbine speed from 550 to 690 seconds after boost pump first start, AC-17.

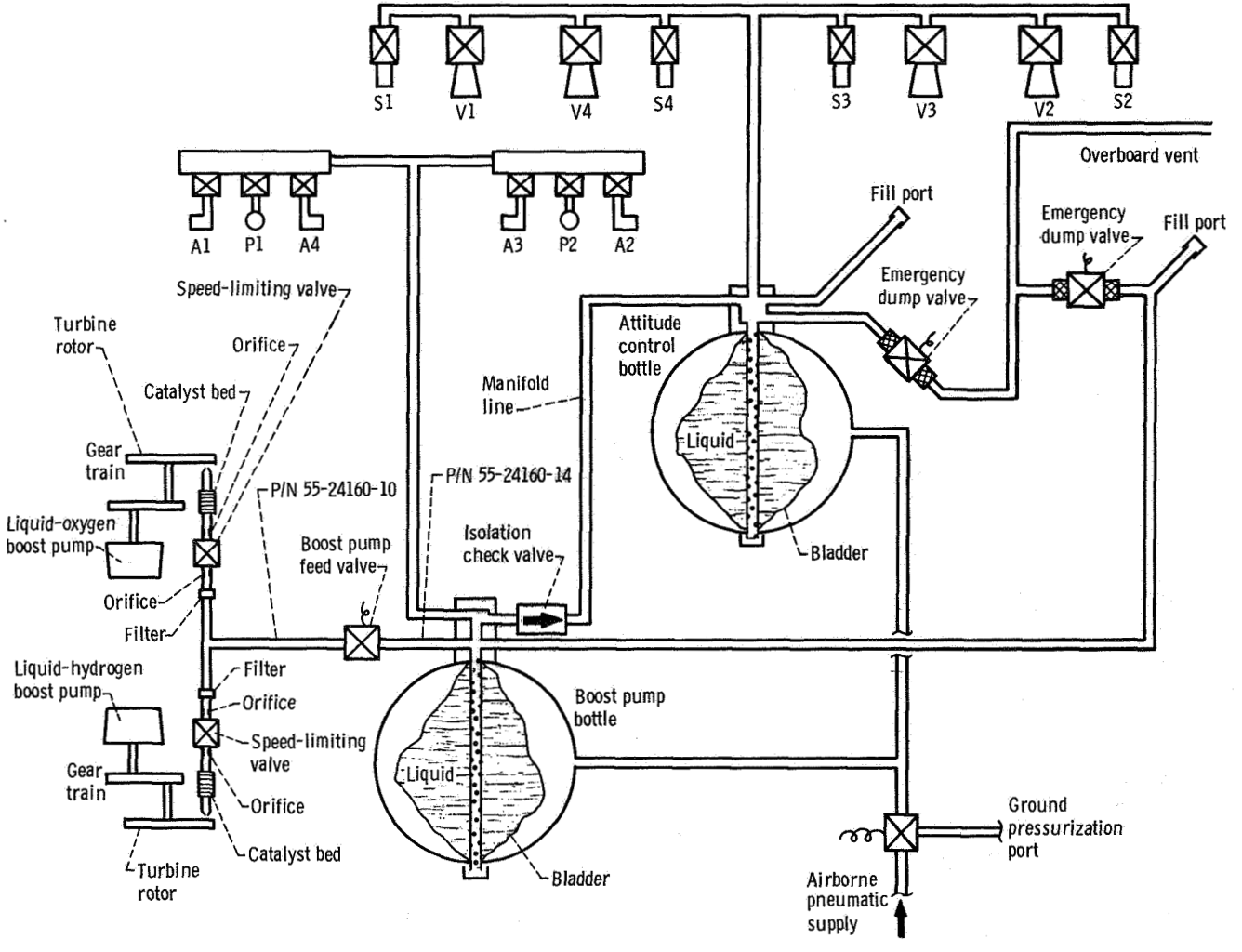

Figure VI-11. - Centaur hydrogen peroxide engine and boost pump system, AC-17.

Engine designation	Thrust	
	N	lbf
V1, V2, V3, V4	222	50
S1, S2, S3, S4	13	3
A1, A2, A3, A4	16	3.5
P1, P2	27	6

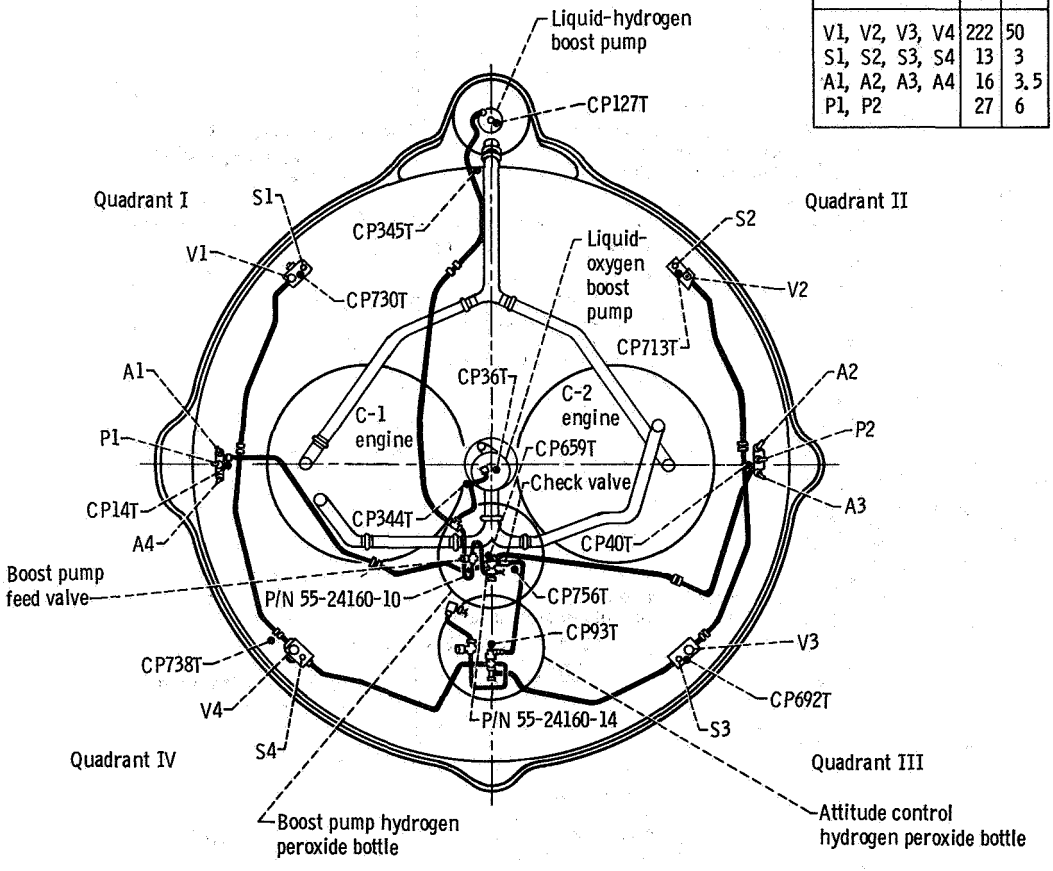

Figure VI-12. - Centaur hydrogen peroxide system, AC-17.

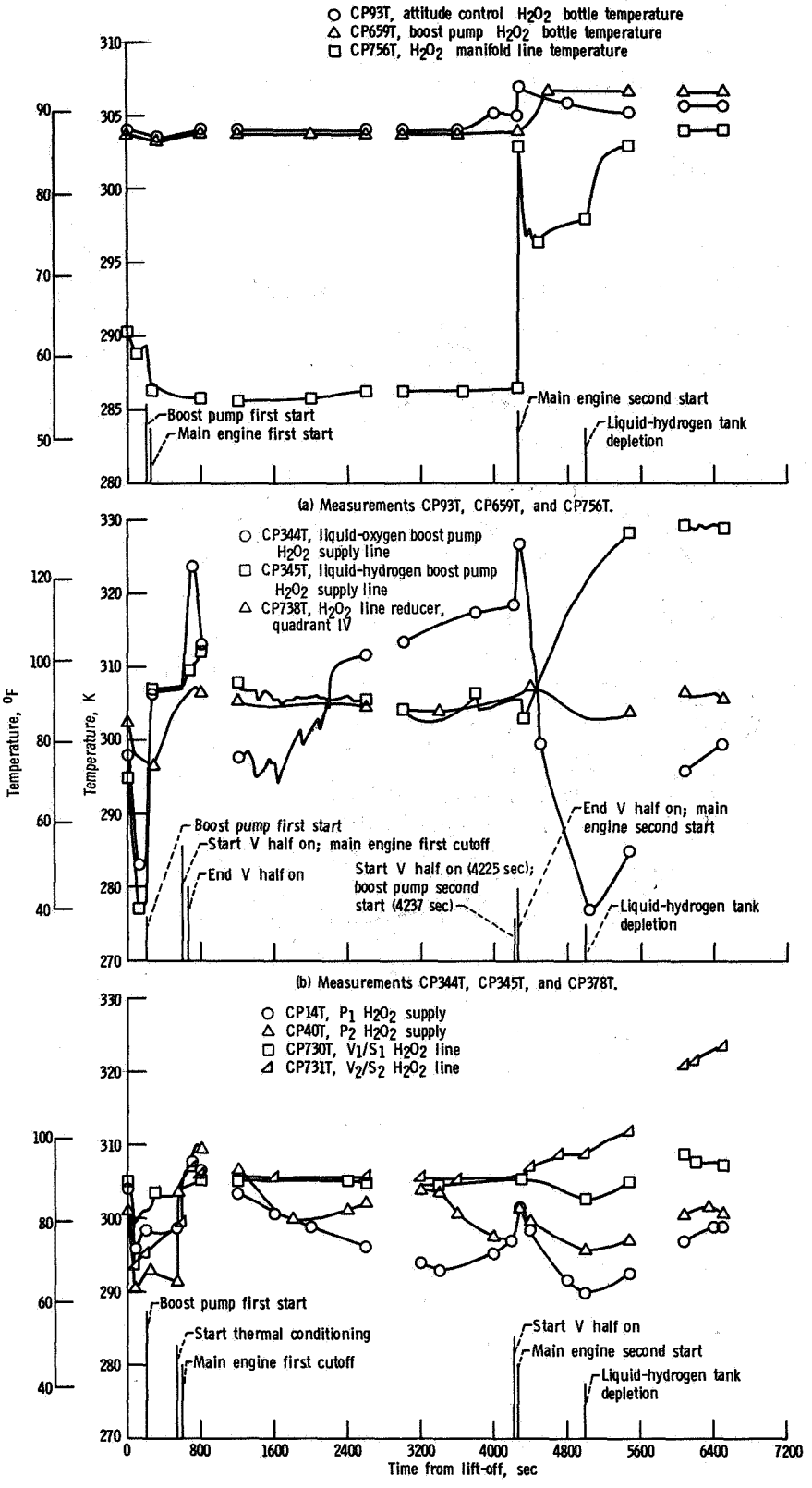

Figure VI-13. - Hydrogen peroxide system temperatures, AC-17.

PROPELLANT LOADING AND PROPELLANT UTILIZATION SYSTEMS

by Richard C. Kalo and Clifford H. Arth

Level Indicating System for Propellant Loading

System description. - The Atlas propellant level indicating system (fig. VI-14) consists of a portable sight gage assembly for RP-1 fuel (kerosene) loading and platinum hot-wire-type sensors for oxidizer (liquid oxygen) loading.

The fuel (RP-1) loading levels are determined by visual observation of the sight gage assembly which is connected to the fuel probe by two temporary sense lines. After tanking, the fuel sight gage assembly and sense lines are removed and the connection points on the vehicle are secured for flight.

The liquid-oxygen loading levels are determined from liquid sensors located at discrete points in the oxidizer (liquid oxygen) tank. The sensing elements are the hot-wire type made with platinum wire (0.025 cm (0.001 in.) which has a linear resistive temperature coefficient. The sensors are supplied with a near-constant current of approximately 200 milliamperes; the voltage drop across a sensor reflects the resistance value of the sensor. When immersed in a cryogenic fluid (covered), it has a low resistance and low voltage drop. When uncovered, the sensor has a higher resistance and therefore a high voltage drop.

The control unit with electronic trigger circuits and control relays supplies a signal to the propellant loading operator. These control relays are activated or deactivated by the voltage level at each sensor (i.e., covered or uncovered).

The Centaur propellant level indicating system (fig. VI-15) utilizes platinum hot-wire level sensors in both the liquid-oxygen and liquid-hydrogen tanks. This sensor system operates identically to those used in the Atlas liquid-oxygen tank.

System performance. - Atlas and Centaur propellant loading was satisfactorily accomplished. The weight of the Atlas fuel (RP-1) tanked was calculated by using a density of 0.8 gram per cubic centimeter (49 lb/ft^3). The weight of the liquid oxygen tanked in the Atlas was calculated by using a density of 1.1 grams per cubic centimeter (69.29 lb/ft^3). Centaur propellant weights were calculated by using a density of 0.06 gram per cubic centimeter (4.2 lb/ft^3) for liquid hydrogen and a density of 1.09 grams per cubic centimeter (68.6 lb/ft^3) for liquid oxygen. These calculated values are

Atlas propellant weight tanked, kg (lbm):

Fuel (RP-1)	38 011 (83 800)
Oxidizer (liquid oxygen)	85 584 (188 680)

Centaur propellant weight at lift-off, kg (lbm):

Fuel (liquid hydrogen)	2377 (5241)
Oxidizer (liquid oxygen)	11 556 (25 476)

Atlas Propellant Utilization System

System description. - The Atlas propellant utilization system (fig. VI-16) consists of two mercury manometer assemblies, a computer-comparator, a hydraulically actuated propellant utilization fuel valve, sense lines, and associated electrical harnessing. The system is used to ensure near-simultaneous depletion of the propellants and minimum propellant residuals at sustainer engine cutoff. This is accomplished by controlling the propellant mixture ratio (oxidizer flow rate/fuel flow rate) to the sustainer engine. During flight, the manometers sense propellant head pressures which are indicative of propellant mass. The mass ratio is then compared to a reference ratio (at lift-off the ratio is 2.27) in the computer-comparator. If needed, a correction signal is sent to the propellant utilization valve controlling the main fuel flow to the sustainer engine. The oxidizer flow is regulated by the head suppression valve. This valve senses propellant utilization valve movement and moves in a direction opposite to that of the propellant utilization valve. This opposite movement thus alters propellant mixture ratio to maintain constant propellant mass flow to the engine. The propellant utilization valve operates at null position for the first 13 seconds of flight to prevent oscillations of the valve during lift-off.

System performance. - The Atlas propellant utilization system operated satisfactorily. The propellant utilization system valves angles are shown in figure VI-17. During the flight the valve was in the fuel-rich position from T + 13 seconds to approximately T + 200 seconds, then operated alternately in the oxygen- and fuel-rich positions until T + 230 seconds, when the valve was commanded to the oxygen-rich stop to ensure liquid-oxygen depletion at sustainer engine cutoff.

The predicted and actual residual propellant weights above the pump inlets at the time of sustainer engine cutoff are shown in the following table:

Atlas propellant residuals	Units	Predicted	Actual
Fuel (RP-1)	kg	101	125
	lbm	223	276
Liquid oxygen	kg	141	220
	lbm	311	487

These residuals were calculated by using the time from when the head sensing port uncovers to sustainer engine cutoff and a flow rate. The flow rate used accounts for the decay typical of a liquid-oxygen depletion.

Centaur Propellant Utilization System

System description. - The Centaur propellant utilization (PU) system (fig. VI-18) is used during flight to control the ratio of propellants consumed by the main engines and to assure minimum propellant residuals. The probes (sensors) of the PU system are also used during tanking to indicate propellant levels within the range of these probes. In flight, the mass of propellant in each tank is sensed by a capacitance probe and compared in a bridge balancing circuit. If the mass ratio of propellants in the tanks varies from the predetermined value (5:1 oxidizer to fuel), an error signal is sent to the proportional servopositioners which control the liquid-oxygen flow control valves (one on each engine). When the mass ratio is greater than 5:1, the liquid-oxygen flow is increased to return the ratio to 5:1. When the ratio is less than 5:1, the liquid-oxygen flow is decreased. The sensing probes do not extend to the top of the tanks, and therefore are not used for control until after the probes are uncovered at approximately 90 seconds after Centaur main engine first start. For this 90 seconds, the liquid-oxygen flow control valves are maintained at approximately 5:1 propellant mixture ratio. The valves are also commanded to the null position at approximately a 5:1 propellant mixture ratio 27 seconds before Centaur main engine second cutoff. This is done because the probes do not extend to the bottom of the tanks, and system control is lost when the liquid level depletes below the bottom of the probes.

System performance. - The Centaur propellant utilization system operated satisfactorily. The liquid-oxygen valve angles during flight are shown in figure VI-19. System control was enabled by the vehicle programmer at 89.6 seconds prior to main engine first start. The valves at this time moved to the liquid-oxygen-rich stop, reaching the stop by 93.5 seconds prior to main engine first start. They remained on the stop for approximately 71 seconds. During this time the system corrected for 206.6 kilograms (456 lbm) of excess liquid oxygen. This correction consisted of

(1) Engine consumption rate error accumulated during the first 90 seconds of engine firing

(2) Propellant loading error

(3) System bias to ensure liquid-oxygen depletion

(4) System bias to compensate for differential propellant boiloff during coast

The liquid-oxygen level passed the top of the probe at 95 seconds after main engine first start. The liquid-hydrogen probe uncovered 7.5 seconds later.

The Centaur propellant residuals at main engine first cutoff were as follows:

Centaur propellant residuals	Units	Actual
Fuel (liquid hydrogen)	kg lbm	643 1417
Oxidizer (liquid oxygen)	kg lbm	2966 6540

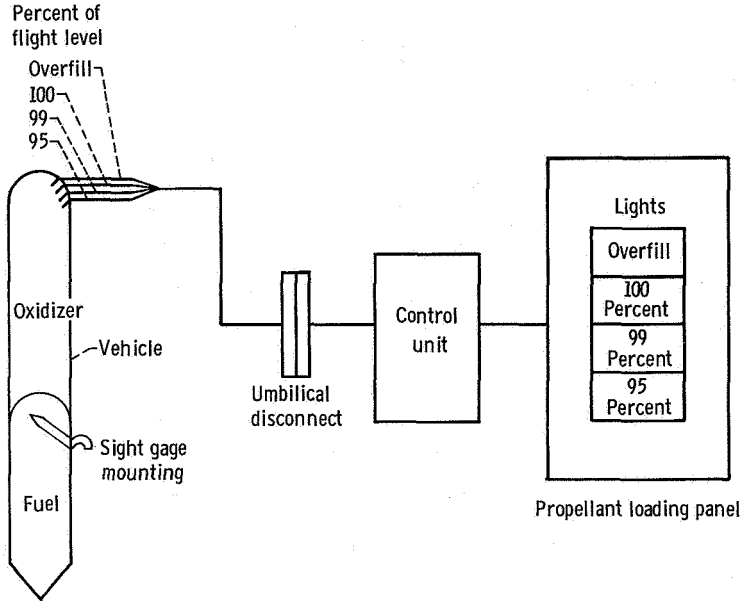

Figure VI-14. - Propellant level indicating system for Atlas propellant loading, AC-17.

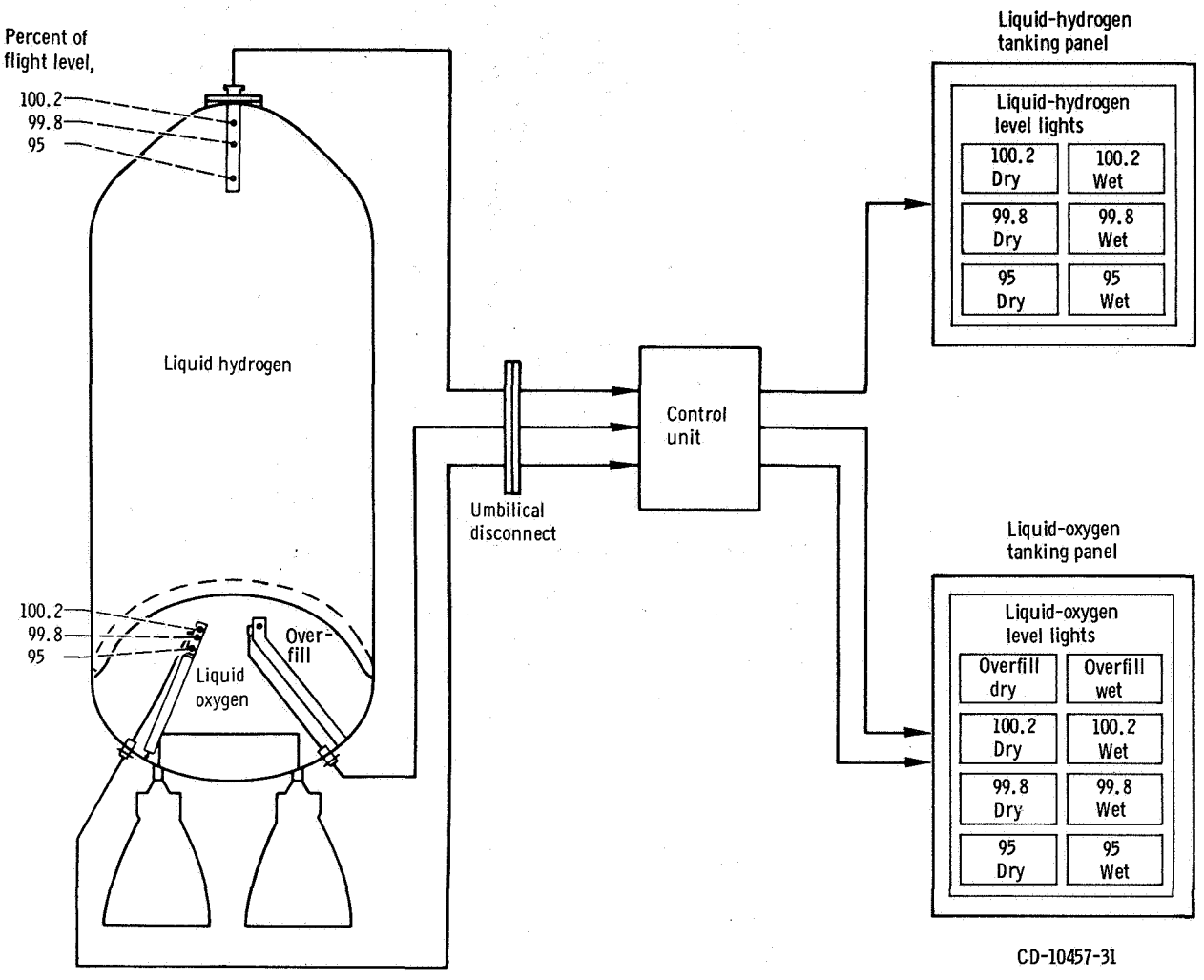

Figure VI-15. - Propellant level indicating system for Centaur propellant loading, AC-17.

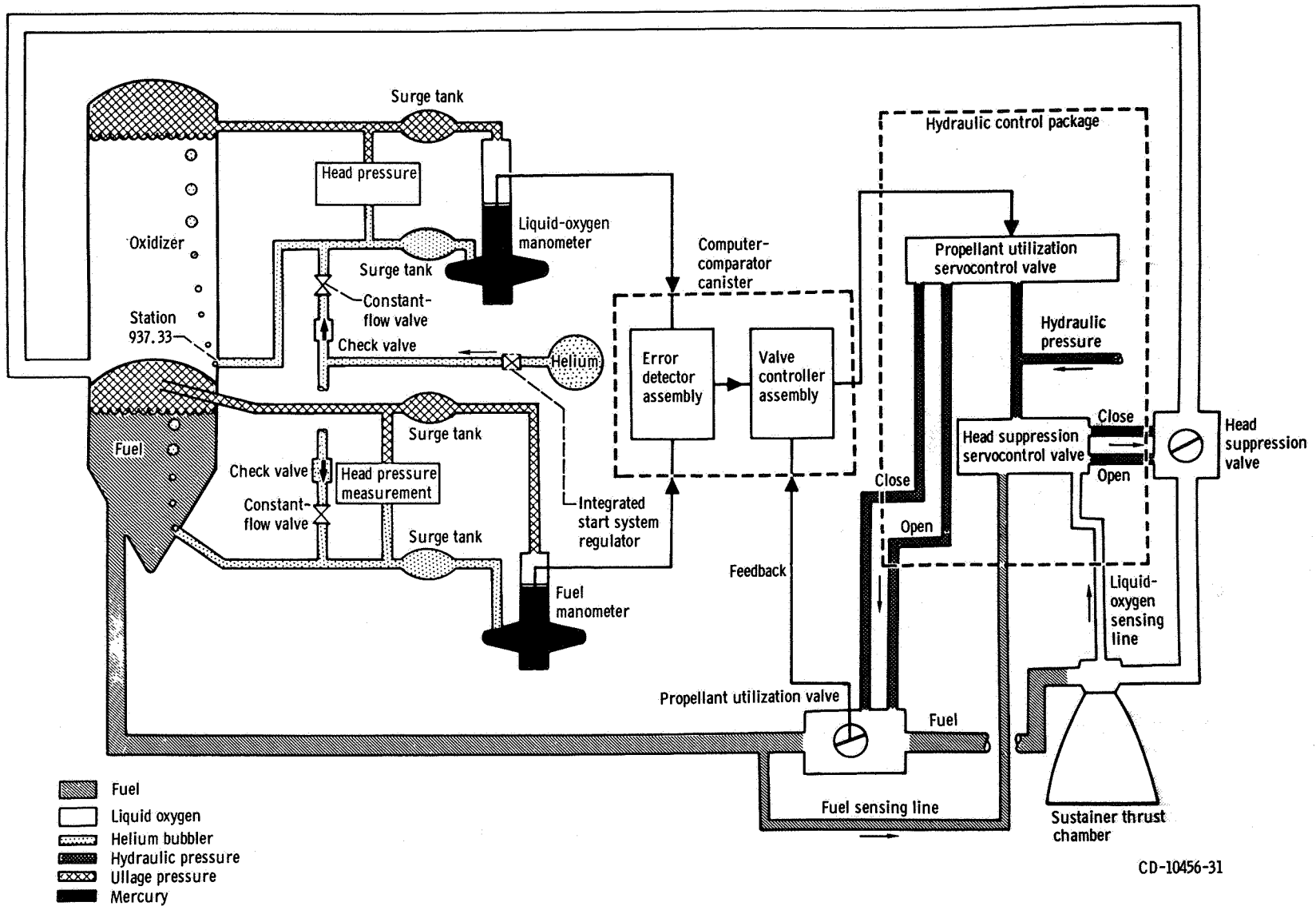

Figure VI-16. - Atlas propellant utilization system, AC-17.

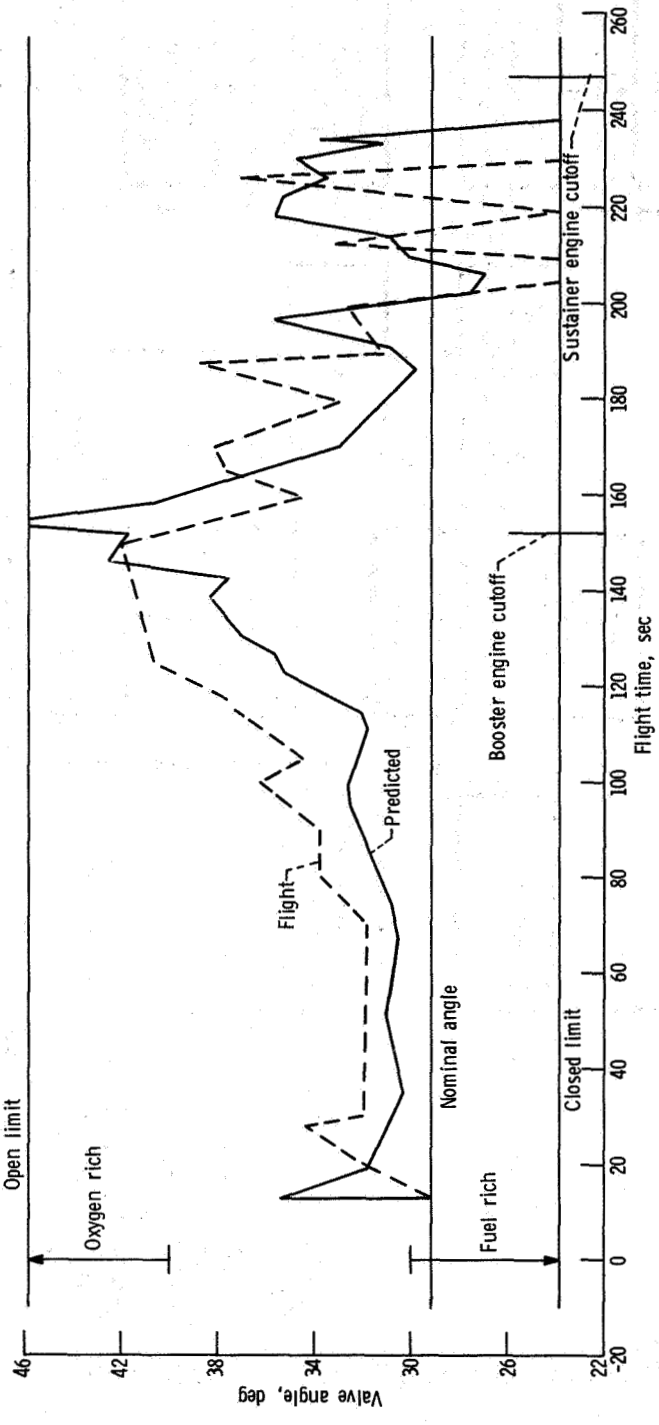

Figure VI-17. - Atlas propellant utilization valve angle prediction and flight data, AC-17.

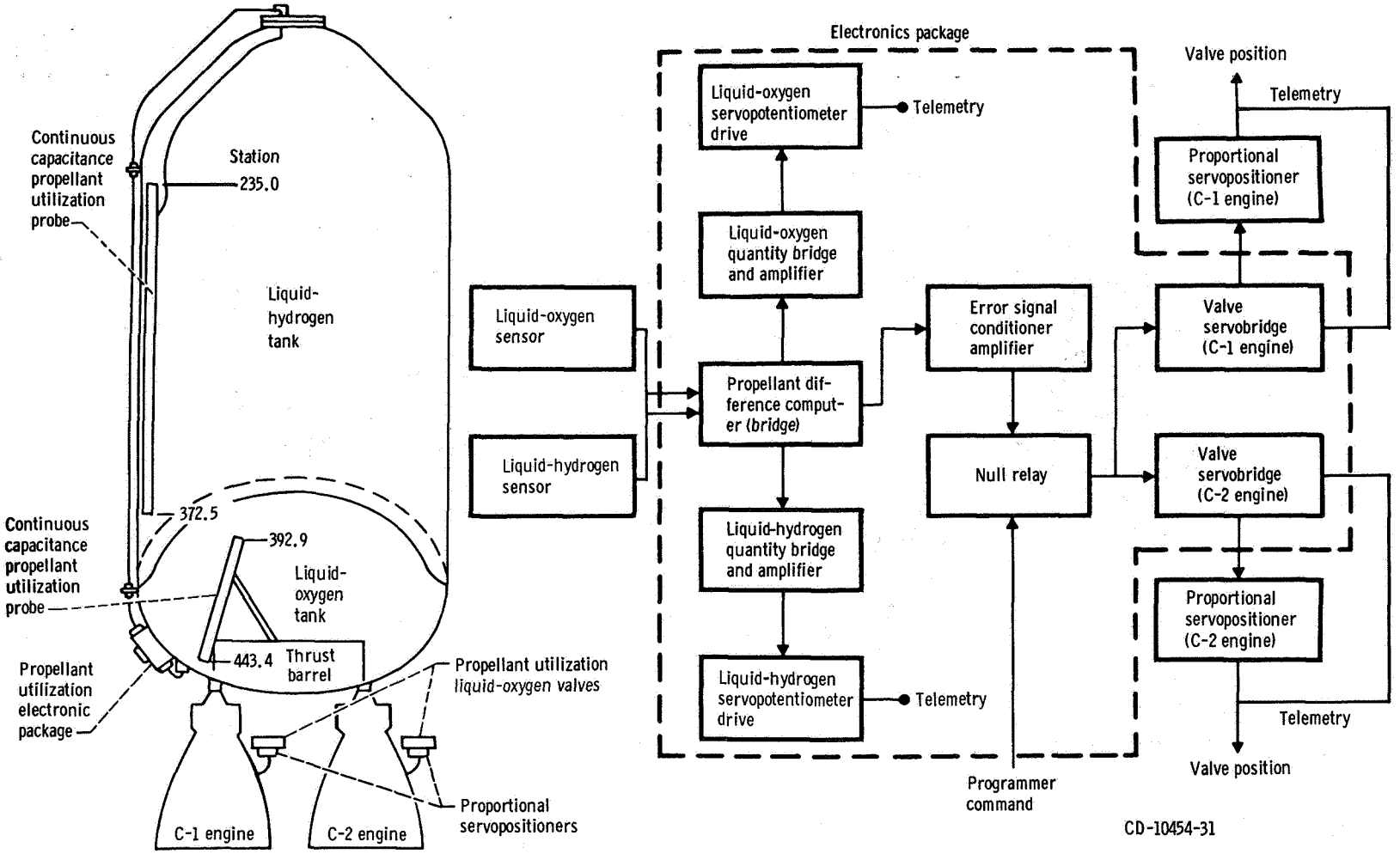

Figure VI-18. - Centaur propellant utilization system, AC-17.

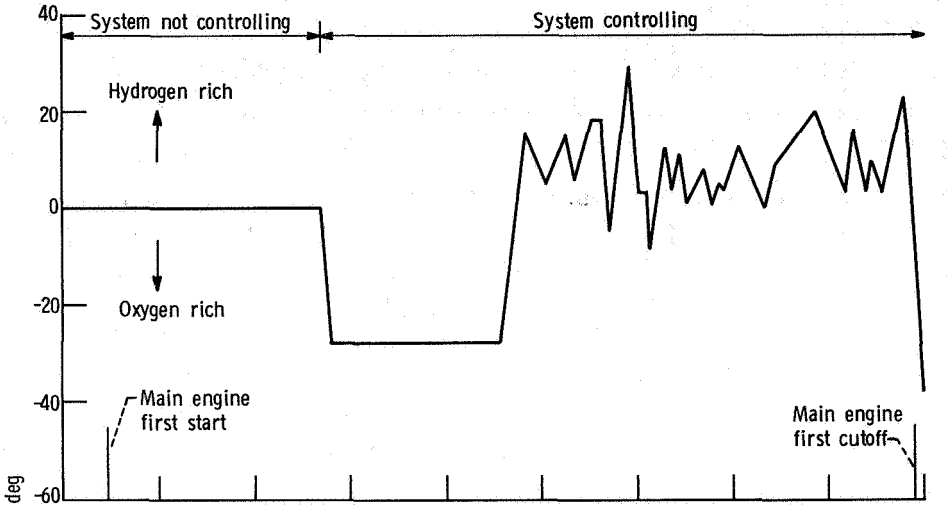

(a) C-1 engine.

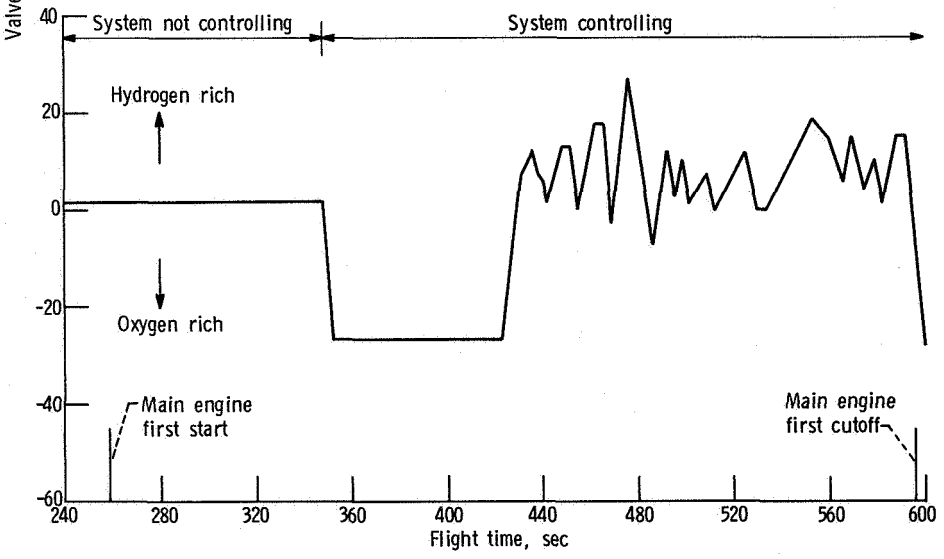

(b) C-2 engine.

Figure VI-19. - Centaur propellant utilization valve angle, AC-17.

PNEUMATIC SYSTEMS

by Eugene J. Fourney and Richard W. Heath

Atlas

System description. - The Atlas pneumatic system supplies helium gas for tank pressurization and for various vehicle control functions. The system is comprised of three independent subsystems: propellant tank pressurization, engine control, and booster section jettison. This system schematic is shown in figure VI-20.

Propellant tank pressurization subsystem: This subsystem uses helium gas to maintain propellant tank pressures at required levels to support the pressure-stabilized tank structure and to satisfy the inlet pressure requirements of the engine turbopumps. In addition, helium is supplied from the fuel tank pressurization line to pressurize the hydraulic reservoirs and turbopump lubricant storage tanks. The subsystem consists of eight shrouded helium storage bottles, a heat exchanger, and fuel and oxidizer tank pressure regulators and relief valves.

The eight shrouded helium storage bottles with a total capacity of 967 000 cubic centimeters (59 000 cu in.) are mounted in the jettisonable booster engine section. The bottle shrouds are filled with liquid nitrogen during prelaunch operations to chill the helium in order to provide a maximum storage capacity at a pressure of 2373 N/cm^2 (3400 psia). The liquid nitrogen drains from the shrouds at lift-off. During flight the cold helium passes through a heat exchanger located in the booster engine turbine exhaust duct and is heated before being supplied to the tank pressure regulators. The pressurization control of the propellant tank pressurization subsystem is switched from the ground to the airborne system at about T - 60 seconds. Airborne regulators are set to control fuel tank gage pressure between 44.1 and 46.2 N/cm^2 (64 and 67 psi) and the oxidizer tank pressure between 19.58 and 24.13 N/cm^2 (28.4 and 35.0 psi). From approximately T - 60 seconds to T + 20 seconds the liquid-oxygen regulator sense line is biased by a helium "bleed" flow into the liquid-oxygen tank regulator sensing line which senses ullage pressure. The bias causes the regulator to control tank pressure at a lower level than the normal regulator setting. Depressing the liquid-oxygen tank pressure increases the differential pressure across the bulkhead between the propellant tanks. The increased differential pressure counteracts the launch transient loads that act in a direction to cause bulkhead reversal. At T + 20 seconds the bias is removed by closing an explosively actuated valve and the ullage pressure in the liquid-oxygen tank increases to the normal regulator control range. The increased pressure then provides sufficient vehicle structural stiffness to withstand bending loads during the remainder of the ascent.

Pneumatic regulation of tank pressure is terminated at booster engine section jettison. Thereafter the fuel tank pressure decays slowly, but the oxidizer tank pressure is augmented by liquid-oxygen boiloff.

Engine controls subsystem: This subsystem supplies helium pressure for actuation of engine control valves, for pressurization of the engine start tanks, for purging booster engine turbopump seals, and for the reference pressure to the regulators which control oxidizer flow to the gas generator. Control pressure in the system is maintained through Atlas/Centaur separation. The pneumatic requirements are supplied from a 76 000-cubic-centimeter (4650-cu-in.) helium storage bottle pressurized to a gage pressure of about 2342.6 N/cm^2 (3400 psi) at lift-off.

Booster engine jettison subsystem: This subsystem supplies pressure for release of the pneumatic staging latches to separate the booster engine section. A command from the Atlas flight control system opens two explosively actuated valves to supply helium pressure to 10 piston-operated staging latches. Helium for the system is supplied by a single 14 260-cubic-centimeter (870-cu-in.) bottle charged to a gage pressure of 2342.6 N/cm^2 (3400 psi).

System performance. - The Atlas pneumatic system performance was satisfactory throughout the AC-17 flight. Pneumatic system performance during flight is shown in table VI-5. The individual subsystem performance during flight was as follows:

Propellant tank pressurization subsystem: Control of propellant tank pressures was switched from the ground Pressurization Control Unit (PCU) to the airborne regulators at approximately T - 62 seconds. Ullage pressures were properly controlled throughout the flight.

The fuel tank pressure regulator controlled at a gage pressure of about 44.7 N/cm^2 (64.7 psi) until termination of pneumatic control at booster engine section jettison. During the sustainer phase the fuel tank pressure decreased normally, and was 36.19 N/cm^2 (52.49 psi) at sustainer engine cutoff (SECO).

The oxidizer tank ullage pressure was steady at 21.34 N/cm^2 (30.95 psi) after switching from the PCU to "pneumatics internal" at approximately T - 62 seconds. The pressure decreased to 20.10 N/cm^2 (29.15 psi) at engine start and increased slightly until T + 20 seconds. At T + 20 seconds the oxidizer ullage tank pressure was 20.37 N/cm^2 (29.55 psi). At this time the regulator sense line bias was terminated, and pneumatic regulation increased the ullage pressure to 23.10 N/cm^2 (33.5 psi). It required 3 seconds for the ullage pressure to stabilize. The liquid-oxygen tank pressure remained within the required limits until termination of pneumatic regulation at booster staging. After booster engine section jettison the ullage pressure decreased from 22.75 N/cm^2 (32.95 psi) to 21.92 N/cm^2 (31.79 psi) by the time SECO occurred.

Engine control subsystem: The booster and sustainer engine control regulators provided the required helium pressure for engine control throughout the flight.

Booster engine section jettison subsystem: Subsystem performance was satisfactory. The explosively actuated valve was opened on command, allowing high-pressure helium to actuate the 10 booster staging latches.

Centaur

System description. - The Centaur pneumatic system (fig. VI-21) consists of five subsystems: propellant tank venting, propellant tank pressurization, propulsion pneumatics, helium purge pneumatics, and nose fairing pneumatics.

Propellant tank venting subsystem: The structural stability of the propellant tanks is maintained throughout the flight by the propellant boiloff gas pressures. These pressures are controlled by a vent system on each propellant tank. The hydrogen tank vent system is comprised of two pilot-controlled, pressure-actuated vent valves and ducting. The hydrogen primary vent valve is fitted with a solenoid valve which locks the vent valve, preventing its opening. The hydrogen secondary vent valve does not have the control solenoid. The relief range of the secondary valve is 17.1 to 18.5 N/cm^2 (24.8 to 26.8 psia) and is above that of the primary valve, which is 13.1 to 14.8 N/cm^2 (19 to 21.5 psia). This prevents overpressurization of the hydrogen tank when the primary vent valve is locked. The vented hydrogen gas is ducted overboard through a single vent in the nose fairing. After fairing jettison the gas is vented overboard through two opposed nozzles so as to produce no thrust. The oxygen tank vent system uses a single vent valve which is fitted with the control solenoid valve. Its operating range is 20 to 22 N/cm^2 (29 to 32 psia). The vented oxygen gas is ducted overboard through the interstage adapter. The duct, which remains with the Centaur after separation from the interstage adapter, is oriented to aline the venting thrust vector with the vehicle center of gravity.

The vent valves are commanded to the locked mode at specific times (1) to permit the hydrogen tank pressure to increase during the atmospheric ascent to satisfy the structural requirements of the pressure-stabilized tank, (2) to permit controlled pressure increases in the tanks to satisfy the boost pump pressure requirements, (3) to restrict oxygen venting during nonpowered flight to avoid vehicle disturbing torques, and (4) to restrict hydrogen venting to nonhazardous times. (A fire could conceivably occur during the early part of the atmospheric ascent if a plume of vented hydrogen "washes" back over the vehicle and is exposed to an ignition source. A similar hazard could occur at Atlas booster engine staging when residual oxygen envelopes a large portion of the vehicle.)

Propellant tank pressurization subsystem: The propellant tank pressurization subsystem supplies helium gas in controlled quantities for in-flight pressurization in addition to that provided by the propellant boiloff gases. It consists of a normally closed solenoid valve and orifice for each propellant tank and a pressure switch assembly which

senses oxygen tank pressure. The solenoid valves and orifices provide a metered flow of helium to both propellant tanks, for step pressurization during the main engine start sequence, and to the oxygen tank at main engine cutoff. The pressure sensing switch controls the pressurization of the oxygen tank during the main engine start sequence.

Propulsion pneumatic subsystem: The propulsion pneumatic subsystem supplies helium gas at regulated pressures for actuation of main engine control valves and pressurization of the hydrogen peroxide storage bottle. It consists of two pressure regulators, which are referenced to ambient pressure, and two relief valves. Pneumatic pressure supplied through the engine controls regulator is used for actuation of the engine inlet valves, the engine chilldown valves, and the main fuel shutoff valve. The hydrogen peroxide pressure regulator, located downstream of the engine controls regulator, further reduces the pressure to provide expulsion pressurization for the hydrogen peroxide storage bottle and the boost pump feedline purge. The boost pump feedline purge was used for the first time on this flight. A relief valve is located downstream of each regulator to prevent overpressurization.

Helium purge pneumatic subsystem: A ground/airborne helium purge subsystem is used to prevent cryopumping and icing under the insulation panels and in propulsion system components. A common airborne distribution system is used for prelaunch purging from a ground helium source and in-flight purging from an airborne helium storage bottle. This subsystem distributes helium gas for purging the cavity between the hydrogen tank and the insulation panels, the seal between the cylindrical section of the nose fairing and the forward bulkhead, the propellant feedlines, the boost pumps, the ducts for the engine chilldown vents, the engine thrust chambers, and the hydraulic power packages. The umbilical connection for charging the airborne bottle could also be used to supply the purge from the ground source should an abort occur after disconnection of the ground purge supply line.

Nose fairing pneumatic subsystem: The nose fairing pneumatic subsystem provides the thrust required to jettison the nose fairing. It consists of a nitrogen storage bottle and an explosive actuated valve with an integral thruster nozzle in each fairing half. Release of the gas through the nozzles provides the necessary thrust to propel the fairing halves away from each other and from the vehicle.

System performance. - The performance of the Centaur pneumatic system was satisfactory. The individual subsystem performance during flight was as follows:

Propellant tank pressurization and venting subsystems: The ullage pressures in the hydrogen and oxygen tanks during the flight are shown in figure VI-22. The hydrogen tank absolute pressure was 15.1 N/cm^2 (21.9 psi) at T - 7.5 seconds, when the primary hydrogen vent valve was locked. After vent valve lockup the tank absolute pressure increased, at an average rate of 2.40 N/cm^2/minute (3.48 psi/min), to 18.2 N/cm^2 (26.4 psi) at T + 70 seconds. At this time the secondary vent valve relieved and

regulated tank pressure until T + 90 seconds, when the primary vent valve was enabled. The tank pressure was then reduced and was regulated by the primary vent valve.

At T + 152 seconds the primary hydrogen vent valve was locked and remained locked for 8.0 seconds during Atlas booster engine section jettison. Following booster engine section jettison the primary vent valve was enabled and allowed to regulate tank pressure. At T + 247 seconds the primary hydrogen vent valve was again locked, and the tank was pressurized with helium for 1 second. The tank absolute pressure increased from 14.3 N/cm^2 to 15.8 N/cm^2 (20.8 psi to 22.9 psi). The pressure remained at that level until engine prestart (T + 249.7 sec) and then began to decrease. At Centaur main engine first start (T + 257.7 sec) the absolute pressure was 14.5 N/cm^2 (21.0 psi).

The ullage absolute pressure in the oxygen tank was 21.3 N/cm^2 (30.9 psi) at lift-off. After lift-off the increasing vehicle acceleration suppressed the propellant boiling and caused the pressure to decrease. At T + 80 seconds the vent valve reseated and venting ceased. The pressure then varied between the operating limits of the vent valve until Atlas booster engine cutoff. At that time the sudden reduction in the acceleration caused an increase in the liquid-oxygen boiloff and a resulting pressure rise in the tank. As thermal equilibrium was reestablished in the tank, the ullage pressure decreased to 21.3 N/cm^2 (30.9 psi).

At T + 214 seconds the oxygen tank vent valve was locked, and the helium pressurization of the tank began. The tank absolute pressure increased to 27.4 N/cm^2 (39.8 psi), at which pressure the pressurization switch opened and the pressurization was terminated. As the warm helium gas cooled in the tank, the absolute pressure decreased to 26.2 N/cm^2 (38.0 psi), at which pressure the pressure switch closed and additional helium was injected into the tank. After the second cycle, the heat input from the boost pump recirculation flow increased the boiloff and caused the pressure to increase before it reached the lower limit of the pressurization switch again. At engine prestart the absolute pressure was 28.2 N/cm^2 (40.9 psi). After engine prestart the absolute pressure decreased to 26.8 N/cm^2 (38.9 psi) at main engine first start and decreased thereafter to its saturation value of approximately 21.0 N/cm^2 (30.5 psi).

The ullage pressures in both propellant tanks decreased normally during main engine first firing. At engine cutoff the ullage absolute pressures in the hydrogen and oxygen tanks were 11.3 N/cm^2 (16.4 psi) and 18.9 N/cm^2 (27.4 psi), respectively. The primary hydrogen vent valve was enabled after main engine cutoff, while the oxygen tank vent valve remained locked.

During the portion of the coast period from T + 805 to T + 1205 seconds when no telemetry data were available the hydrogen tank pressure increased until it reached the regulating range of the primary vent valve and was regulated by that valve for the duration of the coast period. The oxygen tank ullage absolute pressure increased to 19.9 N/cm^2 (28.9 psi), decreased to 18.6 N/cm^2 (27.0 psi), and then remained essentially constant for the remainder of the coast period.

At T + 4226 seconds the primary hydrogen vent valve was locked, and at the same time helium was injected into both propellant tanks. The step pressurization of the oxygen tank was timed to last 18 seconds. The pressure sensing switch, used prior to the main engine first start, was electrically bypassed. During the 18-second pressurization period, the oxygen tank ullage absolute pressure increased from 18.9 N/cm^2 (27.4 psi) to 20.6 N/cm^2 (29.9 psi). The step pressurization of the hydrogen tank was also a timed function, lasting 40 seconds until the scheduled main engine second start. The absolute pressure increased from 13.2 N/cm^2 (19.2 psi) to 17.3 N/cm^2 (25.1 psi), when the relief setting of the secondary valve was reached. The tank pressure was then regulated by that valve until the scheduled main engine second start.

Propulsion pneumatic subsystem: The engine controls regulator output absolute pressure was 322 N/cm^2 (467 psi) at T - 0. After lift-off the pressure increased to 351 N/cm^2 (509 psi) and then leveled off, indicating relief valve actuation. At boost pump first start the pressure dropped abruptly to 307 N/cm^2 (445 psi) and remained relatively constant thereafter. The hydrogen peroxide bottles pressure regulator output absolute pressure was 222 N/cm^2 (322 psi) at T - 0. After lift-off the absolute pressure decreased with a corresponding decrease in ambient pressure to 211 N/cm^2 (306 psi) and remained relatively constant thereafter.

Helium purge subsystem: The total helium purge flow rate to the vehicle prior to lift-off was 89 kilograms per hour (196 lb/hr). The differential pressure across the insulation panels after hydrogen tanking was 0.18 N/cm^2 (0.26 psi). The minimum allowable differential pressure to prevent air ingestion is 0.02 N/cm^2 (0.03 psi). At T - 12.4 seconds the airborne purge system was activated, and at T - 4 seconds the ground purge was terminated. The helium in the airborne purge bottle was depleted during the booster phase of the flight.

Nose fairing pneumatic subsystem: There is no airborne instrumentation in this system, but proper jettisoning of the nose fairing indicated proper functioning of the nose fairing pneumatic subsystem.

TABLE VI-5. - ATLAS PNEUMATIC SYSTEM PERFORMANCE, AC-17

Performance parameter	Measurement	Units	Design range	Flight values at-						Remarks
				T - 10 sec	T - 0 sec	T + 20 sec	T + 23 sec	Booster engine cutoff	Sustainer and vernier engine cutoff	
Oxidizer tank ullage pressure, gage	AF1P	N/cm^2 psi	(a) (b)	21.34 30.95	20.10 29.15	20.37 29.55 (c)	23.10 33.5 (d)	22.72 32.95 (e)	21.92 31.79	Actual relief valve crack 26.0 N/cm^2 (37.8 psi) at validation
Fuel tank ullage pressure, gage	AF3P	N/cm^2 psi	44.13 to 46.19 64.0 to 67.0	44.4 64.4	44.4 64.4	44.55 64.7	44.61 65.0	44.44 64.45 (e)	36.19 52.49	Actual relief valve crack 48.4 N/cm^2 (70.2 psi) at validation
Intermediate bulkhead differential pressure	AF116P	N/cm^2 psi	0.345 (min.) 0.5 (min.)	13.45 19.5	14.13 20.5	11.72 17.0	8.62 12.5	17.24 25.0	16.07 23.3	
Sustainer controls helium bottle pressure, absolute	AF291P	N/cm^2 psi	2137 (max.) 3100 (max.)	2117 3070	2041 2960	2000 2900	2000 2900	1738 2520	1703 2470	
Booster helium bottle pressure, absolute	AF246P	N/cm^2 psi	2137 (max.) 3100 (max.)	2062 2990	2041 2960	1586 2300	1531 2220	476 690 (e)	-----	
Booster helium bottle temperature	AF247P	K ^oF	139.67 to 160.67 K -299^o to 320^o F (prior to T - 0)	140.17 -319.5	140.17 -319.5	129.07 -330.6	127.67 -332.0	8067 -379.0 (e)	-----	

[a] 19.58 to 22.27 N/cm^2 (28.4 to 32.3 psi) from T - 0 to T + 20 sec.

[b] 22.06 to 24.13 N/cm^2 (32.0 to 35.0 psi) after T + 23 sec.

[c] Signal from programmer to fire programmed pressure valves.

[d] Liquid-oxygen-tank pressure at termination of programmed pressure.

[e] Helium supply bottles jettisoned with booster at BECO + 3 sec.

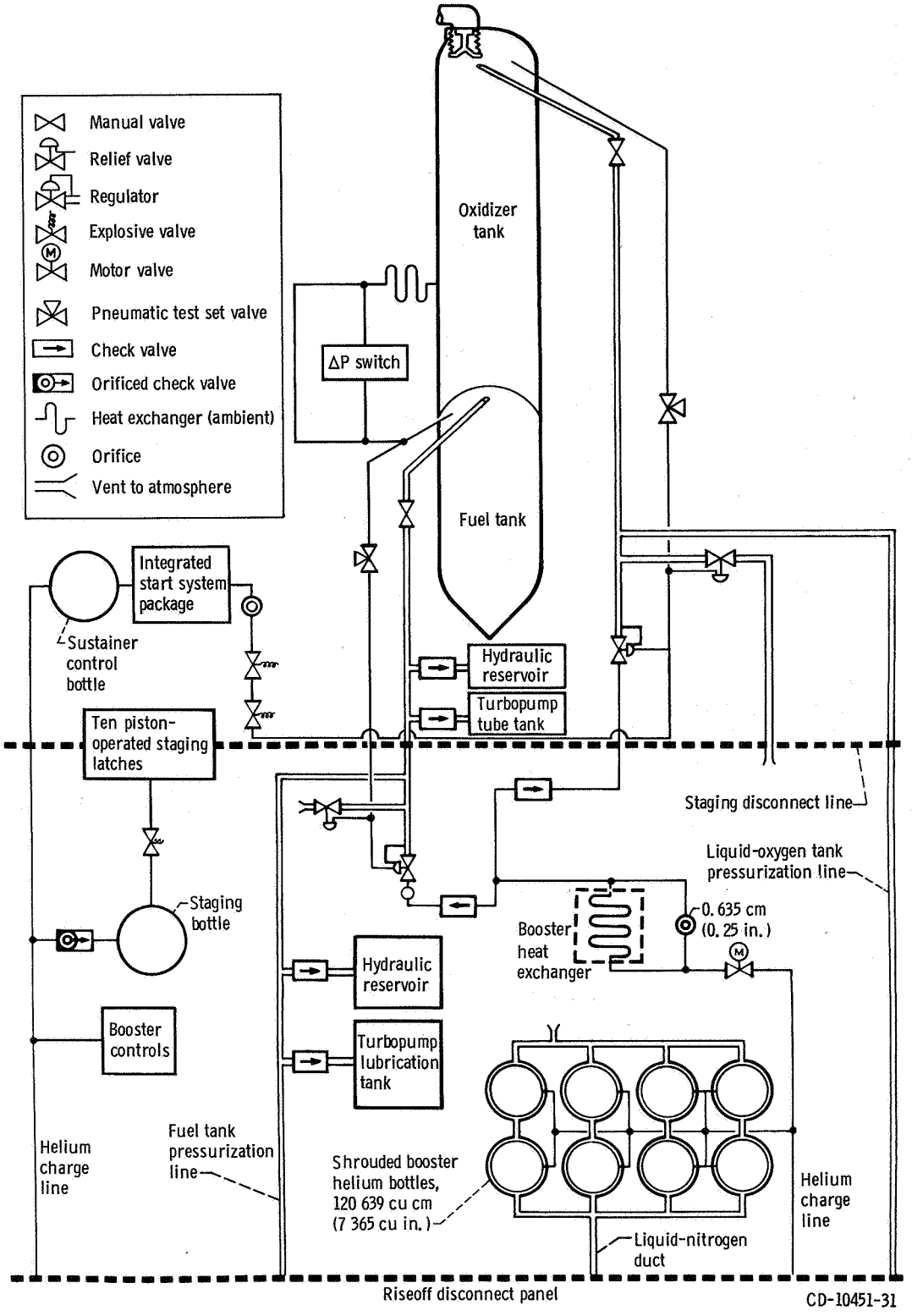

Figure VI-20. - Atlas vehicle pneumatic system, AC-17.

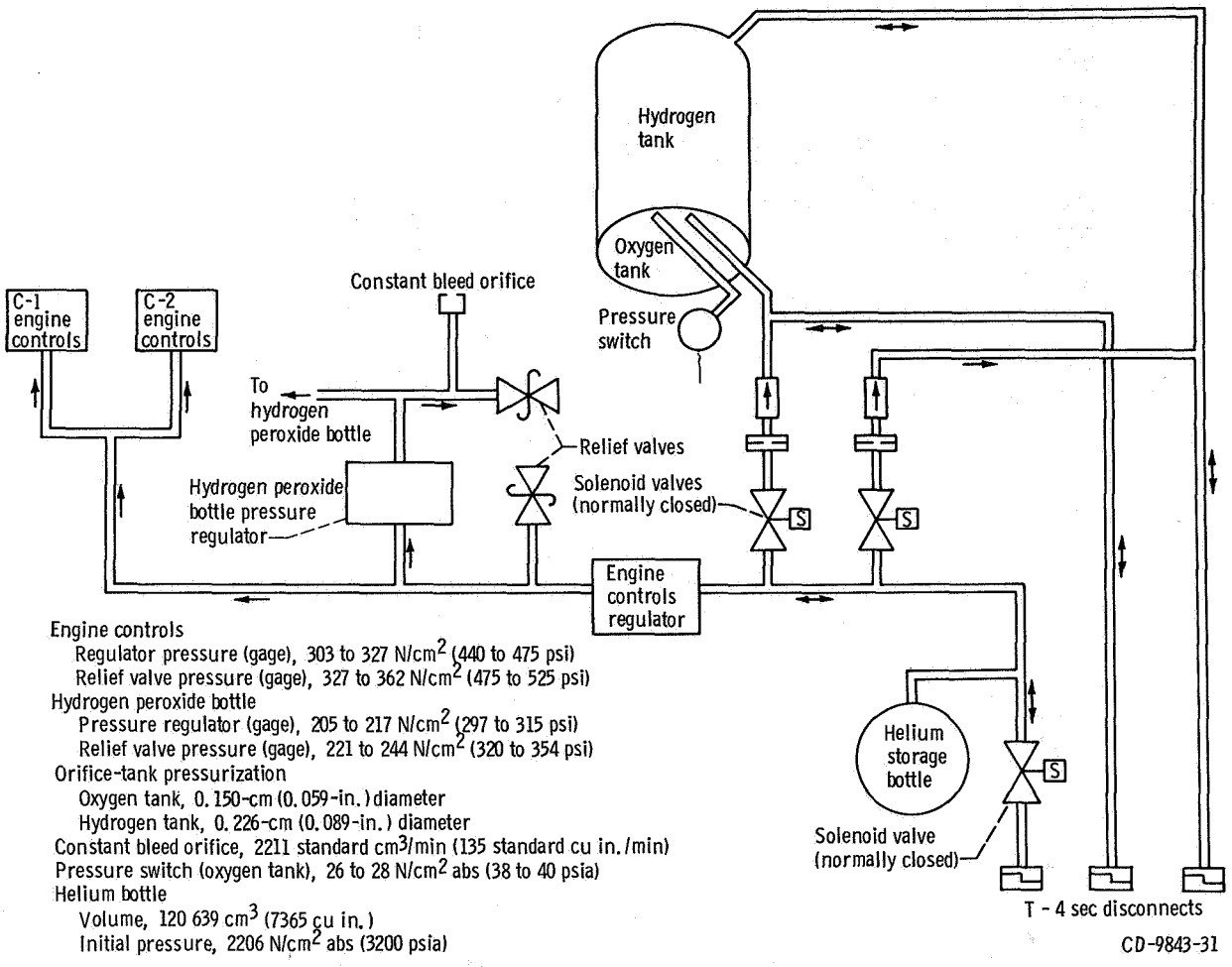

Engine controls
- Regulator pressure (gage), 303 to 327 N/cm^2 (440 to 475 psi)
- Relief valve pressure (gage), 327 to 362 N/cm^2 (475 to 525 psi)

Hydrogen peroxide bottle
- Pressure regulator (gage), 205 to 217 N/cm^2 (297 to 315 psi)
- Relief valve pressure (gage), 221 to 244 N/cm^2 (320 to 354 psi)

Orifice-tank pressurization
- Oxygen tank, 0.150-cm (0.059-in.) diameter
- Hydrogen tank, 0.226-cm (0.089-in.) diameter

Constant bleed orifice, 2211 standard cm^3/min (135 standard cu in./min)

Pressure switch (oxygen tank), 26 to 28 N/cm^2 abs (38 to 40 psia)

Helium bottle
- Volume, 120 639 cm^3 (7365 cu in.)
- Initial pressure, 2206 N/cm^2 abs (3200 psia)

(a) Tank pressurization and propulsion pneumatics subsystems.

Figure VI-21. - Centaur pneumatic system, AC-17.

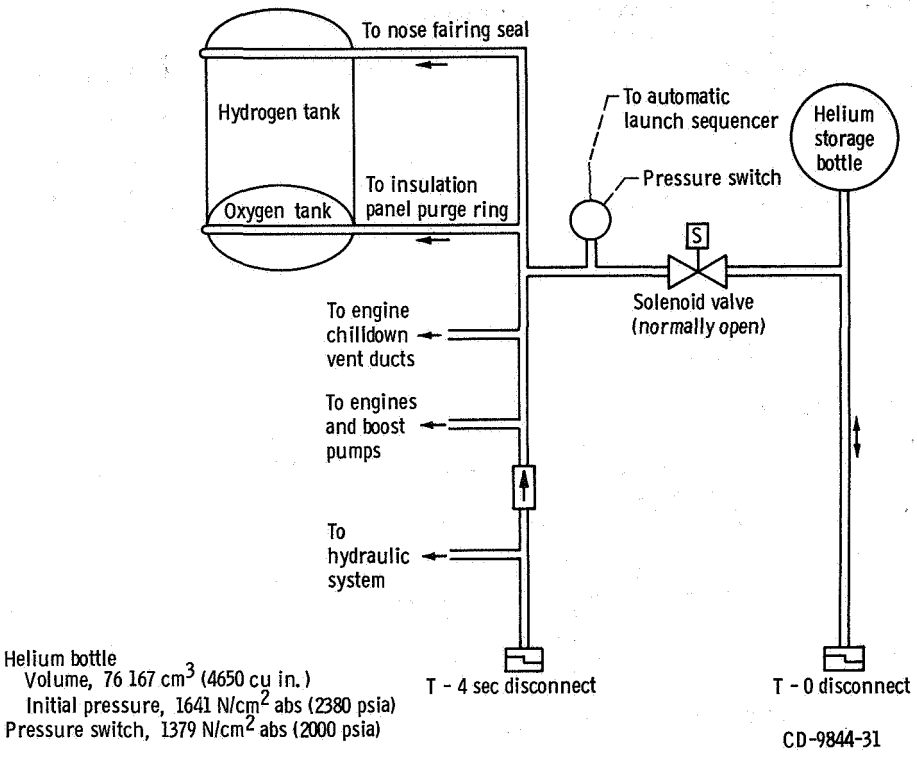

(b) Helium purge subsystem.

Figure VI-21. - Concluded.

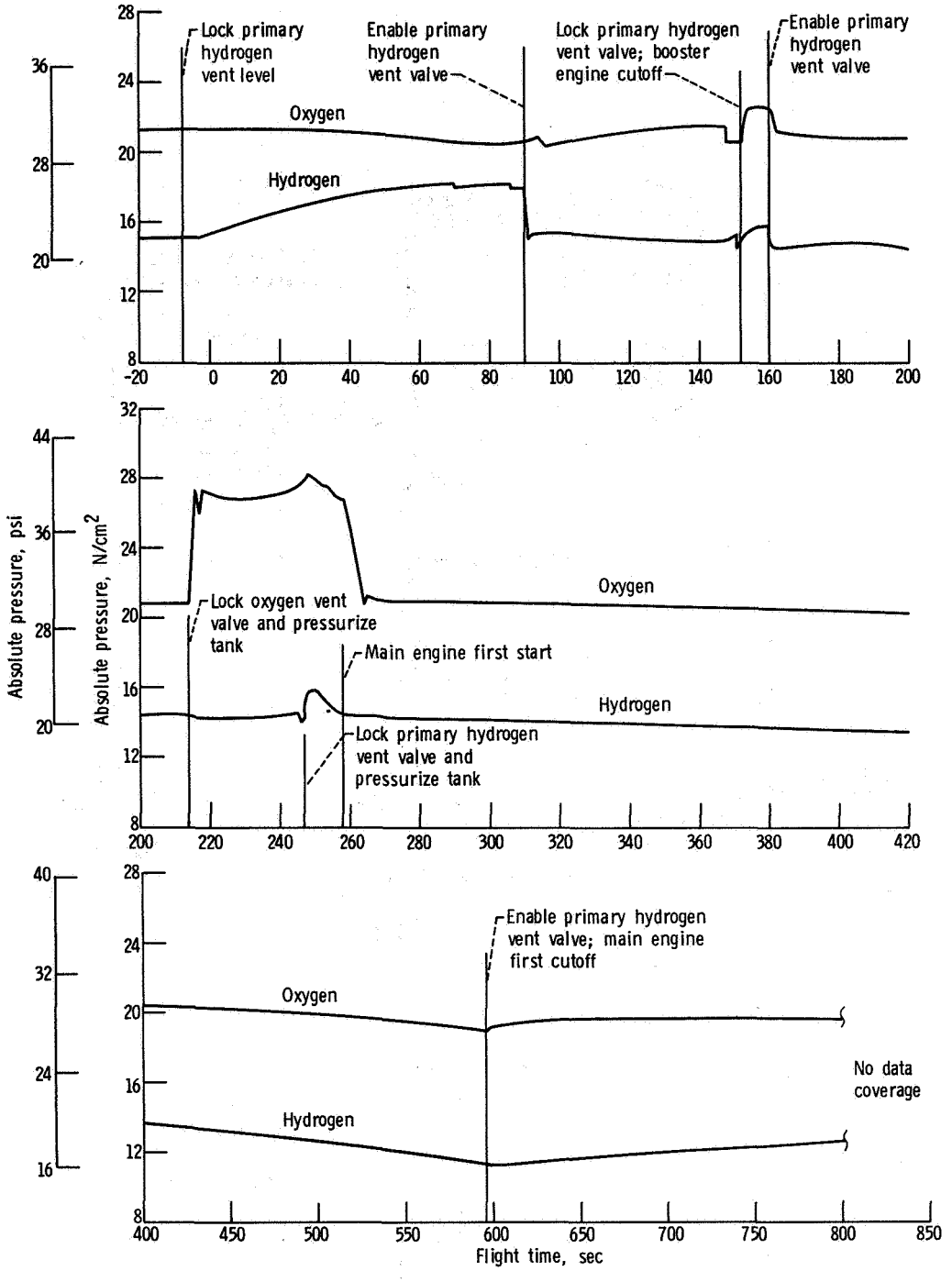

Figure VI-22. - Centaur tank pressure history, AC-17.

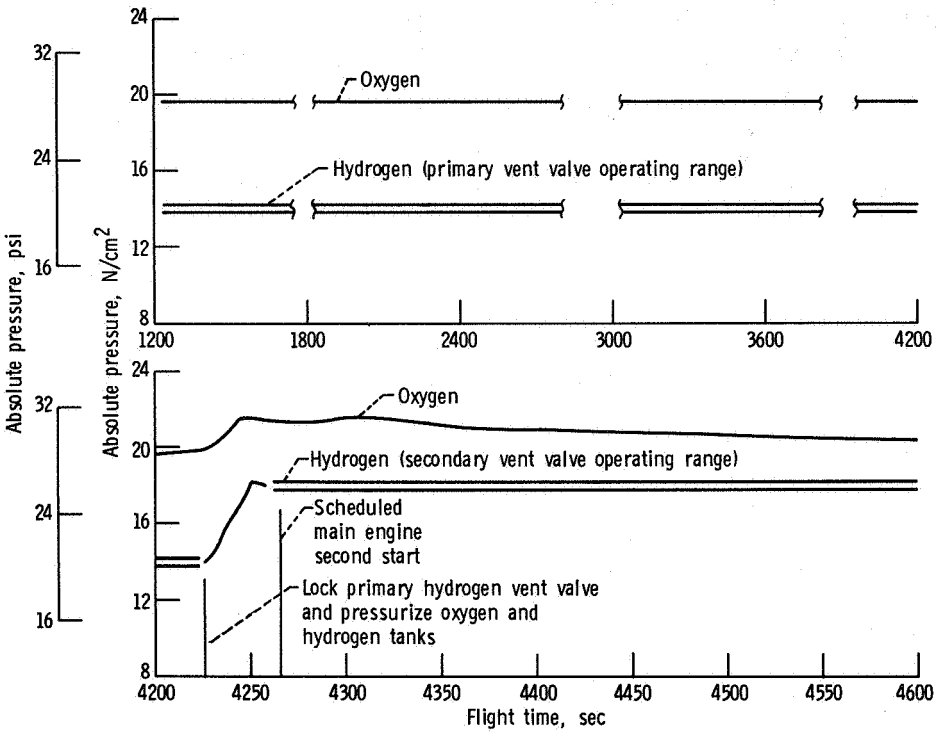

Figure VI-22. - Concluded.

HYDRAULIC SYSTEMS

by Eugene J. Fourney

Atlas

System description. - Two hydraulic systems, as shown in figures VI-23 and VI-24. are used on the Atlas vehicle to supply fluid power for operation of sustainer engine control valves and for thrust vector control of all engines. One system is used for the booster engines and the other for the sustainer and vernier engines.

The booster hydraulic system provided power solely for gimbaling the two booster thrust chambers. System pressure is supplied by a single, pressure-compensated, variable displacement pump driven by the engine turbopump accessory drive. Additional components of the system included four servocylinders, a high-pressure relief valve, two accumulators, and a reservoir. Engine gimbaling in response to flight control commands is accomplished by the servocylinders which provide separate pitch, yaw, and roll control during the booster phase of flight.

The sustainer and vernier hydraulic system is similar to that of the booster in components and to the booster hydraulic system in function. In addition, the sustainer and vernier hydraulic system provides hydraulic power for sustainer engine control valves and for gimbaling the two vernier engines. Vehicle roll control is accomplished during the sustainer phase by differential gimbaling of the vernier engines.

System performance. - Atlas hydraulic system performance was normal throughout the flight. Pressures were stable. The transfer of fluid power from ground to airborne hydraulic systems was normal. Booster pump discharge absolute pressures increased from 1290 N/cm^2 (1870 psi) at T - 2 seconds to flight levels of 2165 N/cm^2 (3141 psi) in less than 2 seconds. Starting transients produced a normal overshoot of about 10 percent in the pump discharge pressure. The booster system stabilized at 2149 N/cm^2 (3115 psi). Absolute pressure in the sustainer hydraulic system stabilized at 2151 N/cm^2 (3119 psi). Flight data for AC-17 are presented in figure VI-25.

Centaur

System description. - Two separate but identical hydraulic systems, shown in figure VI-26, are used on the Centaur stage. Each system gimbals one engine for pitch, yaw, and roll control. Each system consists of two servocylinders and an engine-coupled power package containing a high- and low-pressure pump, a reservoir, an accumulator, a pressure-intensifying bootstrap piston, and relief valves for pressure regulation. High pressure and flow are provided by a constant-displacement vane-type

pump driven by the liquid-oxygen turbopump accessory drive shaft. An electrically powered recirculation pump is used to provide low pressure for engine gimbaling requirements during prelaunch checkout, to aline the engines prior to main engine start, and for limited thrust vector control during the Centaur post-separation maneuver. Two thermostats are contained in each hydraulic system to start and stop the recirculation pumps in order to control hydraulic fluid temperature (between 261 K (10^{o} F) and 270 K (30^{o} F)) during the coast phase.

System performance. - The performance of the hydraulic systems was satisfactory. System pressures and temperatures as they varied with flight time are shown in figures VI-27.

Activation of the low-pressure recirculation pumps provided absolute hydraulic pressures of 90.6 N/cm^2 (131 psi) for the C-1 engine system and 87 N/cm^2 (126 psi) for the C-2 engine system. These pumps provided pressure and flow for centering the engines prior to main engine first and the attempted second start.

The main hydraulic system provided absolute hydraulic pressures at 755 N/cm^2 (1095 psi) to the hydraulic systems for the C-1 and C-2 engines throughout Centaur main engine first firing. During the attempted main engine second start, the hydraulic pressure increased to an absolute pressure of 748 N/cm^2 (1085 psi) when the main engine system started momentarily. However, the pressure abruptly decreased to zero when the engine failed to continue operating.

System fluid temperatures were below the specified maximum limit of 408 K (275^{o} F) and above the minimum limit of 239 K (-30^{o} F) throughout the flight. Manifold fluid temperature increased from 292 K (66^{o} F) and 293 K (68^{o} F), respectively, for C-1 and C-2 at main engine first start to 347 K (165^{o} F) and 345 K (162^{o} F) by the time of main engine first cutoff. After engine cutoff the fluid temperature at the C-1 manifold decreased to a low of 291 K (64^{o} F), and the C-2 manifold fluid temperature decreased to a low of 287 K (57^{o} F) by the time of the attempted main engine second start. After the attempted main engine second start the manifold fluid temperature was 301 K (82^{o} F) for C-1 and C-2.

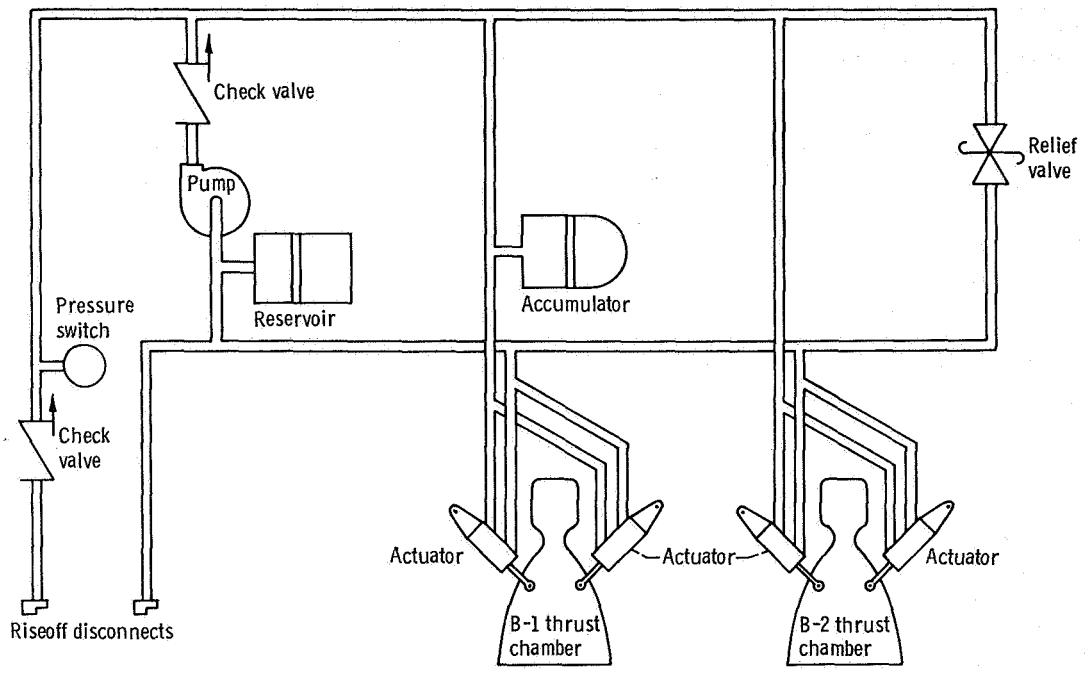

Figure VI-23. - Atlas booster hydraulic system, AC-17.

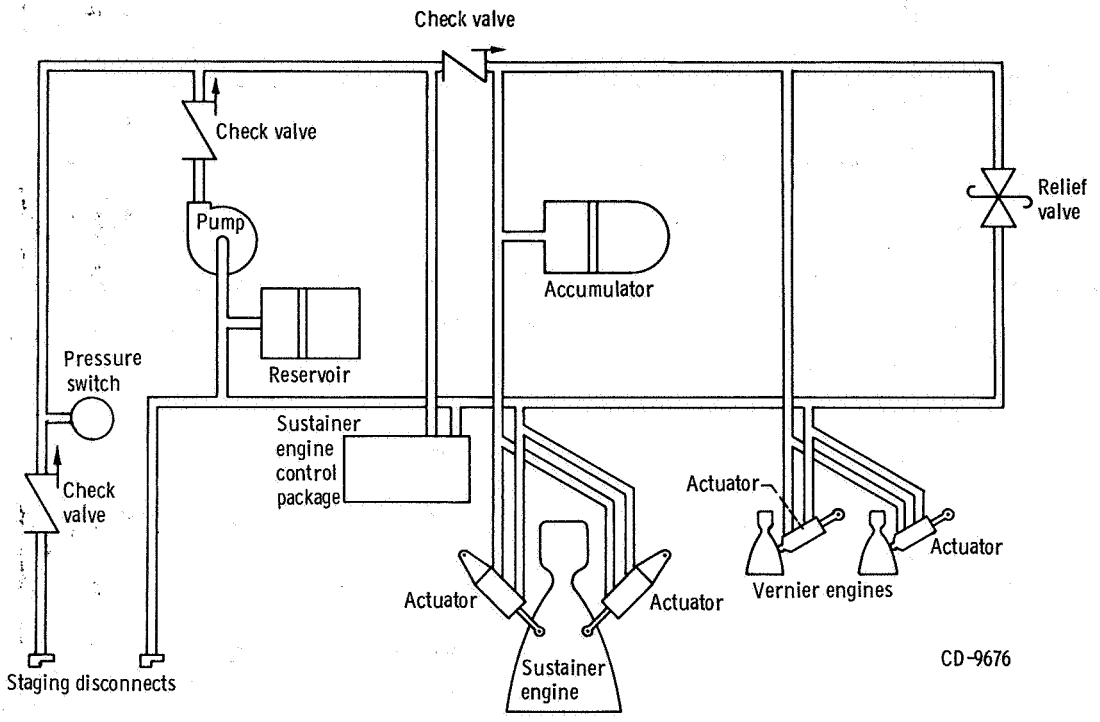

Figure VI-24. - Atlas sustainer hydraulic system, AC-17

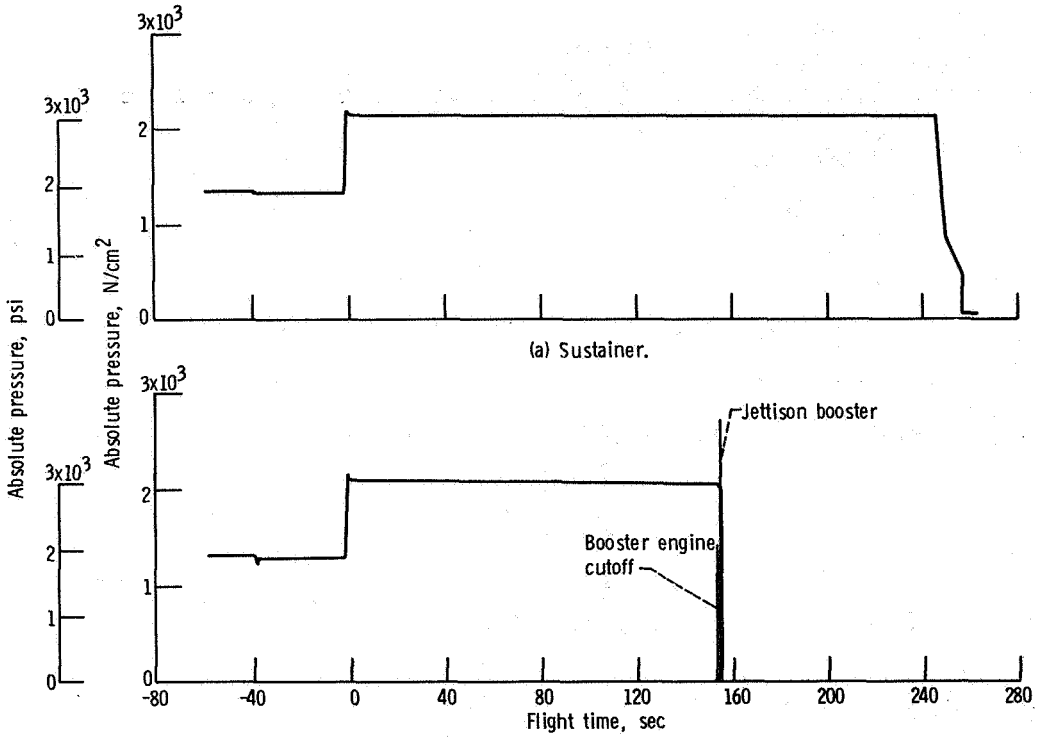

(a) Sustainer.

(b) Booster.

Figure VI-25. - Atlas booster and sustainer hydraulic pressures, AC-17.

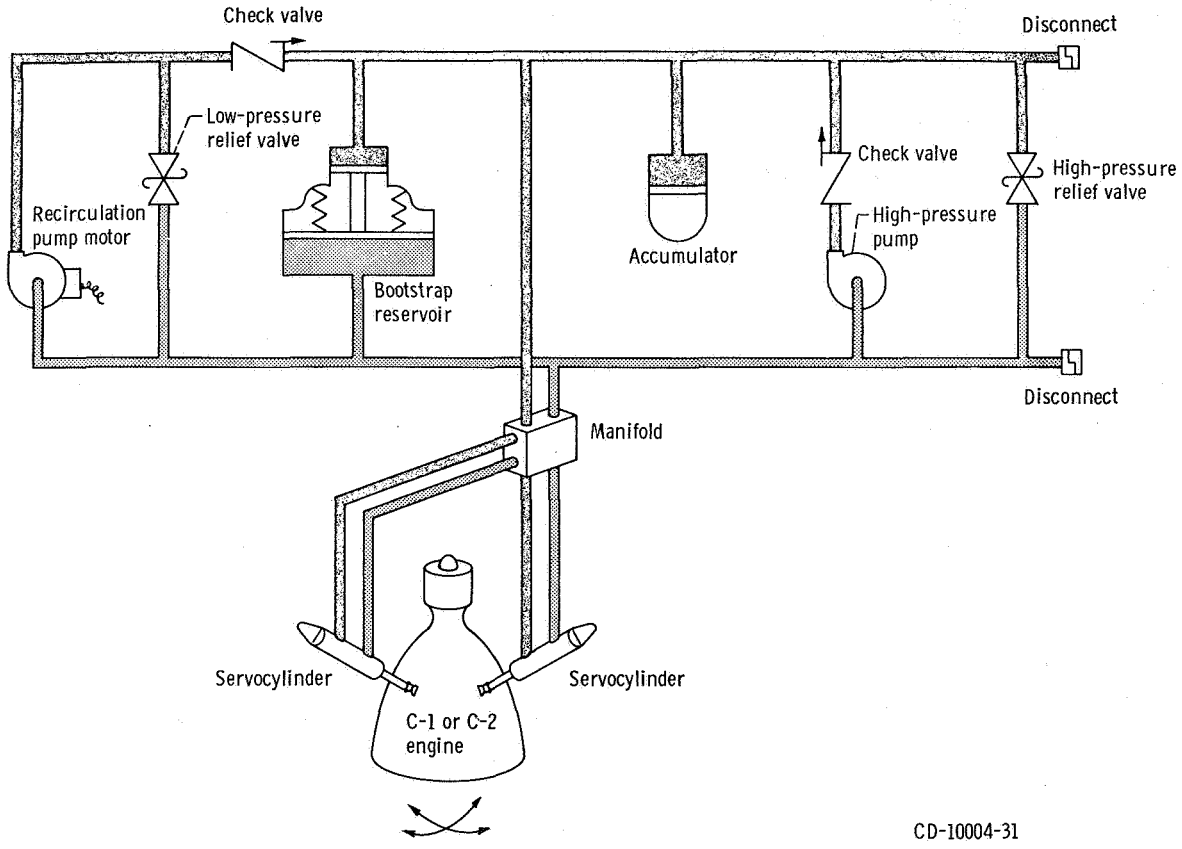

Figure VI-26. - Centaur hydraulic system, AC-17.

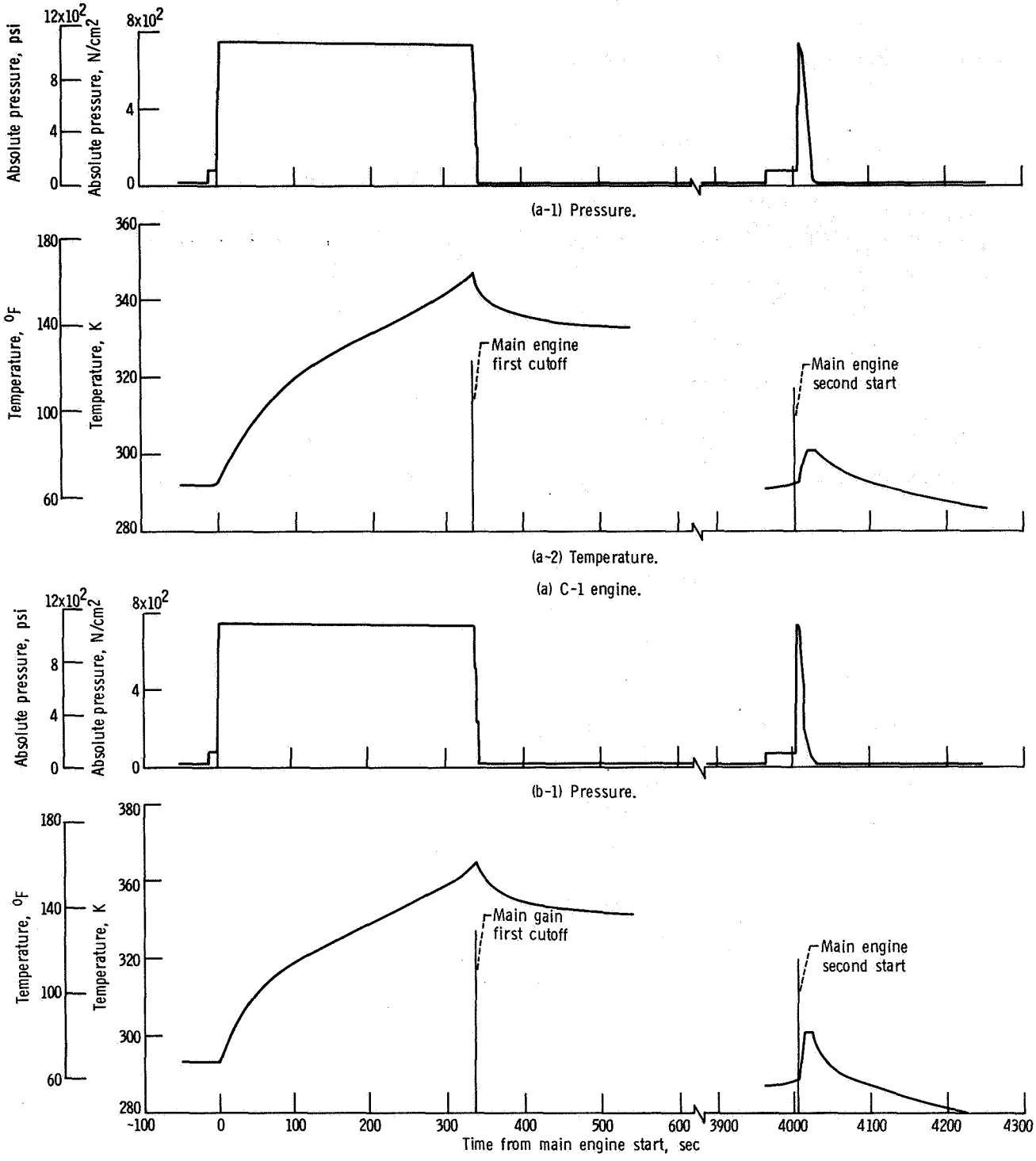

(a-1) Pressure.

(a-2) Temperature.

(a) C-1 engine.

(b-1) Pressure.

(b-2) Temperature.

(b) C-2 engine.

Figure VI-27. - Hydraulic system temperature and pressure, AC-17.

STRUCTURES

by James F. Harrington, Charles W. Eastwood, Jr., William M. Prati, Dana H. Benjamin, Thomas L. Seeholzer, Robert C. Edwards, and John C. Estes

Atlas and Interstage Adapter

System description - Atlas. - The Atlas structure consists primarily of a tank section and a jettisonable booster engine section. The forward end of the tank section mates with the interstage adapter and supports the Centaur and payload. The aft end mates with the booster engine section and supports the thrust loads of the booster and sustainer engines. The tank section is divided into a fuel tank and an oxidizer tank by an intermediate bulkhead. An ellipsoidal bulkhead encloses the forward end of the tank section and a thrust cone encloses the aft end. The sustainer engine is mounted on the thrust cone. Fairings on the tank section protect electronic equipment.

The primary structure is the propellant tanks. These tanks are thin-walled, pressure-stabilized, monocoque sections of welded stainless-steel construction (see fig. VI-28). They require internal pressure in order to maintain structural stability. The tensile strength of the tank material determines the maximum allowable pressure in the propellant tanks.

The maximum allowable and minimum required tank pressures are presented in figure VI-29. They are computed using maximum design loads (as opposed to actual flight loads) with appropriate factors of safety. These tank pressure limits are not constant because of varying aerodynamic loads, inertia loads, and ambient pressure during flight.

The Atlas vehicle is subjected to its highest bending load between T + 40 and T + 110 seconds. The bending, inertia, and aerodynamic drag create compressive loads in the fuel and oxidizer tank skin. These loads are resisted by internal pressure to prevent buckling of the skin.

The maximum allowable differential pressure between the oxidizer and fuel tanks is limited by the strength of the Atlas intermediate bulkhead. The fuel tank pressure must always be greater than the oxidizer tank pressure to stabilize the intermediate bulkhead (prevent bulkhead reversal).

The booster engine section structure consists of a thrust cylinder, nacelles, and fairings which house the booster engines and associated equipment. This section is attached to the tank section by 10 helium-gas-operated latch mechanisms. These latches, as shown in figures VI-30 and VI-31, are located circumferentially around the Atlas aft bulkhead thrust ring at station 1133. An explosively actuated valve supplies helium at a gage pressure of 2068 N/cm^2 (3000 psi) to the distribution manifold. The actuation of the latch mechanism results in the disengagement of the booster engine from the Atlas

vehicle. Two jettison tracks (fig. VI-32) attached to the thrust ring are used to guide the booster engine section as it separates from the Atlas.

System description - interstage adapter. - The interstage adapter structure is a cylinder of aluminum skin, stringer, and ring construction that provides the structural tie between the Atlas and Centaur stages. The Atlas/Centaur staging system, shown in figure VI-33, consists of a flexible linear shaped charge mounted circumferentially which severs the forward end of the interstage adapter at Centaur station 413; Atlas deceleration is provided by eight retrorockets mounted near the aft end of the Atlas.

System performance. - The Atlas ullage and bulkhead differential pressure profiles are compared with the design limits in figure VI-29. The Atlas oxidizer and fuel tank ullage pressures did not approach the maximum allowable pressure during flight. The oxidizer and fuel tank ullage pressures were greater than the minimum required to resist the combined bending and axial design loads between T + 40 and T + 110 seconds. The bulkhead differential pressure was also within the maximum allowable and minimum required pressure limits for all periods of flight.

The increase of longitudinal inertia force was as expected. A maximum value of 5.74 g's was reached at booster engine cutoff. This value was less than the 5.81 g's maximum allowable.

Booster engine cutoff (BECO) occurred at T + 152.0 seconds and booster engine section staging occurred at T + 155.1 seconds. Staging was verified by data from the B-1 booster thrust chamber pitch actuator position instrumentation and from the vehicle axial (fine) accelerometer. Atlas/Centaur staging was successful. Vehicle staging was commanded at T + 248.1 seconds, and the flexible linear shaped charge severed the interstage adapter at station 413. The eight retrorockets, mounted around the aft end of the Atlas, fired 0.1 second later to decelerate the Atlas and provide separation from the Centaur. Accelerometer and other data indicated that all eight retrorockets functioned as expected for the flight. Figure VI-34 shows the separation distance, as a function of time, between the Atlas and the Centaur for the flight. This figure also indicates clearance losses due to pitch and yaw motions of the Atlas during separation.

Following is a summary of shaped charge firing time, retrorocket firing time, and the results of the pitch and yaw motions as the Atlas cleared the aft end of the Centaur engines:

Shaped charge firing time, sec	T + 248.1
Retrorocket firing time, sec	T + 248.2
Nominal pitch clearance, cm (in.)	27.9 (11)
Pitch clearance loss, cm (in.)	6.6 (2.6)
Actual pitch clearance, cm (in.)	21.3 (10.4)
Nominal yaw clearance, cm (in.)	78.7 (31)
Yaw clearance loss, cm (in.)	10.8 (4.3)
Actual yaw clearance, cm (in.)	67.9 (26.7)

Centaur

System description. - The Centaur structures consist of propellant tanks with an intermediate bulkhead, main engine thrust barrel, electronic equipment mounting structure, and adapters to support the payload. The Centaur primary vehicle structure is provided by the propellant tanks. These tanks are thin-walled, pressure-stabilized, monocoque sections of welded stainless-steel construction (fig. VI-35). They require internal pressure in order to maintain structural stability. The tensile strength of the tank material determines the maximum allowable pressure in the propellant tanks.

The tank locations and criteria which determine the maximum allowable and minimum required tank pressures during different phases of flight are described in figure VI-36. The maximum allowable and minimum required tank pressures, presented in figure VI-37 are computed using maximum design loads (as opposed to actual flight loads) with appropriate factors of safety. These tank pressure limits are not constant because of varying loads and varying ambient pressure during flight.

The margin between oxidizer tank pressure and the maximum allowable pressure is least at booster engine cutoff (T + 152.0 sec), when the high inertia load causes maximum tension stresses on the aft bulkhead (fig. VI-37, top part). The minimum required oxidizer tank pressure for intermediate bulkhead stability is always greater than the minimum pressure required for aft bulkhead stability.

The strength of the fuel tank is governed by the capability of the conical section of the forward bulkhead to resist hoop stress. Thus, the differential pressure across the forward bulkhead determines the maximum allowable fuel tank pressure. The margin between fuel tank ullage pressure and the minimum required pressure is least during the following times:

(1) Prior to launch, when the payload and nose fairing impose compression loads on the cylindrical skin at station 409.6 because of gravity and ground winds

(2) From T + 0 to T + 10 seconds, when the payload and nose fairing impose compression loads on the cylindrical skin at station 409.6 from the longitudinal and lateral inertial loads and from the vibration loads

(3) From T + 40 to T + 110 seconds, when the Centaur is subjected to maximum bending moments: The combined loads from the inertia, aerodynamic drag, and bending impose compression on the cylindrical skin at station 409.6

(4) At nose fairing jettison, when the nose fairing exerts inboard radial loads at station 218.9

The maximum differential pressure between the oxidizer and fuel tanks is limited by the strength of the Centaur intermediate bulkhead. This maximum allowable differential pressure is 15.9 N/cm^2 (23.0 psi). The oxidizer tank pressure must always be greater than the combined fuel tank pressure and hydrostatic pressure of the liquid hydrogen to stabilize the intermediate bulkhead (prevent bulkhead reversal).

There are three adapters that provide the structural tie between the Centaur and the separable payload (see figs. III-3 and III-4). The aft adapter mounts on the Centaur forward bulkhead, the transition adapter mounts on the aft adapter, and the spacecraft adapter mounts on the transition adapter. The aft adapter is a truncated cone of aluminum sheet and stringer construction. The transition adapter is an inverted truncated cone of aluminum sheet and stringer construction with a fiber-glass thermal diaphragm containing air-conditioning ducts and nozzles. It is a new design similar to the adapter used on Surveyor missions. The spacecraft adapter is provided by the spacecraft agency. The spacecraft is attached to the spacecraft adapter by a V-band clamp. Two explosive bolts, located 180° apart in the clamp, are fired by the Centaur. Each explosive bolt contains one squib with dual bridgewires. When the bolts are severed, the V-band clamp is released and 10 springs between the spacecraft and the adapter provide the separation force. Eight lanyards and tension springs attached from the periphery of the V-band to the spacecraft adapter limit band excursion.

System performance. - The Centaur fuel and oxidizer tank ullage pressure profiles are compared with the design limits in figures VI-37. The oxidizer tank pressure was less than the maximum allowable at booster engine cutoff and all other periods of flight. The oxidizer tank pressure was maintained above the minimum required for aft bulkhead stability during all periods of flight. The fuel tank ullage pressure was above the minimum required pressure and was below the maximum allowable pressure during all periods of flight. The differential pressure across the Centaur intermediate bulkhead was less than the maximum allowable for all periods of flight. The oxidizer tank ullage pressure was always greater than the combined fuel tank ullage pressure and hydrostatic pressure of liquid hydrogen.

The events programmed to follow main engine second start were not accomplished because main engine second start did not occur. Therefore, separation of the spacecraft from the Centaur vehicle was not achieved. (Refer to GUIDANCE AND FLIGHT CONTROL SYSTEMS sections for details on the sequencing of events for spacecraft separation.)

Jettisonable Structures

System description. - The Atlas-Centaur vehicle jettisonable structures are the hydrogen tank insulation panels and a nose fairing.

The hydrogen tank insulation consists of four polyurethane-foam-filled fiber-glass honeycomb panels bolted together along the longitudinal axis to form a cylindrical cover around the Centaur tank. The panels are bolted at their aft end to a support on the Centaur vehicle (fig. VI-38). At the forward end a circumferential Tedlar and fiber-glass laminated cloth forms a seal between the panels and the base of the nose fairing at station 219 (fig. VI-39). Separation of the four insulation panels is accomplished by firing of flexible linear shaped charges located at the forward, aft, and longitudinal seams. The shaped charge at the panel forward seam simultaneously severs the aft attachment of the nose fairing preparatory to fairing jettison at a later time in flight. Immediately following shaped charge firing, the panels rotate about hinge points at their aft end (fig. VI-40) from the preload hoop tension, center-of-gravity offset, and in-flight residual purge pressure. The panels jettison free of the Centaur vehicle after approximately 45^{o} of panel rotation on the hinge pins.

The nose fairing is a fiber-glass skin and honeycomb structure of the type used on Surveyor missions. It consists of a cylindrical section approximately 1.83 meters (6 ft) long bolted to a conical section approximately 4.87 meters (16 ft) long. It is assembled in two jettisonable halves with the split line along the X-X axis, as shown in figure VI-41. A subliming agent is applied to the fairing to limit temperature to maintain structural integrity. In addition to the flexible linear shaped charge which severs the aft attachment, the nose fairing separation system consists of latches and thrusters. Eight pyrotechnically operated pin-puller latches release the fairing halves along the split line, as shown in figure VI-41. Separation force is provided by two nitrogen gas thrusters located at the forward end of the nose cone, one in each fairing half. Each fairing half is hinged at a single point on the Centaur hydrogen tank at station 219 on the Y-Y axis (fig. VI-41). The following modifications were made to the Surveyor-type nose fairing for the ATS missions:

(1) Two 22.9-centimeter (9-in.) access doors, two electrical disconnects and harness assemblies, and four antenna ramps were added.

(2) Removable metal air-conditioning ducts replaced fiber-glass ducts bonded to the fairing.

(3) Split lines of the thermal bulkhead were modified to clear the transition adapter at nose fairing jettison.

System performance. - Flight data indicated that the insulation panels were jettisoned satisfactorily. The insulation panel jettison sequence was initiated by a command signal issued from the Atlas programmer at T + 196.751 seconds. Following issuance of the command, the linear shaped charge fired to sever the panel attachments. Shaped

charge firing times were determined from accelerometers mounted on the payload aft adapter. At 35° of panel rotation, breakwire transducers provided event time data. These transducers were attached to one hinge arm of each panel as shown in figure VI-42. Since the breakwire data were monitored on commutated channels, the panel 35°-position event times in the following table are mean times:

Insulation panel location, quadrant	Instrumented hinge arm location, quadrant	Insulation panel 35°-rotation-position event time, sec
I-II	I	T + 197.213
II-III	III	T + 197.196
III-IV	III	T + 197.185
IV-I	I	T + 197.236

The rotational velocity of each panel, assuming first motion at shaped charge firing, was determined from the mean time of the 35° position. Panel velocities are presented in the following table.

Panel location, quadrant	Insulation panel average rotational velocities from shaped charge firing to mean time of 35° position, deg/sec
I-II	78.4
II-III	81.4
III-IV	83.6
IV-I	74.5

The vehicle rates and dynamics response data indicated a completely satisfactory insulation panel jettison sequence.

The nose fairing was successfully jettisoned. The nose fairing jettison system was initiated by a command from the Atlas programmer at T + 233.0 seconds. The eight pyrotechnically operated pin pullers then unlatched the nose fairing split line. Approximately 0.5 second later the two nitrogen thrusters operated, causing the fairing halves to begin rotation about their hinge points. Nose fairing latch actuation and initiation of the thruster operation were determined from accelerometer data. Rotation of each fairing half was sensed by disconnect pins in the electrical connectors which separated after

approximately 3^{o} of fairing rotation. The following table summarizes significant nose fairing separation event times:

Event	Nose fairing jettison event times, sec
Split line latch actuation	T + 233.031
Nitrogen thruster actuation	T + 233.493
3^{o} rotation position	[a]T + 233.529
(each fairing half)	[a]T + 233.771

[a]Commutated data.

During fairing jettison the payload compartment pressure remained at zero with no pressure surge occurring at thruster bottle discharge.

Vehicle Dynamic Loads

The Atlas-Centaur launch vehicle experiences dynamic loads from four major sources: effects resulting from aerodynamic and acoustic loads; transients from starting and stopping of the engines; transients from operation of the separation systems; and effects from dynamic coupling between major systems.

The instruments used on AC-17 to determine dynamic loads and the parameters measured are tabulated below:

Instruments	Corresponding parameters
Low-frequency accelerometer	Vehicle longitudinal acceleration and vibration
Low-frequency accelerometers (6)	Spacecraft transition adapter longitudinal and tangential acceleration
Centaur pitch-rate gyro	Vehicle pitch-plane angular rate
Centaur yaw-rate gyro	Vehicle yaw-plane angular rate
Angle-of-attack sensor	Vehicle aerodynamic loads
High-frequency accelerometers (2)	Local spacecraft vibration

Launch vehicle longitudinal vibrations measured on this flight are compared with four other flights in figure VI-43. The frequency and amplitude of all other vibration data measured on AC-17 are shown in table VI-6. Longitudinal vibrations were excited at lift-off by the launch release transient. The amplitude and frequency of these vibrations were similar to those observed on prior vehicles. Atlas intermediate bulkhead pressure oscillations were the most significant effects produced by the launcher-induced longitudinal vibrations. These oscillations presented no problem because the measured minimum differential pressure was 8.5 N/cm^2 (12.3 psi) (see fig. VI-29), while the minimum design allowable differential pressure across the bulkhead is 1.4 N/cm^2 (2.0 psi).

Between T + 70 and T + 153 seconds, intermittent longitudinal vibrations of 0.1 g (11 to 12 Hz) were observed on the Atlas fuel tank skin. These vibrations are caused by dynamic coupling between structure, engines, and propellant lines (commonly referred to as "POGO"). For a detailed discussion of this POGO effect see reference 1. During Atlas booster engine thrust decay, short-duration longitudinal vibrations of 0.6 g (13 Hz) were observed. Post-flight load analyses indicate that these transients did not result in any significant structural loading.

During the Atlas phase of flight, the vehicle vibrates in the pitch plane and the yaw plane as an integral body at its natural frequencies. Previous analyses and tests have defined these natural frequencies and the modes which the vehicle assumes when it is dynamically excited. The rate gyros on the Centaur provide data for determining modal deflections. The maximum first-mode deflection occurred in the pitch plane at T + 148 seconds (fig. VI-44). This pitch deflection was less than 10 percent of the allowable. The maximum second-mode deflection occurred in the yaw plane at T + 42 seconds (fig. VI-45). The yaw deflection was less than 25 percent of the allowable.

Structural loading due to upper-air winds is minimized during the booster phase of Atlas flight by the preflight selection of pitch and yaw programs from within a family of available predetermined programs. The pitch and yaw programs are chosen just prior to launch on the basis of calculated vehicle response to measured upper-air wind profiles. The wind profiles are obtained from weather balloons released at established intervals during the hours prior to launch. The programs selected are those that are calculated to give the least critical predicted peak booster engine gimbal angle and predicted peak vehicle structural load.

Vehicle structural loads are expressed as structural capability ratios - the ratios of predicted load to allowable load at each of the locations being considered. Structural capability ratio is the algebraic sum of the ratio of predicted to allowable axial load plus the ratio of predicted to allowable bending moment. Predicted bending moment includes the root sum square of bending moments due to random dispersions, in addition to the bending moments calculated to result from angles of attack predicted from measured wind profiles.

The flight time envelope of maximum predicted structural capability ratios for this flight is shown in figure VI-46. The peak structural capability ratio predicted for this flight was 0.73 at station 906 at T + 75.5 seconds. These capability ratios are based on pitch program Code PP31, yaw program Code YP6, and the calculated response to the winds measured by the T + 7-minute weather balloon.

Angles of attack experienced during actual flight are computed from differential pressure measurements in the fairing nose cap. Figures VI-47 and VI-48 compare these pitch and yaw angle-of-attack histories to those calculated from the winds measured by the T + 7-minute weather balloon. Analysis of dynamic pressure and angle-of-attack data showed that the structural capability ratio was maximum at T + 78.3 seconds and occurred 2.8 seconds later than the predicted time of T + 75.5 seconds. The combined pitch and yaw angle of attack at T + 78.3 seconds slightly exceeded the maximum value predicted to occur at T + 75.5 seconds. This would indicate that the actual structural capability ratio slightly exceeded the predicted value of 0.73 at the critical Atlas station 906. However, the predicted structural capability ratio equation includes a sizeable allowance for dispersions. From an evaluation of the flight dispersions, it was judged that the actual dispersions were appreciably less than the equation allowance. It was therefore concluded that the maximum structural capability ratio was no greater than the predicted value of 0.73.

An investigation of the vibration environmental data indicated that the vibration levels were comparable to those experienced on other Centaur flights. Two piezoelectric high-frequency accelerometers were located 25 centimeters (10 in.) vertically below the spacecraft center of gravity at Centaur station 109. These accelerometers together with their amplifiers had a flat frequency response to 2100 hertz. However, the telemetry channel Inter-Range Instrumentation Group (IRIG) filter frequency was less than 2100 hertz. Therefore, the frequency range (for unattenuated data) was limited by the standard IRIG filter frequency for that channel.

The steady-state vibration levels were highest near lift-off as expected. The maximum level of the shock loads (over 20 g's) occurred at insulation panel jettison and Atlas/Centaur separation. These shock loads were of short duration (about 0.025 sec) and did not provide significant loads.

In addition to these accelerometers, there were six servo-type low-frequency accelerometers installed on the payload transition adapter at Centaur station 148 to monitor low-frequency, rigid-body acceleration at the spacecraft interface. Three accelerometers were sensitive in the tangential direction and three in the longitudinal direction. Single amplitude shock and vibration levels recorded by the two spacecraft and six transition adapter accelerometers are shown in table VI-6.

In addition to the levels tabulated, a number of high-frequency shock-type transients were experienced during Atlas and Centaur powered flight. The maximum single amplitude of these transients was about 3 g's. These transients were not correlated with

any flight event and were similar in amplitude and frequency content (about 1500 Hz) to those experienced on previous flights. These shock-type transients are believed to be a result of a combination of thermal effects and static loads in the vehicle structure.

A 37-hertz vibration was observed in the forward end of the Centaur at the start of and during Centaur powered flight. This vibration was measured by the six payload transition adapter accelerometers and the two spacecraft accelerometers. Also, rate gyro response indicated this vibration occurred in pitch, yaw, and roll. The cause of the oscillation is believed to be dynamic coupling between the Centaur engines, the vehicle structure, and the autopilot.

TABLE VI-6. - MAXIMUM SHOCK AND VIBRATIONAL LEVELS OBSERVED AT MARK EVENTS, AC-17

Time of dynamic disturbance, sec after lift-off	Mark event	Accelerometer measurement number							
		CY113O	CY114O	CA647A	CA648A	CA649A	CA650A	CA651A	CA652A
		Accelerometer station location (referenced to Centaur stations)							
		109		148					
		Axis or direction of sensitivity							
		Radial		Longitudinal			Tangential		
		Accelerometer system gain of 0 db limited to approximately-							
		2100 Hz		100 Hz			70 Hz		
		Standard telemetry channel cutoff filter frequency, Hz							
		790		110	160	220	330	450	600
		Accelerometer range, g's							
		±20		-2.9 to 8.9			±1.18		
		Acceleration, g's (zero to peak) Frequency, Hz							
1.0 to 5.0	Launch	5 400	8 540	0.3 6	0.35 6	0.35 6	0.5 100	0.6 100	0.5 100
152.09	Booster engine cutoff	1.5 12	(a) (a)	0.7 13	0.65 13	0.6 13	0.1 4	0.1 4	0.3 4
155.12	Booster jettison	(b) (b)	1 7	(b) (b)	(b) (b)	(b) (b)	0.05 5	0.05 5	0.1 5
197.11	Insulation panel jettison	(c) 550	(c) 550	0.4 30	0.5 30	0.6 30	0.03 5	0.04 5	0.02 5
233.80	Nose fairing jettison	5 450	7 450	0.9 30	1.0 30	1.1 30	0.07 6	0.08 6	0.07 6
246.30	Sustainer engine cutoff	1 90	1.5 90	0.5 40	0.5 40	0.6 40	0.4 85	0.6 85	0.5 85
248.30	Atlas/ Centaur separation	(c) 500	(c) 500	(d) (d)	(d) (d)	(d) (d)	(d) (d)	(d) (d)	(d) (d)
259.08	Main engine first start	1 200	1.2 30	0.2 30	0.2 30	0.2 30	0.05 37	0.07 37	0.05 37
595.8	Main engine first cutoff	0.9 50	1.3 30	1.1 30	1.1 30	1.2 30	0.2 40	0.3 40	0.3 40

[a]No detectable response.

[b]Telemetry signal dropout.

[c]The maximum amplitudes observed for these two flight events exceeded the intelligence band for their respective telemetry channels.

[d]Data frequency was beyond telemetry channel and data recorder frequency limitations.

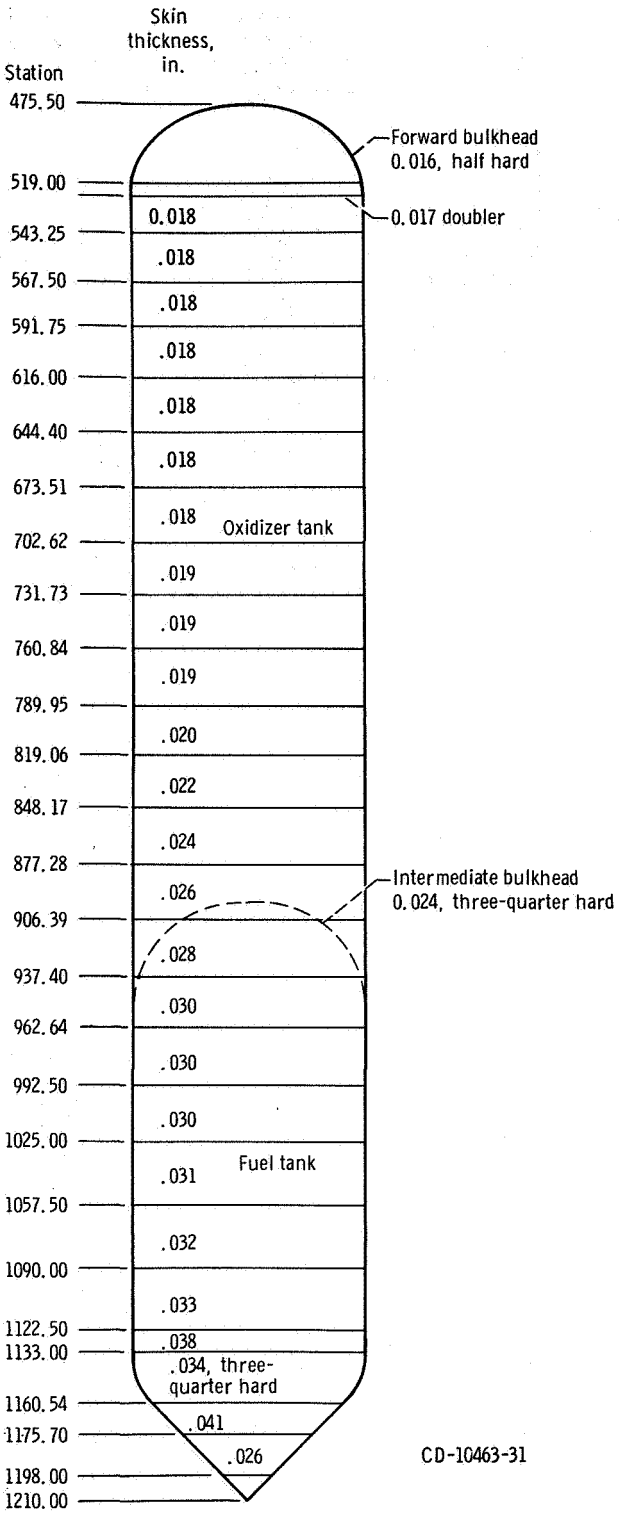

Figure VI-28. - Atlas propellant tanks, AC-17.

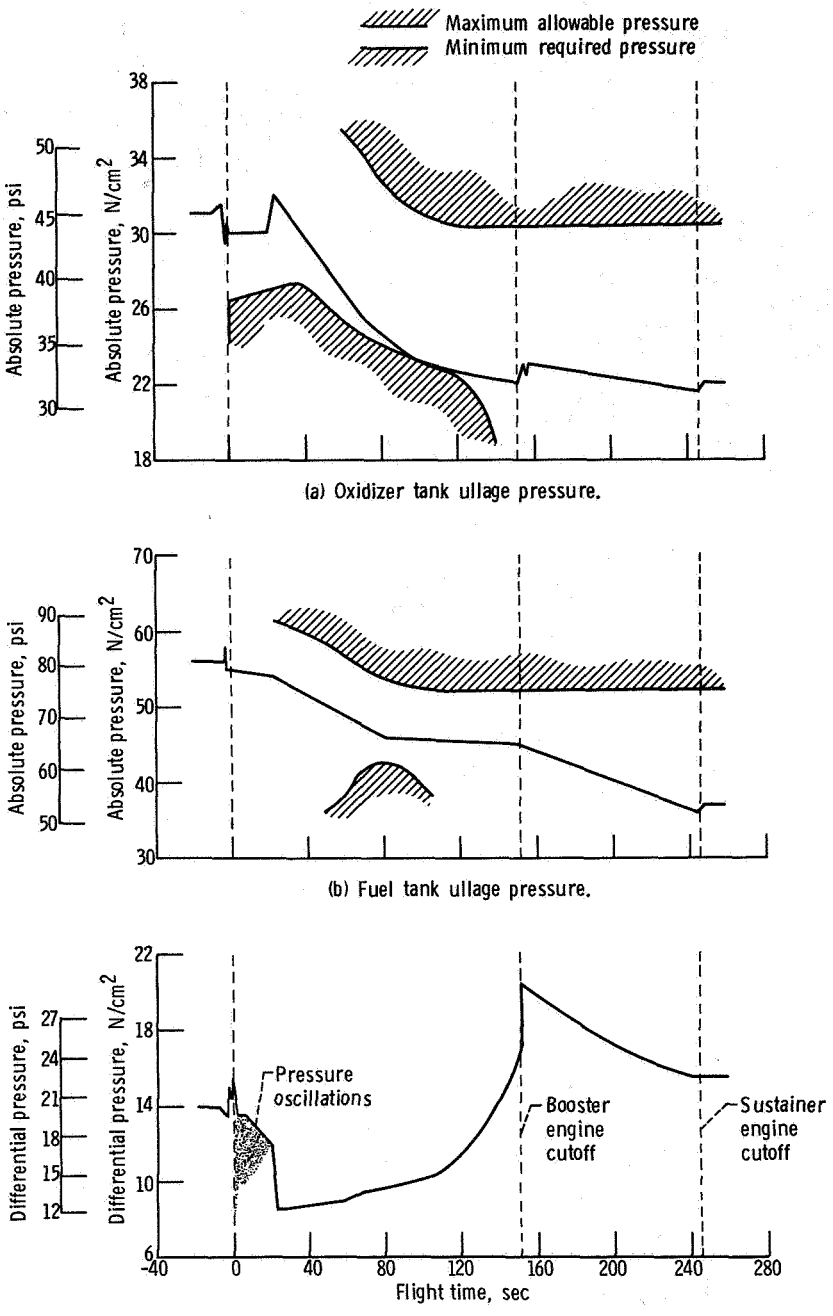

(c) Intermediate bulkhead differential pressure. Maximum allowable differential pressure, 42 N/cm^2; minimum required differential pressure, 1.4 N/cm^2.

Figure VI-29. - Atlas fuel and oxidizer tank pressures, AC-17.

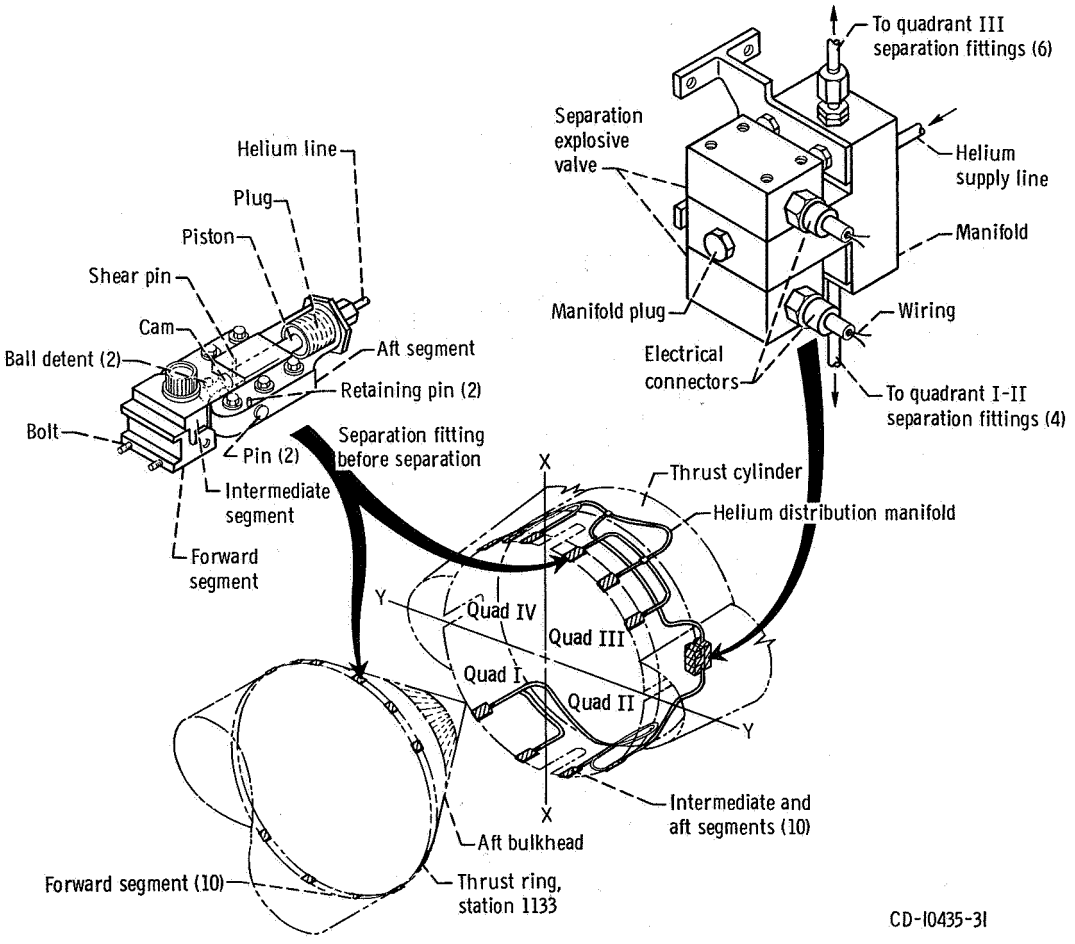

Figure VI-30. - Details of Atlas booster engine section separation system, AC-17.

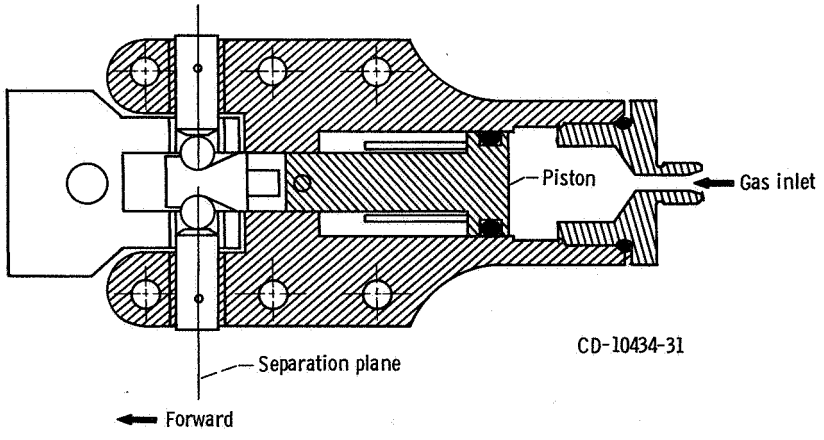

Figure VI-31. - Atlas booster engine section separation fitting, AC-17.

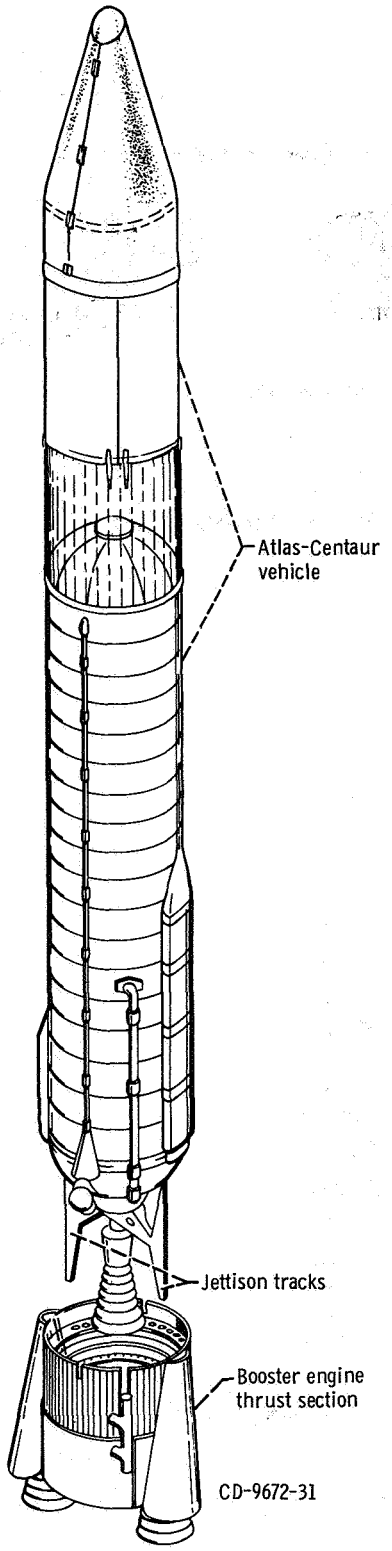

Figure VI-32. - Atlas booster engine section staging system, AC-17.

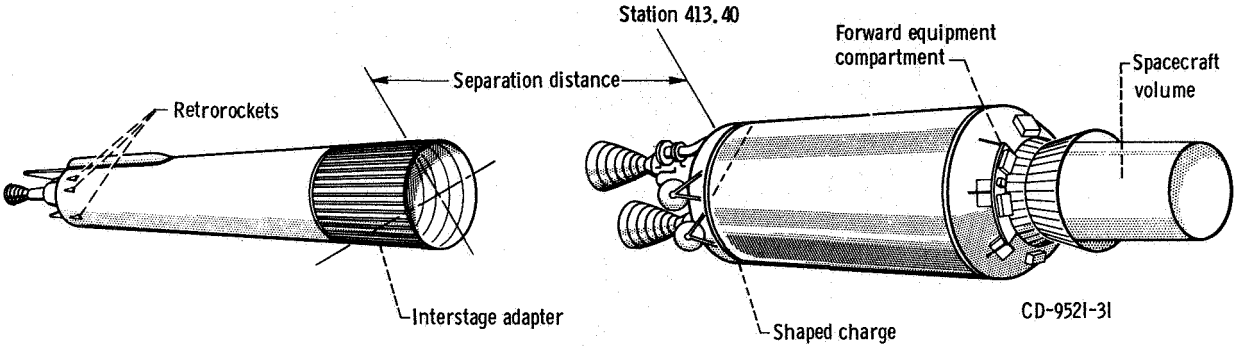

Figure VI-33. - Atlas/Centaur separation system, AC-17.

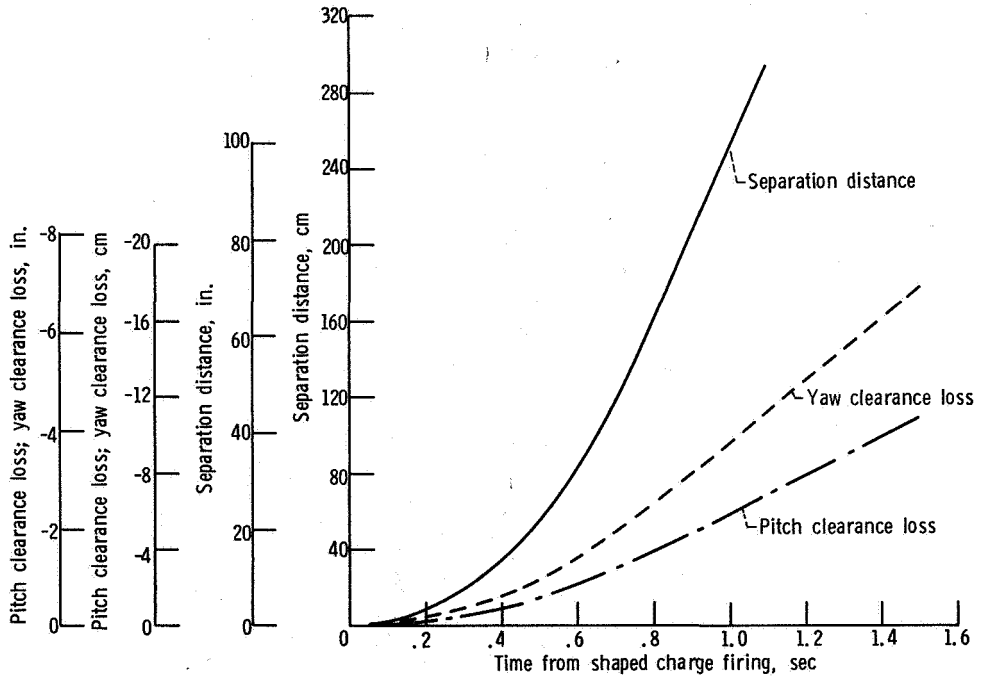

Figure VI-34. - Atlas/Centaur separation distances and clearances, AC-17. All clearance losses referenced to forward end of interstage adapter.

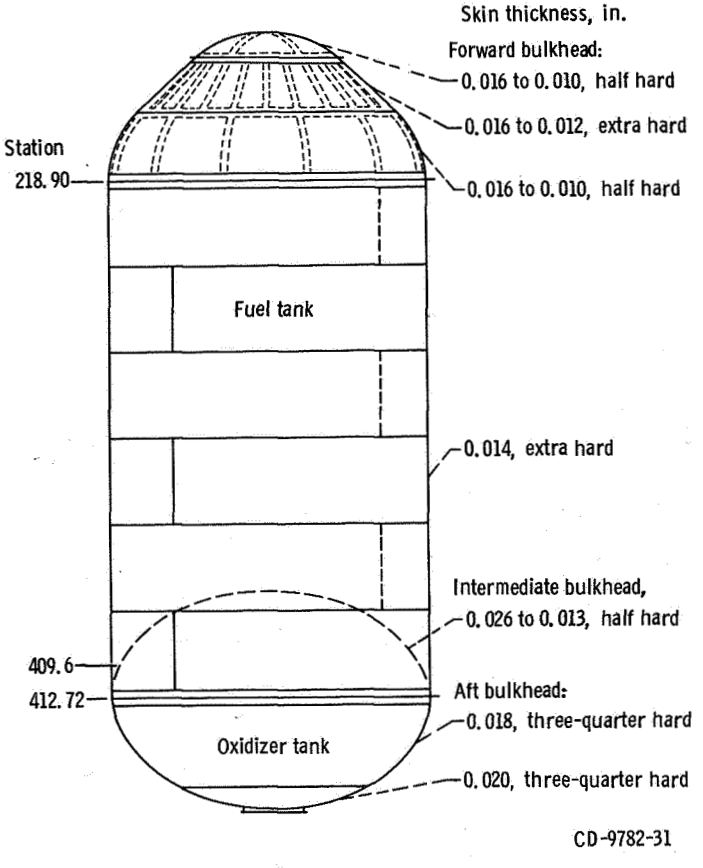

Figure VI-35. - Centaur propellant tanks, AC-17. (All material 301 stainless steel, of hardness indicated.)

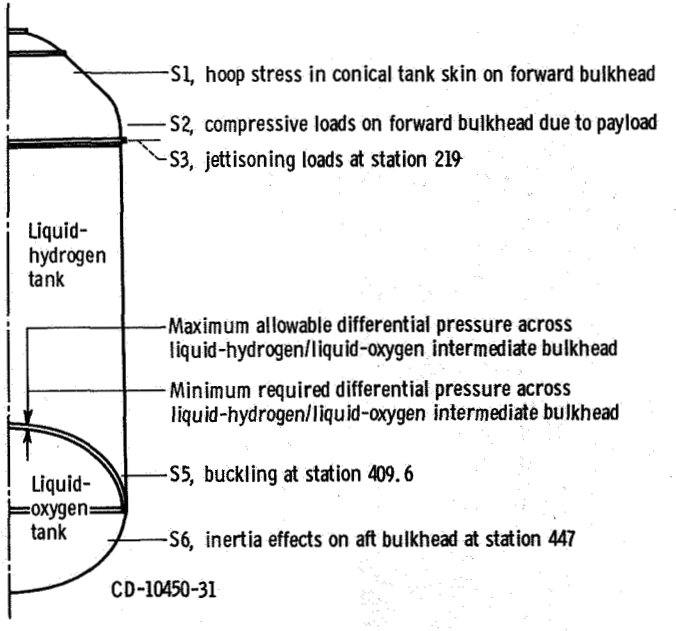

Figure VI-36. - Tank locations and criteria which determine allowable pressures, AC-17.

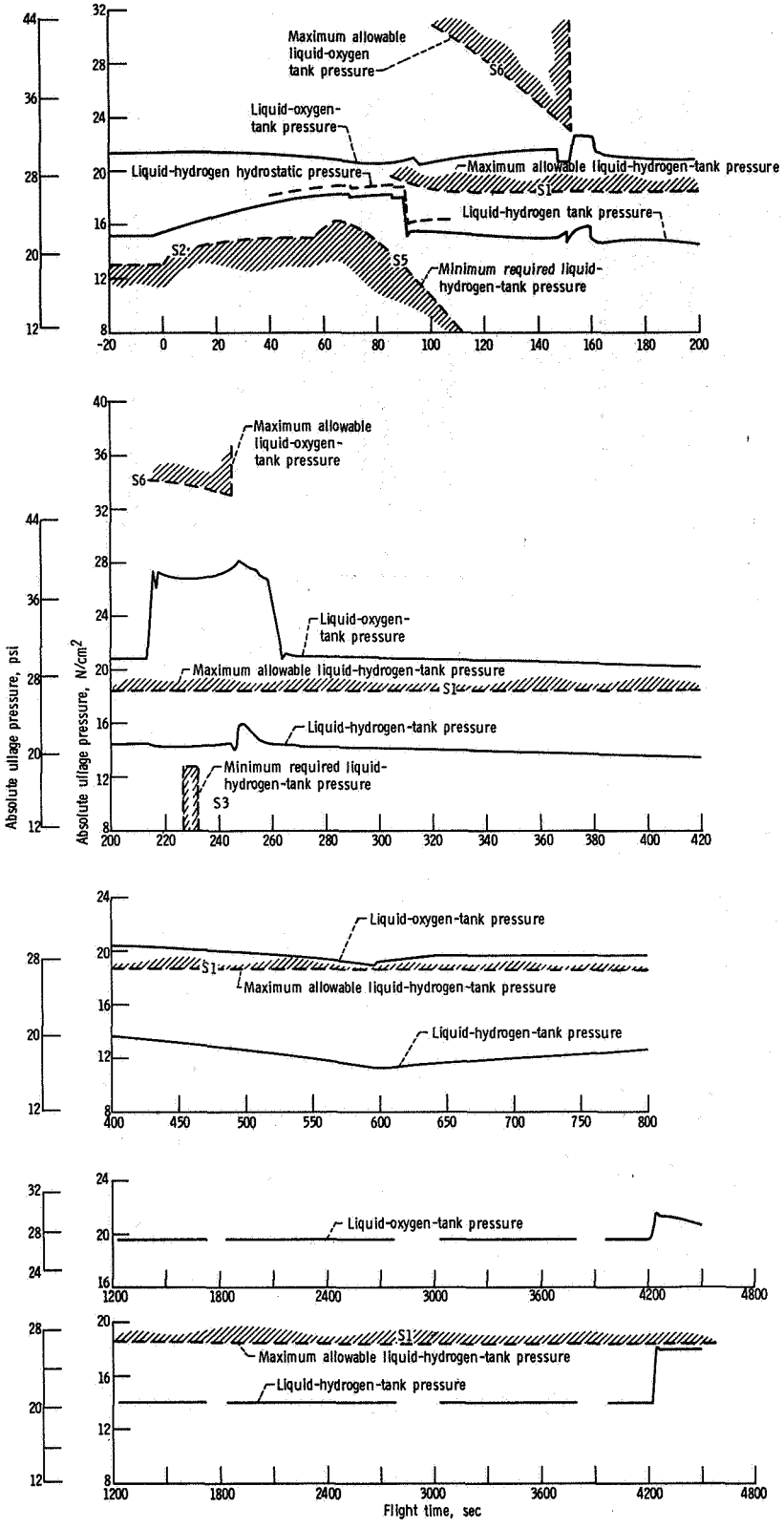

Figure VI-37. - Centaur fuel and oxidizer tank pressures, AC-17. S1, S2, etc., indicate tank structure areas which determine allowable tank structure (see fig. VI-36).

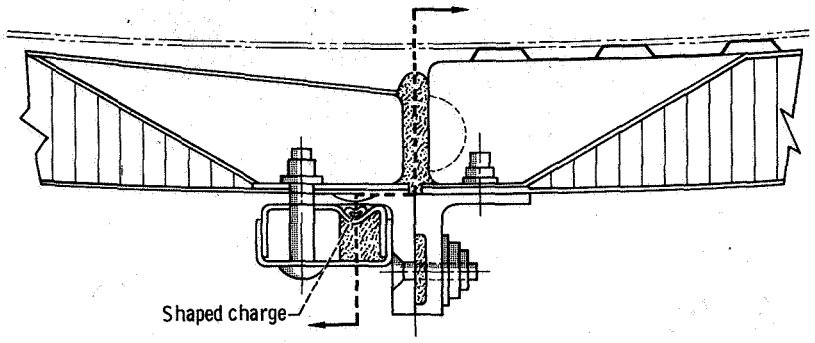

Section B-B: Longitudinal joint

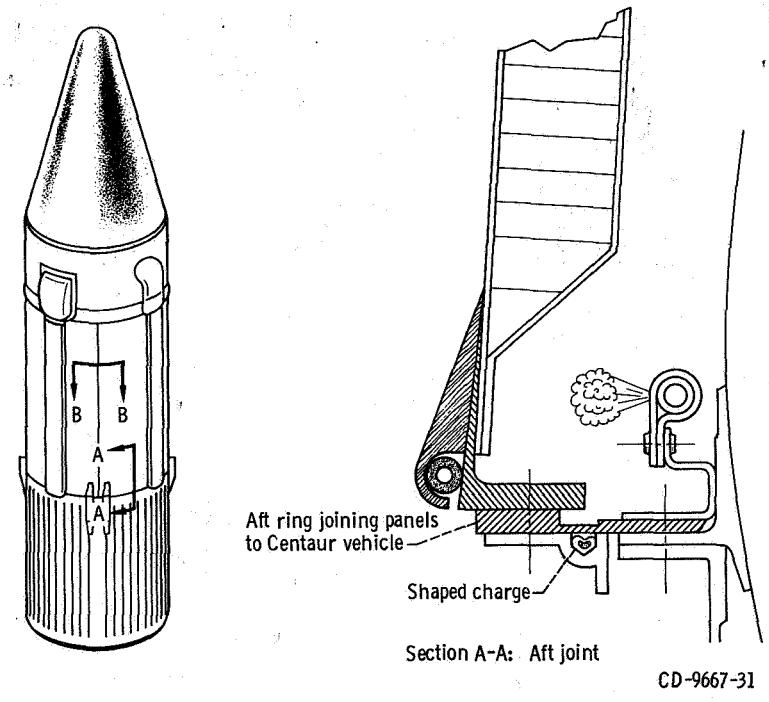

Figure VI-38. - Hydrogen tank insulation panels and separation system, AC-17.

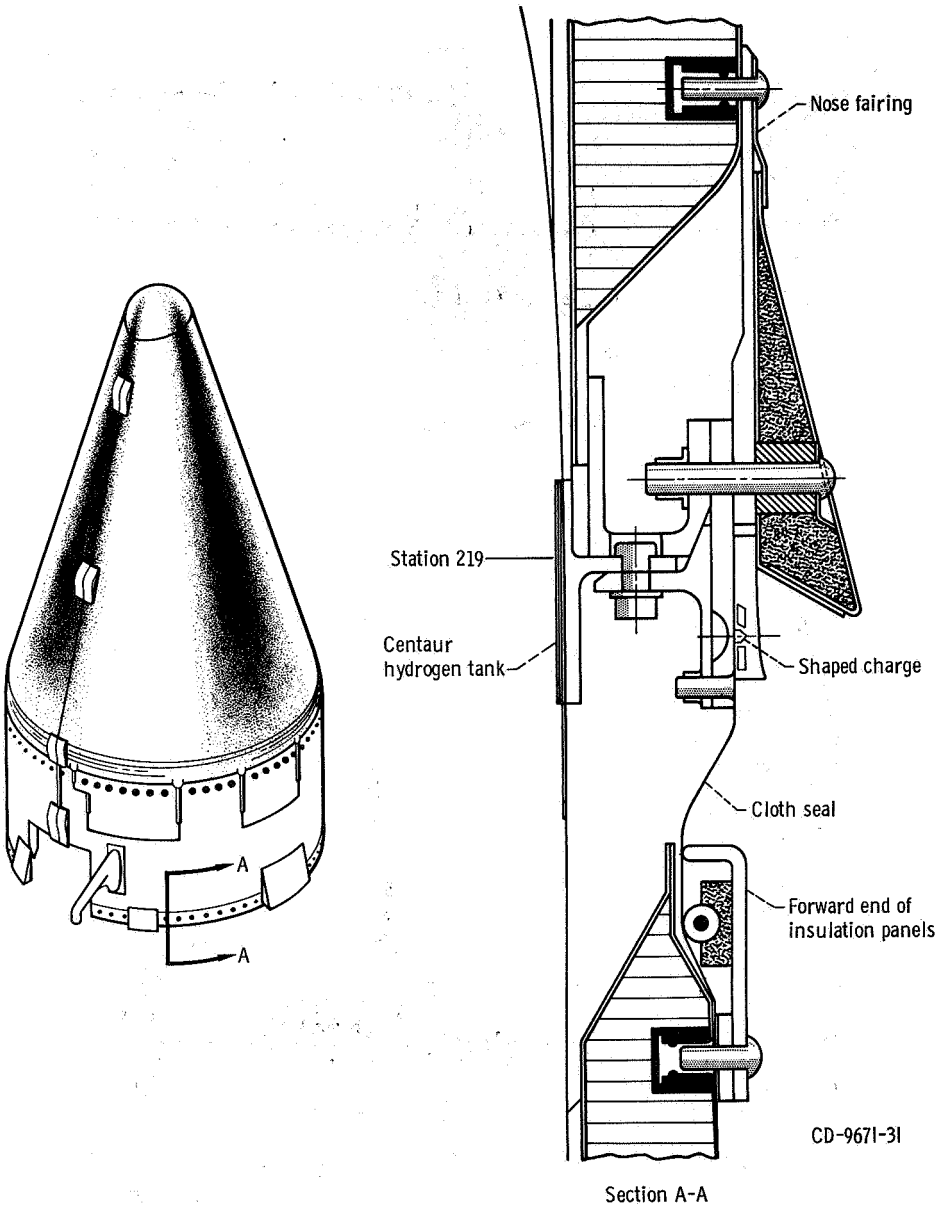

Figure VI-39. - Nose fairing aft separation system, AC-17.

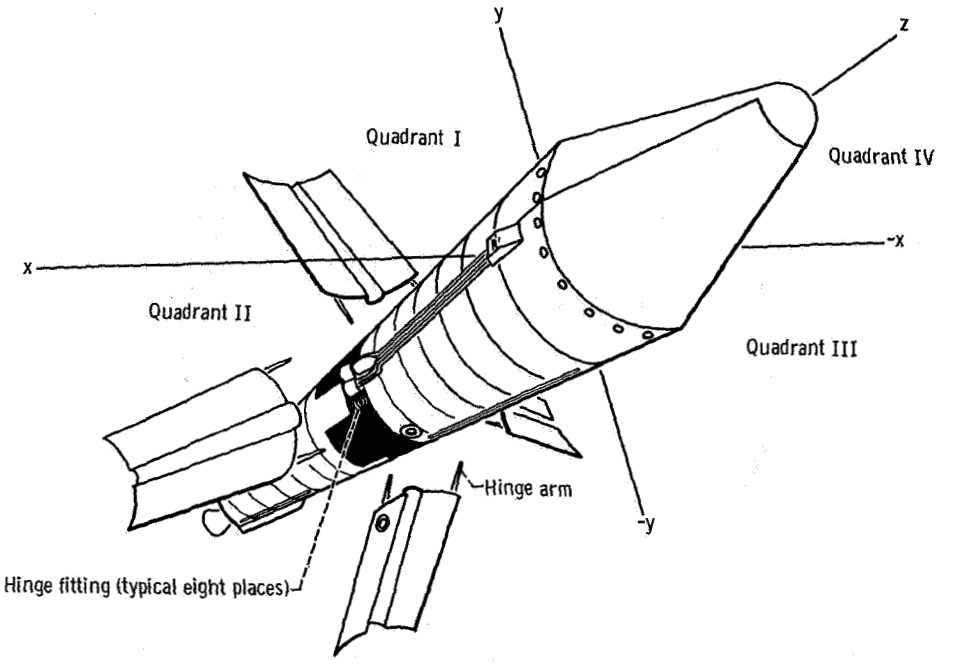

Figure VI-40. - Hydrogen tank insulation panel jettison, AC-17.

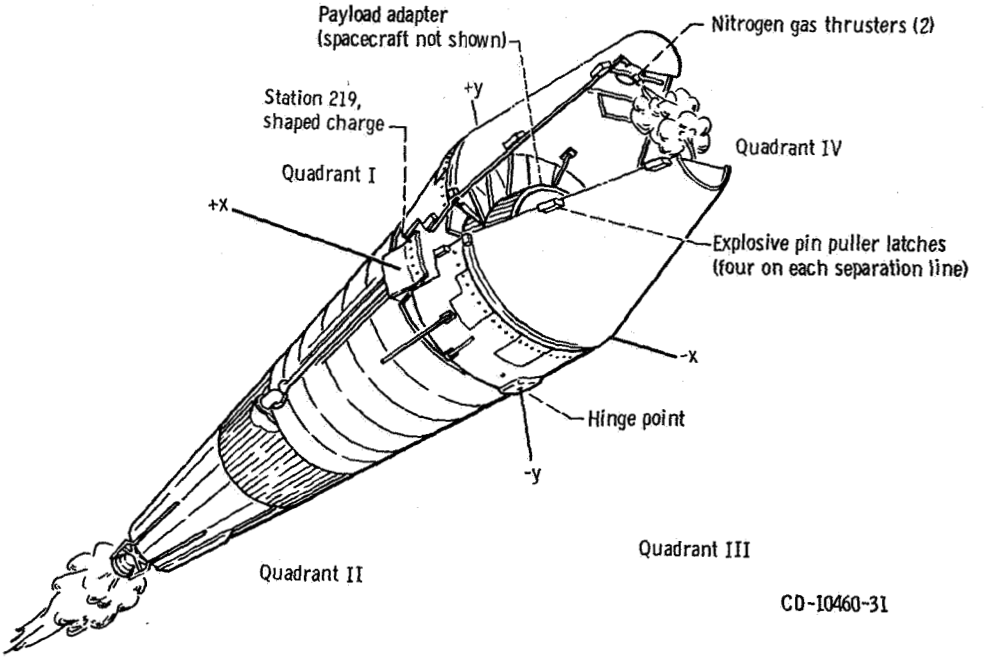

Figure VI-41. - Nose fairing jettison system, AC-17.

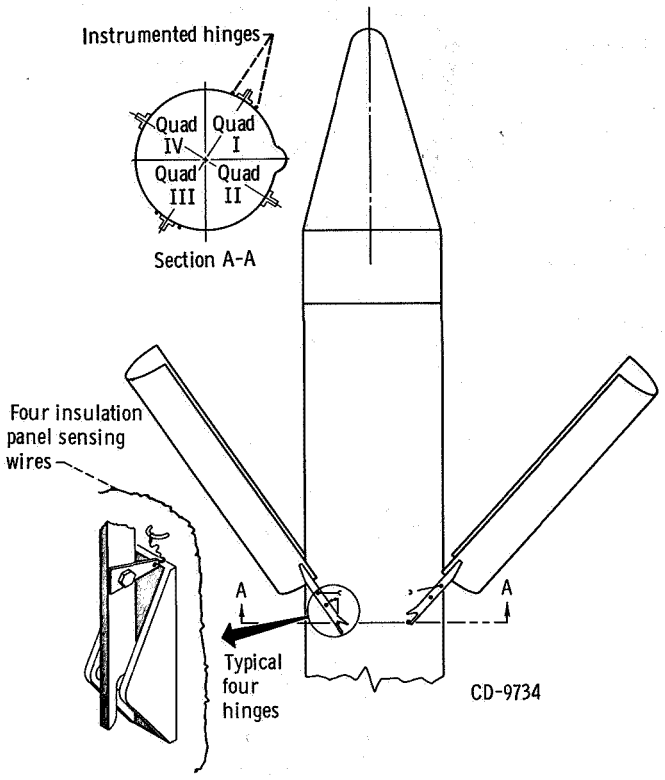

Figure VI-42. - Insulation panel breakwire locations, AC-17.

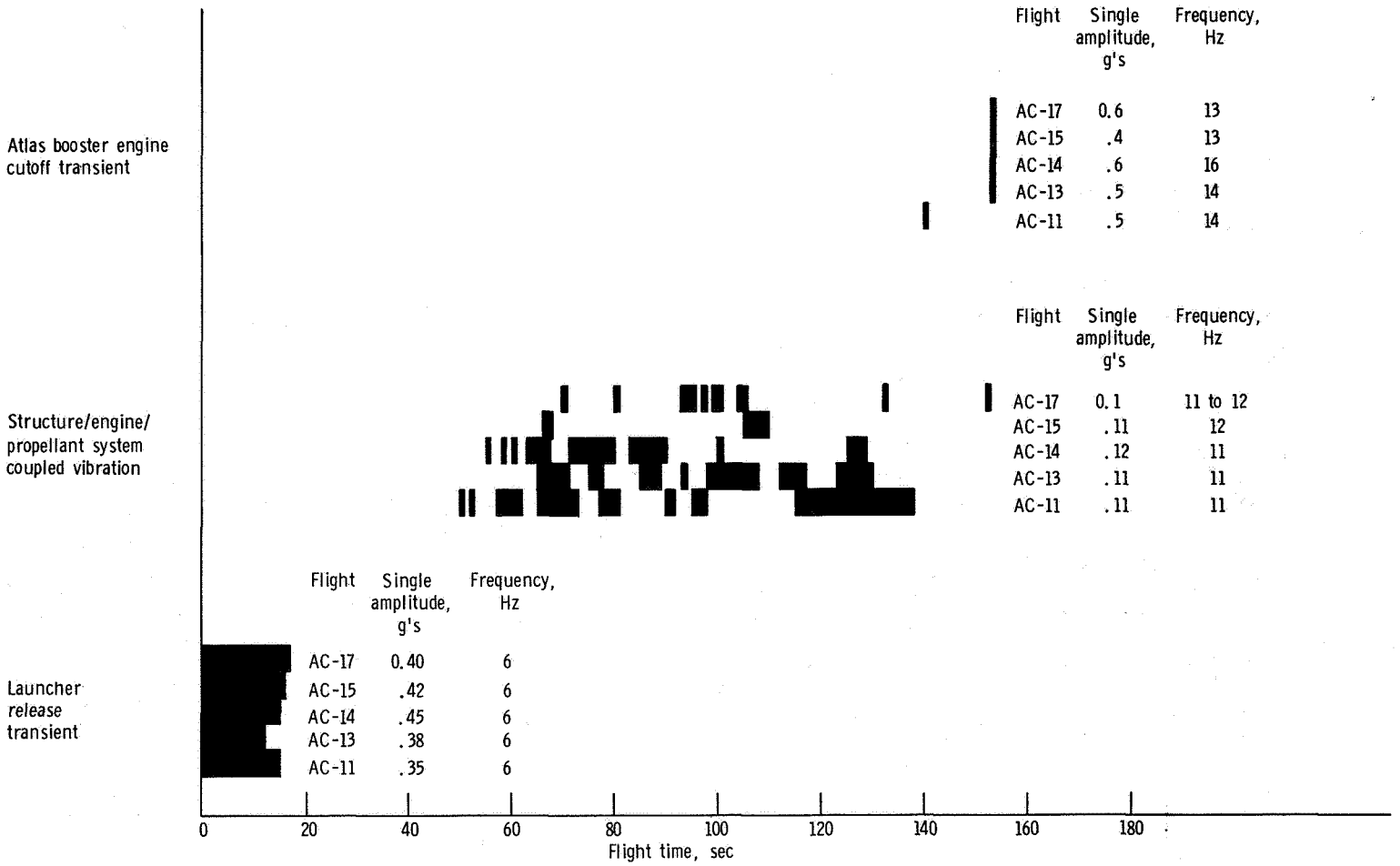

Figure V1-43. - Longitudinal vibrations for Atlas-Centaur flights.

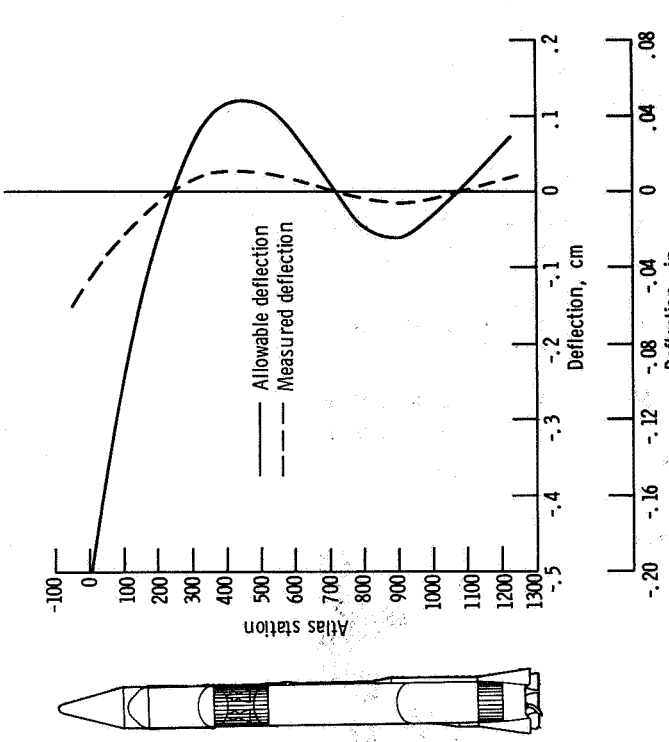

Figure VI-45. - Maximum, yaw plane, second-bending-mode amplitudes at T + 42 seconds, AC-17.

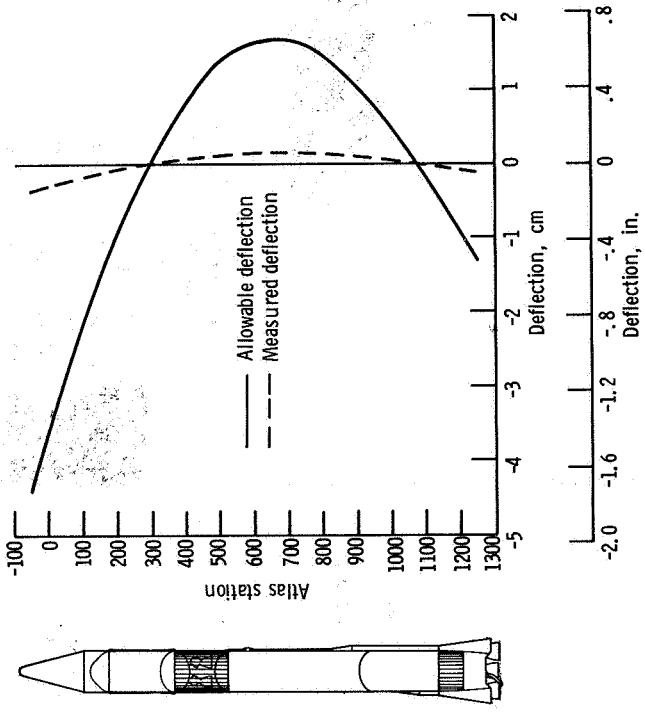

Figure VI-44. - Maximum, pitch plane, first-bending-mode amplitudes at T + 148 seconds, AC-17.

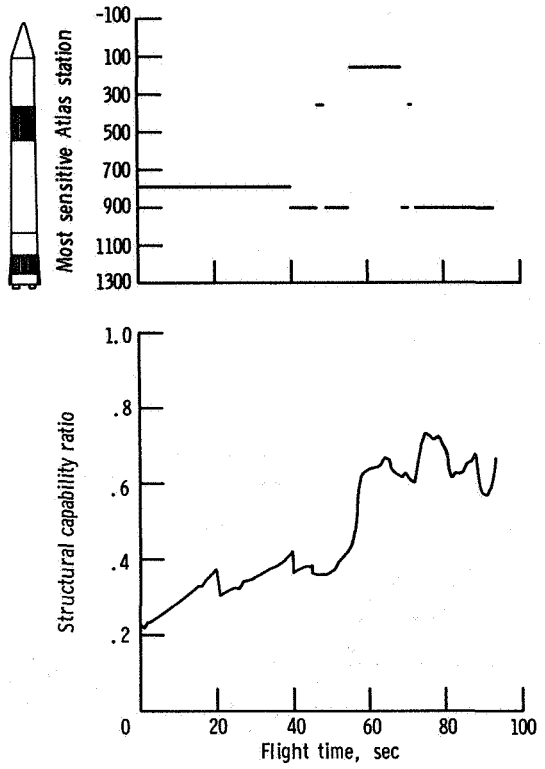

Figure VI-46. - Maximum predicted structural capability ratio (see text) and sensitive station (based on T + 7-min weather balloon), AC-17.

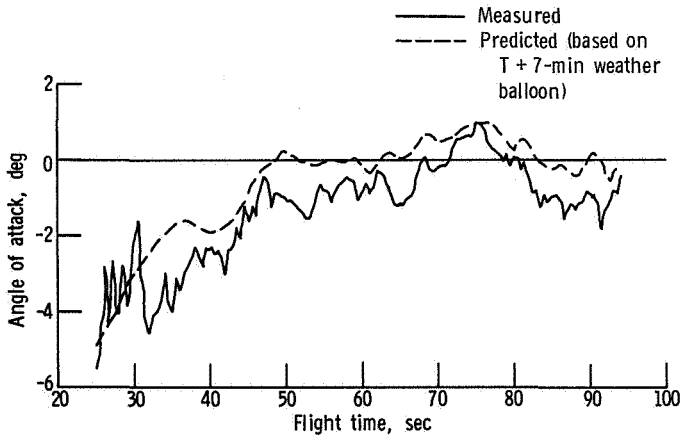

Figure VI-47. - Predicted and measured pitch angles of attack, AC-17.

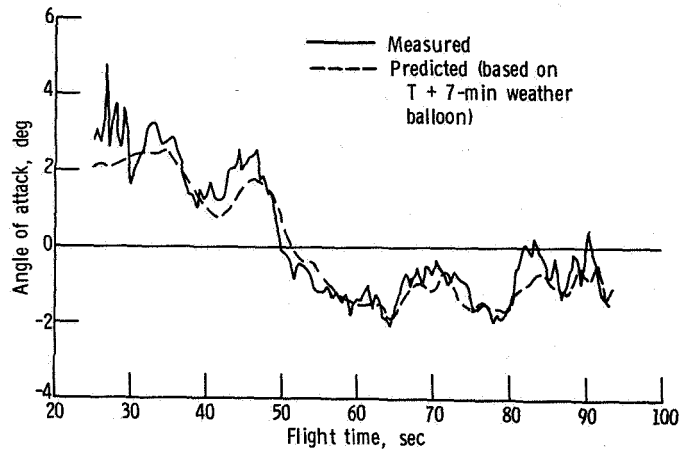

Figure VI-48. - Predicted and measured yaw angles of attack, AC-17.

ELECTRICAL SYSTEMS

by John M. Bulloch and John B. Nechvatal

Power Sources and Distribution

System description - Atlas. - The power supply consists of a power changeover switch; one main battery; one telemetry battery; two independent range safety command (vehicle destruct) system batteries; and a three-phase, 400-hertz rotary inverter. (See fig. VI-49 for the system block diagram.)

System performance - Atlas. - Transfer of the Atlas electrical load from external to internal power was accomplished by the main power changeover switch at T - 2 minutes. Performance of the Atlas electrical system was normal throughout the flight. Voltages and current levels furnished to the dependent systems were within specification limits.

The Atlas main battery supplied the requirements of the user systems at normal levels (25 to 30 V). The battery voltage was 28.1 volts at lift-off and 28.2 volts at sustainer engine cutoff. This is a normal rise of voltage and is caused by battery temperature increase. The telemetry battery and the two range safety command batteries provided normal voltage levels throughout Atlas flight. The voltages at lift-off were 28.4 volts for the telemetry system and 28.8 and 29.0 volts for the two range safety command systems.

The Atlas rotary inverter supplied 400-hertz power within specified voltages and frequency limits. The voltage at lift-off was 115.1 volts and decreased to 114.9 volts at the end of Atlas powered flight (T + 246.2 sec). The inverter frequency at lift-off was 402.2 hertz and increased to 402.7 hertz at the end of Atlas flight. The gradual rise in frequency is typical of the Atlas inverter. The required frequency difference of 1.3 to 3.7 hertz between the Atlas and Centaur inverter frequencies was properly maintained. This difference prevents undesirable beat frequencies in the flight control system; beat frequencies resonant with the slosh and natural structural resonant frequencies of the vehicle may cause the flight control system to issue false commands which may degrade vehicle stability.

System description - Centaur: The electric power system consists of a power changeover switch, a 150-ampere-hour main battery developed for this flight, two independent range safety command (vehicle destruct) batteries, two pyrotechnic system batteries, and a solid-state inverter supplying 400-hertz current to the guidance, flight control, and propellant utilization systems. A block diagram of the system is shown in figure VI-50.

System performance - Centaur: Performance of the Centaur electrical system was satisfactory throughout the flight. Transfer of the Centaur electric load from external

power to the internal battery was accomplished at T - 4 minutes by the power changeover switch and occurred in 250 milliseconds. The maximum voltage excursion at power transfer was 0.5 volt, which is considered negligible.

The main battery voltage was 28.1 volts at lift-off. A low of 27.2 volts was recorded during the main engine first start, and a high of 28.5 volts was reached during the coast phase. The voltage decreased to 28.3 volts at the scheduled main engine second start, and subsequently recovered to 28.8 volts.

Main battery current was 49 amperes at lift-off and reached a maximum of 65.5 amperes at main engine first start and at the scheduled main engine second start. The flight current profile was consistent with ground test values, as programmed, until B timer stop event (T + 4335.1 sec). Since main engine cutoff was not generated, the B timer restart and, therefore, subsequent programmed events did not occur. The vehicle remained in a programmed engine prestart configuration for the remainder of available flight telemetered data (T + 6500 sec). (Refer to GUIDANCE AND FLIGHT CONTROL SYSTEMS section for details on guidance equations switching to the second-powered-phase mode.)

Due to cooling in the aft bulkhead area, the hydraulic recirculator pump was occasionally activated by thermostatic control. This was observed by an increase and subsequent decrease in current demands as recorded on the current profile during the first pass. See figure VI-51 for the flight current profile.

The pyrotechnic battery voltages were 34.8 and 35.2 volts at lift-off. Minimum specification limit is 34.7 volts. Proper operation of the pyrotechnic system batteries and associated relays was verified by instrumentation and by the successful jettison of the insulation panels and nose fairing.

Performance of the two range safety command system batteries was satisfactory. At lift-off, both battery voltages were 33.1 volts. The minimum specification limit is 30 volts.

The Centaur inverter operated satisfactorily throughout the flight. Telemetered voltage levels compared closely to values recorded during preflight testing. The inverter phase voltages at lift-off were as follows: phase A, 115.7 volts; phase B, 115.5 volts; and phase C, 115.1 volts. Voltage changes during flight were small and well within expected values. Maximum phase voltage variation from lift-off was 0.4 volt. Inverter frequency remained constant at 400.0 hertz throughout the flight. Inverter skin temperature was 303 K (85.6° F) at lift-off and reached a high of 354 K (178° F) by T + 6500 seconds (first-orbit telemetry data).

System description - Atlas. - The Atlas telemetry system (fig. VI-52) consists of a RF telemeter unit, two antennas, a telemetry battery, and transducers. It is a pulse amplitude modulation/frequency modulation/frequency modulation (PAM/FM/FM) telemetry system and operates at a carrier frequency of 229.0 megahertz. The PAM technique used on all Atlas-Centaur commutated (sampled) channels makes possible a larger number of measurements on one subcarrier channel. This increases the data handling capability of the telemetry system. The FM/FM technique uses analog values from transducers to frequency modulate the subcarrier oscillators which, in turn, frequency modulate the main carrier (radiofrequency link).

Systems performance - Atlas. - The telemetry coverage for the Atlas portion of the flight (fig. VI-53) extended well beyond Atlas/Centaur separation and met all telemetry coverage requirements. The 106 operational measurements shown in table VI-7 were transmitted through two antennas located on the two equipment pods. All measurements provided useful data. Minor anomalies were experienced by the following measurements:

(1) The pressure measurements on the booster engine thrust chambers B-1 and B-2, both exhibited negative "spiking," which is characteristic of transducer wiper arm lift-off. This has been a common anomaly in the past with this type of transducer. No data were lost because of the momentary wiper arm lift-off.

(2) Data from the nose cap pitch-angle-of-attack measurement, nose cap yaw-angle-of-attack measurement, and nose cap calibrate-angle-of-attack measurement all exhibited bias level shifts from prior to lift-off to nose fairing jettison. Additionally, the nose cap calibrate measurement increased abruptly from 15 percent to 22 percent information bandwidth (IBW) at T - 3.4 seconds. The data remained at this level until T - 1 second and then decreased exponentially back to 15 percent IBW by T + 1.2 seconds. Data from the preceding three measurements were usable. Similar bias shifts were observed prior to lift-off whenever spacecraft telemetry was turned on.

System description - Centaur. - The Centaur telemetry system (fig. VI-54) consists of two RF telemetry systems, one antenna (fig. VI-55), and transducers. It is a PAM/FM/FM system which operates at frequencies of 225.7 and 259.7 megahertz for the RF1 telemetry system and the RF2 telemetry system, respectively. The RF1 telemetry system was used for vehicle operational measurements, and the RF2 telemetry system was used for mission peculiar measurements in order to obtain data (1) on the low-frequency rigid-body vibration environment at the spacecraft interface; (2) on the propellant slosh dynamics during the coast phase; (3) on the thermal environment on vehicle components due to the extended coast period; (4) on heating rates in the main engine compartment resulting from the impingement of the exhaust from the hydrogen peroxide engines during the parking orbit coast phase; and (5) on the alinement of the spacecraft longitudinal axis with respect to the guidance platform.

System performance - Centaur. - A total of 231 measurements, shown in table VI-8, were transmitted to the ground stations. Anomalies were experienced by the following measurements:

(1) The spacecraft adapter longitudinal acceleration measurement (station 135, quadrant 2) did not respond properly to vehicle acceleration during the period from T + 472 to T + 539.6 seconds. At T + 539.6 seconds the measurement began to provide valid data. The data again became invalid after T + 1360 seconds when the measurement started a steady downward drift from 24 percent information bandwidth (IBW) to 0 percent IBW at T + 1800 seconds. Expected value during this portion of the flight is 24 percent IBW. The cause of this failure is unknown.

(2) The C-2 engine fuel pump temperature measurement exhibited a slow response to temperature changes at main engine first start and also unrealistic data during main engine first powered phase. Similar anomalies have occurred on several previous flights and the cause is unknown.

(3) The C-2 engine liquid-oxygen injector differential pressure measurement exhibited a 3 percent bias shift throughout the flight. Review of prelaunch data revealed this bias shift was present throughout the prelaunch activities beginning with the propellant tanking test. No data were lost because of this small bias shift.

Satisfactory telemetry coverage was obtained to T + 5500 and from T + 6000 to T + 6800 seconds, as shown in figure VI-56. Telemetry coverage between Antigua and Ascension (T + 805 to T + 1205 sec), Ascension and Pretoria (T + 1738 to T + 1816 sec), and Tananarive and Carnarvon (T + 2846 to T + 3001 sec) was not obtained because telemetry ships were not available for these areas. Data from the Pretoria receiving station were "noisy" during the interval T + 2164 to T + 2278 seconds. Recurring data "dropouts" of less than 1 second duration occurred at the Kwajalein and Hawaii receiving stations during the interval T + 4553 to T + 5130 seconds, because of varying signal strength. This variation resulted from the changing relative position of the airborne antennas with respect to the ground station because of the vehicle's tumbling motion.

The telemetry in-flight calibration programmed to occur after MECO II plus 566 seconds was not accomplished since the command to calibrate was not issued.

C-Band Tracking System

System description. - An airborne C-band radar system (fig. VI-57) with associated radar ground stations provides real-time position and velocity data for the range safety tracking. These data are also used for post-flight guidance and flight trajectory data analysis. The airborne equipment includes a lightweight transponder, a circulator (to channelize receiving and sending signals), a power divider, and two antennas located on

opposite sides of the Centaur vehicle. The locations of the C-band antennas are shown in figure VI-55.

System performance. - C-band radar tracking was satisfactory; coverage was obtained up to T + 6521 seconds, as indicated in figure VI-58. Bermuda, Antigua, Ascension, Pretoria, Tananarive, and Carnarvon tracking stations provided data for parking orbit calculations. Cape Kennedy, Merritt Island, Patrick Air Force Base, Grand Bahama Island, Grand Turk, and Bermuda tracking stations provided coverage during Atlas-Centaur powered flight.

Grand Bahama Island tracking station did not provide valid data after T + 422 seconds because of ground computer malfunction. The tracking ship USS Watertown did not track because of bias of 3.34° in the azimuth data from the shipboard computer.

Range Safety Command System

System description. - The Atlas and Centaur stages each contained independent vehicle destruct systems. These systems are designed to function simultaneously upon command from the ground stations. Each system includes redundant receivers, a power control unit, a destructor, two antennas, and batteries which operate independently of the main vehicle power system. The locations of the Centaur antennas are shown in figure VI-55. Block diagrams of the Atlas and Centaur vehicle destruct systems are shown in figures VI-59 and VI-60, respectively.

The Atlas and Centaur vehicle destruct systems have the capability of shutting down the engines only or shutting down the engines and destroying the vehicle. Each destruct system consists of an explosive charge which ruptures the propellant tanks of the Atlas and Centaur, dispersing the liquid propellants. In addition, a shaped charge is located on the payload adapter to provide the capability (if required) for destroying the spacecraft apogee motor.

System performance. - The Atlas and Centaur vehicle destruct systems were prepared to execute the destruct command throughout the flight. Engine cutoff or destruct commands were not sent by the range transmitter. The command from the Bermuda ground station to disable the range safety system shortly after Centaur main engine cutoff was properly received and executed. Figure VI-61 depicts ground transmitter coverage to support the vehicle destruct systems. The receiver signal strength measurements indicated a satisfactory received signal strength throughout the flight.

TABLE VI-7. - ATLAS MEASUREMENT SUMMARY, AC-17

System	Measurement type									
	Acceleration	Rotation rate	Displacement	Pressure	Frequency	Rate	Temperature	Voltage	Discretes	Totals
Airframe				3			2		4	9
Range safety								3	1	4
Electrical					1			4		5
Pneumatic				7			1			8
Hydraulic				6						6
Dynamic	1								2	3
Propulsion		3	3	18			6		6	36
Flight control			11			3		4	13	31
Propellant	1			2				1		4
Totals	2	3	14	36	1	3	9	12	26	106

TABLE VI-8. - CENTAUR MEASUREMENT SUMMARY, AC-17

System	Measurement type												
	Acceleration	Rotation rate	Current	Displacement	Vibration	Pressure	Frequency	Rate	Temperature	Digital	Voltage	Discretes	Totals
Airframe	8			5					19			3	35
Range safety											2	3	5
Electrical			1				1		2		4		8
Pneumatic						8			6			2	16
Hydraulic						2			2				4
Guidance									3	1	16		20
Propulsion		4			1	21			41			20	87
Flight control								6			4	36	46
Propellant				2							2		4
Spacecraft					2	1			1			2	6
Totals	8	4	1	7	3	32	1	6	74	1	28	66	231

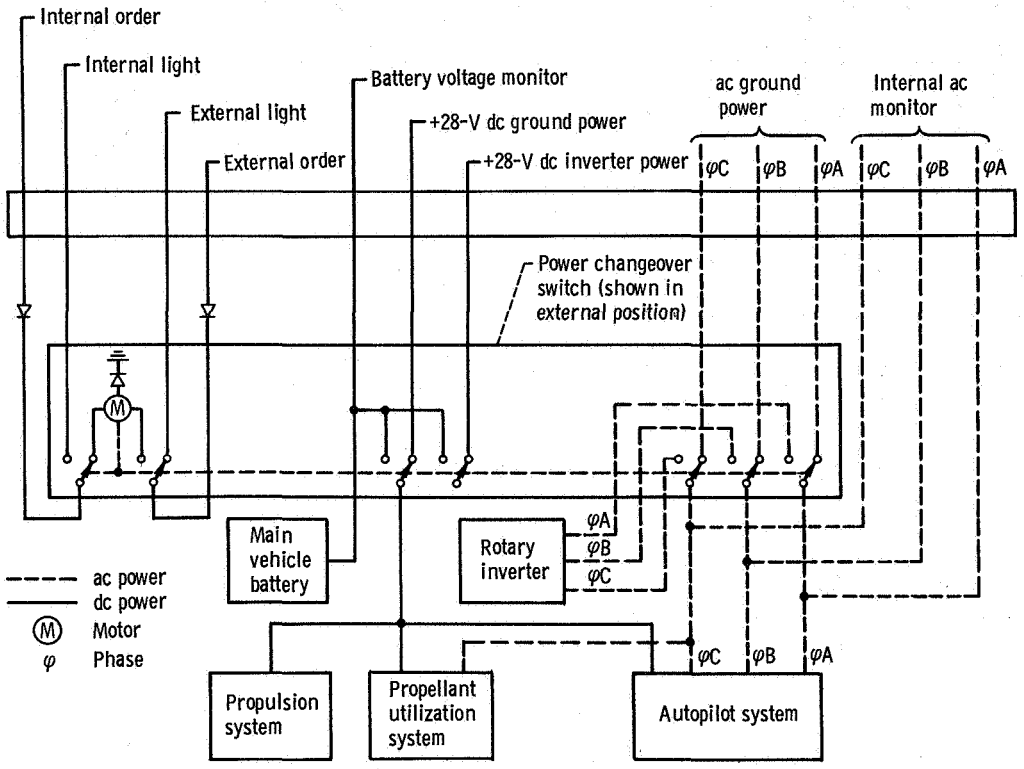

Figure VI-49. - Block diagram of Atlas electrical system, AC-17.

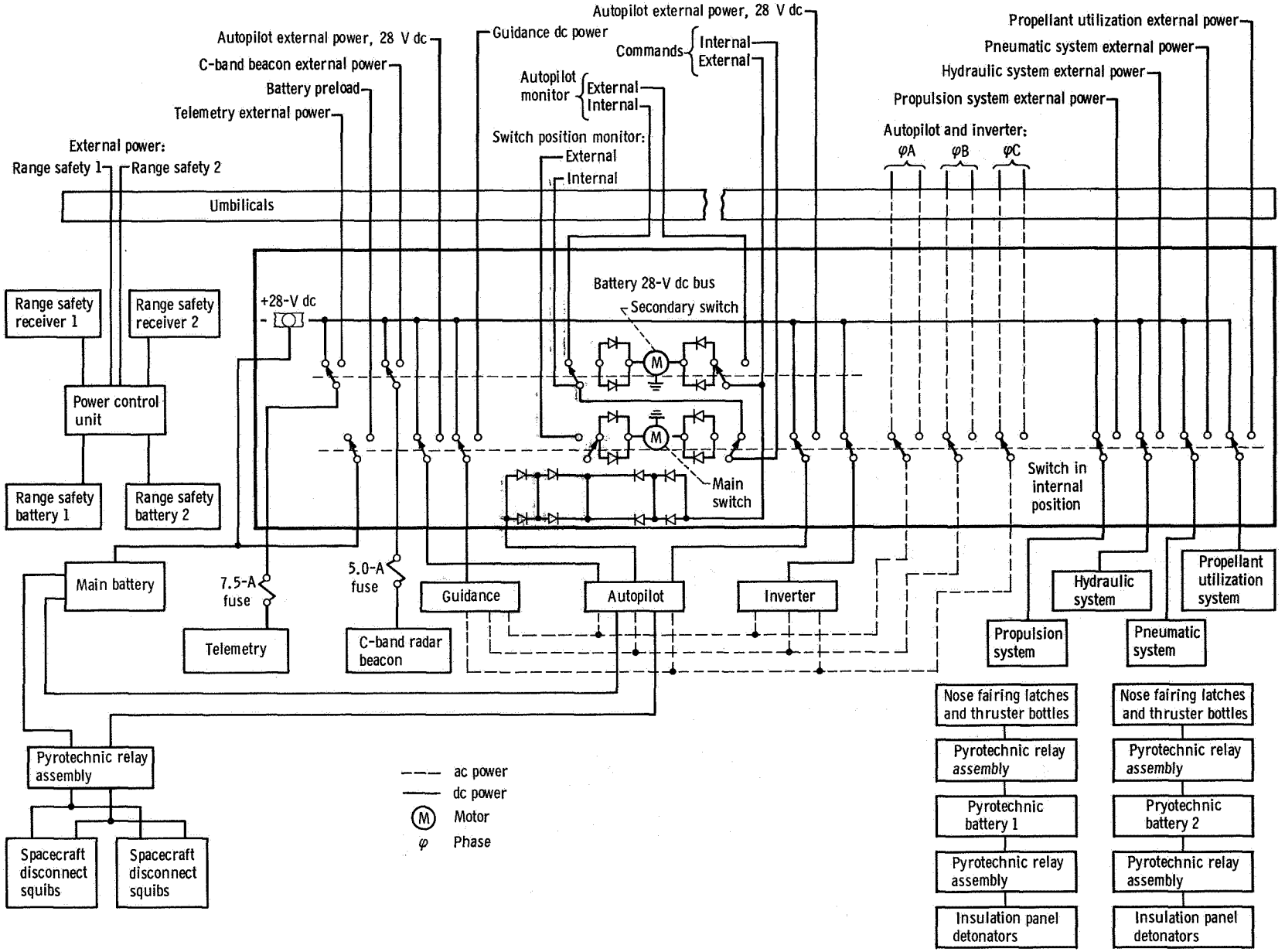

Figure VI-50. - Block diagram of Centaur electrical system, AC-17.

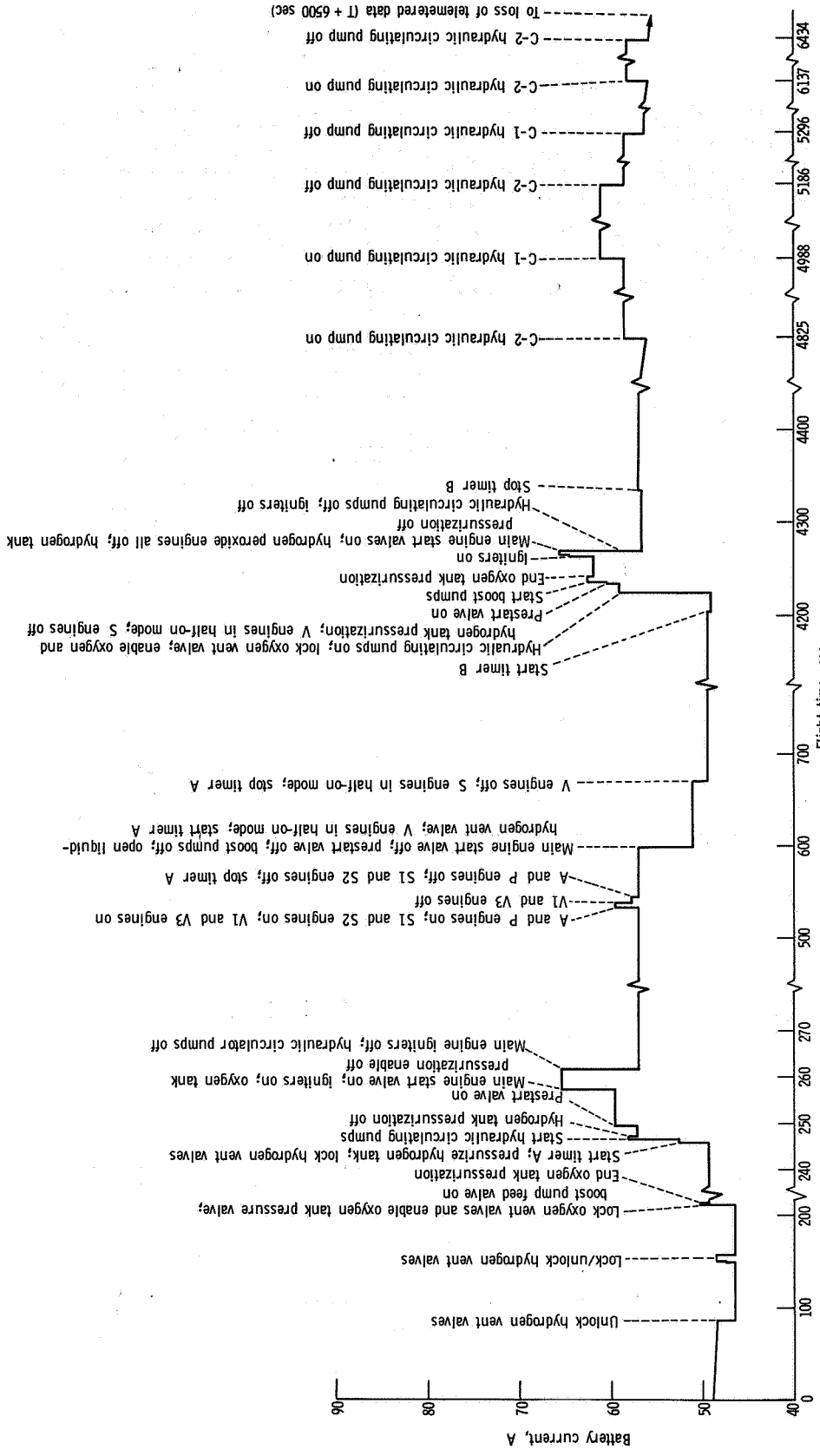

Figure VI-51. - Centaur main battery current profile, AC-17. (Note breaks and changes in time scale.)

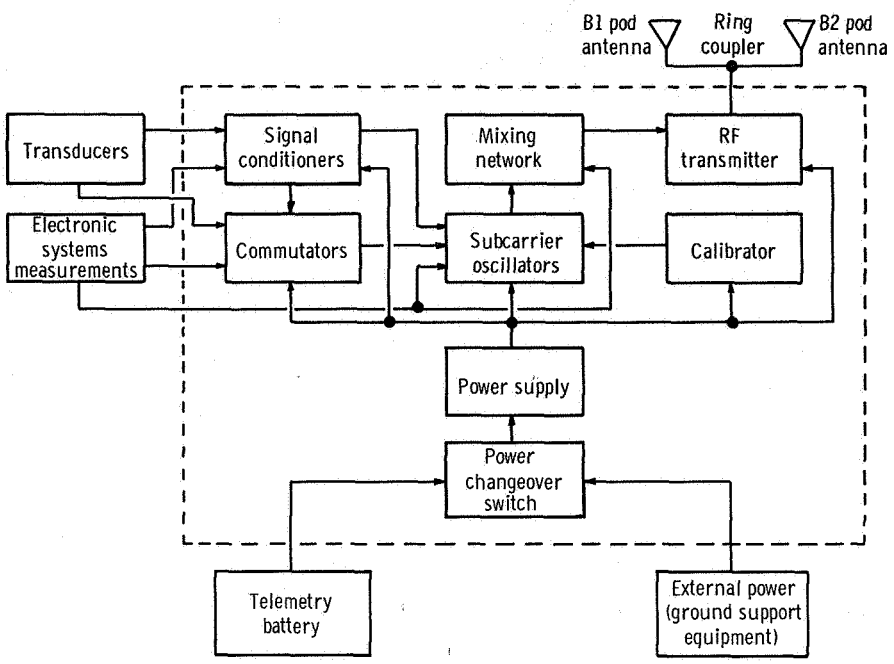

Figure VI-52. - Block diagram of Atlas telemetry system, AC-17.

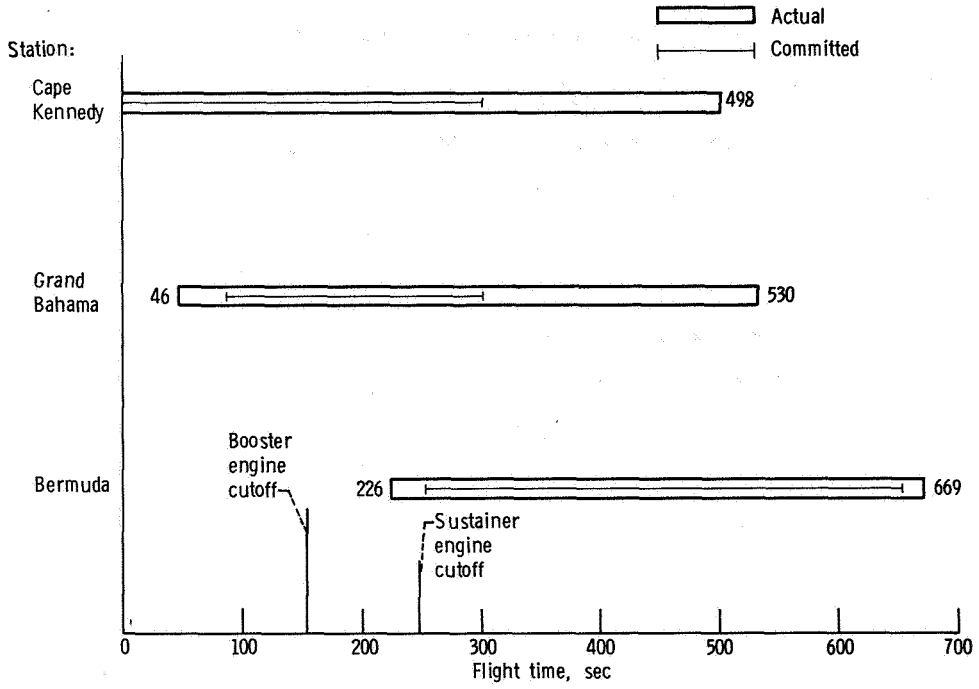

Figure VI-53. - Atlas telemetry coverage, AC-17.

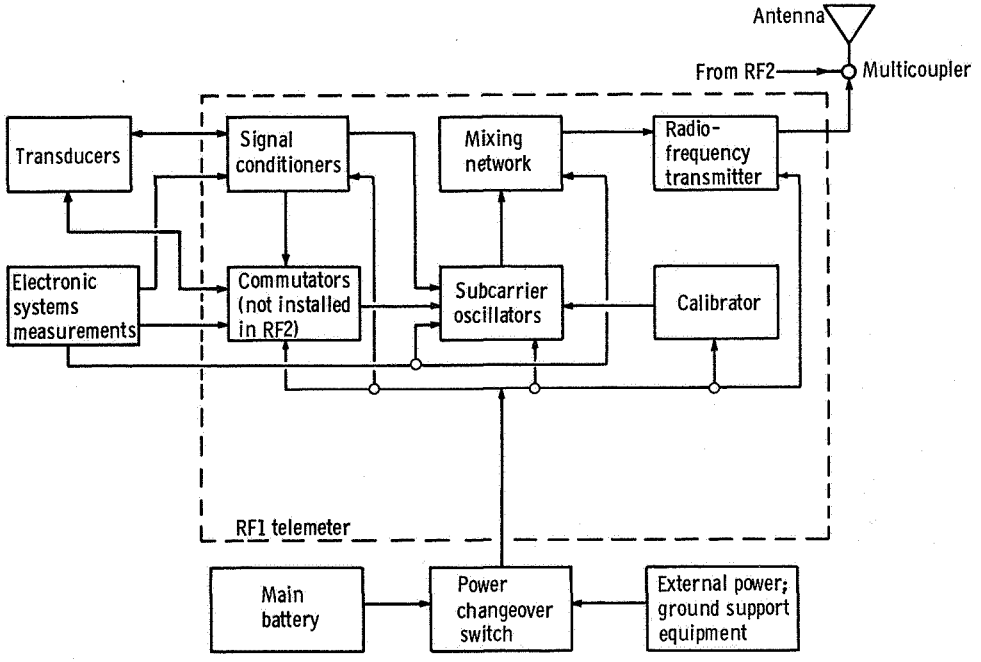

Figure VI-54. - Centaur telemetry system, typical each telemeter, AC-17.

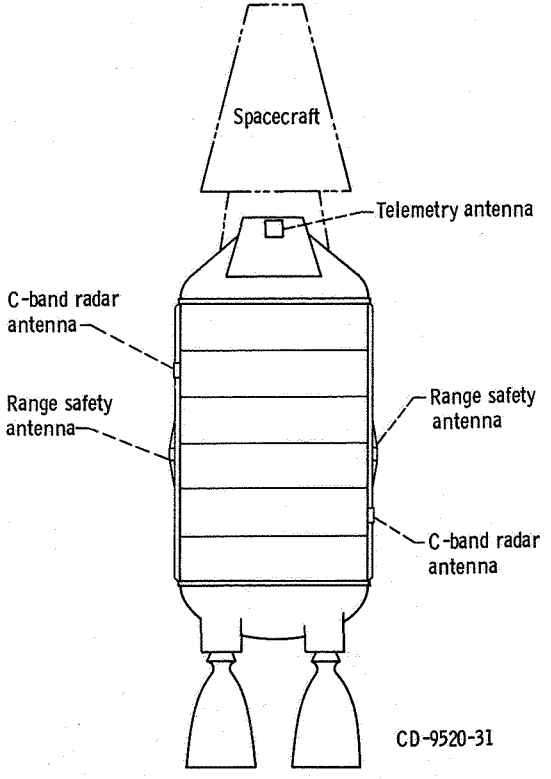

Figure VI-55. - Locations of Centaur antennas, AC-17.

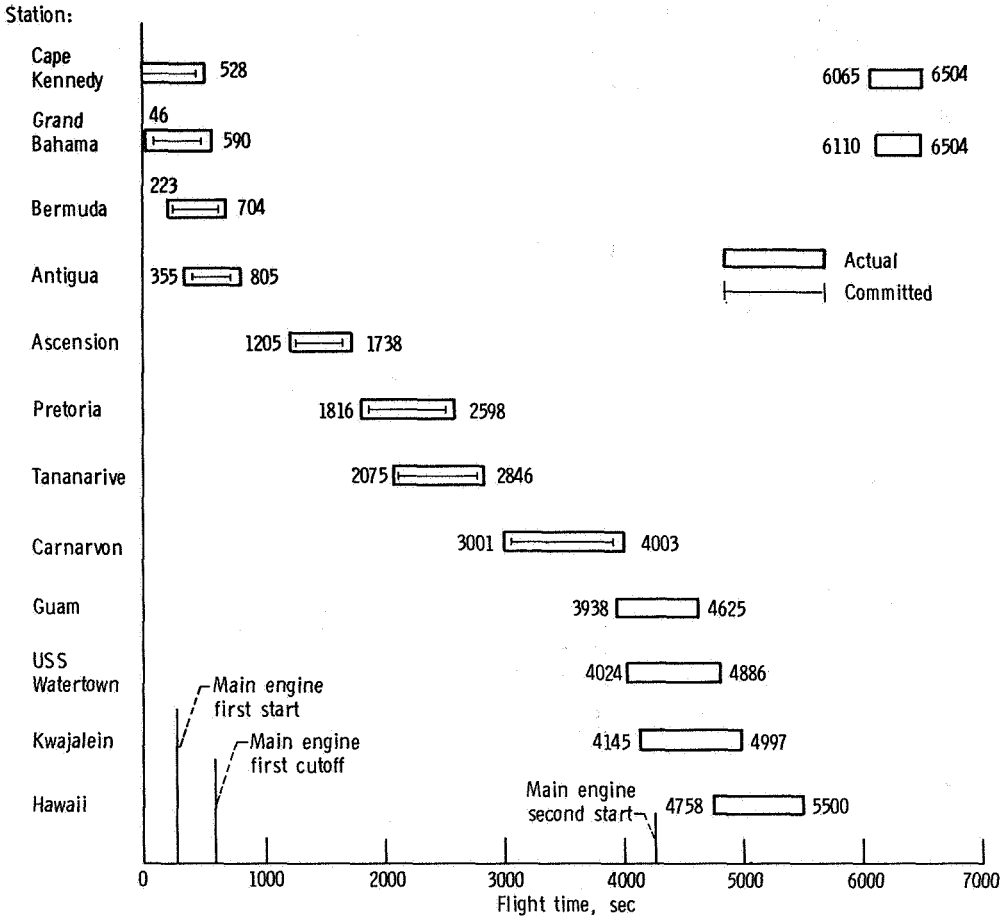

Figure VI-56. - Centaur telemetry coverage, AC-17.

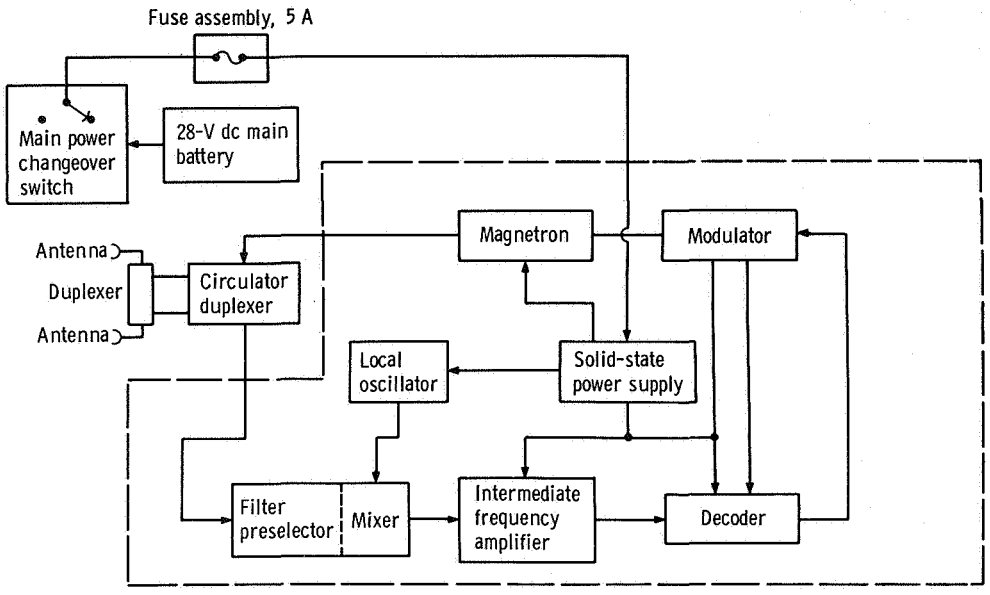

Figure VI-57. - Centaur C-band radar (airborne) system, AC-17.

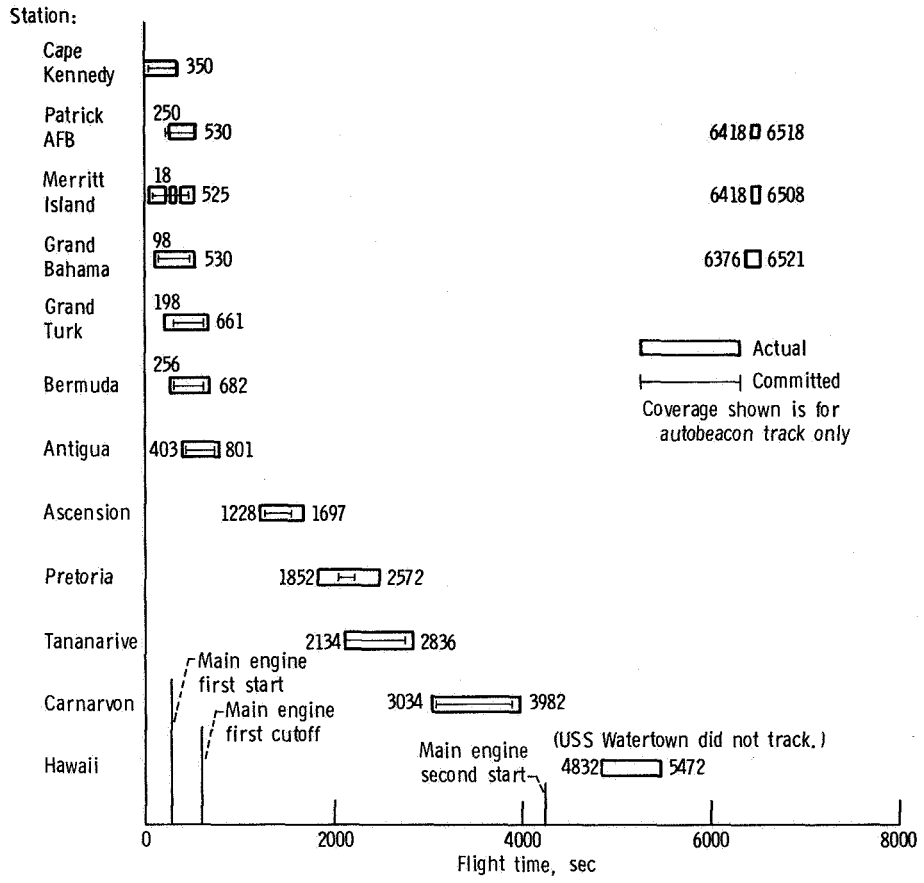

Figure VI-58. - C-band radar coverage, AC-17.

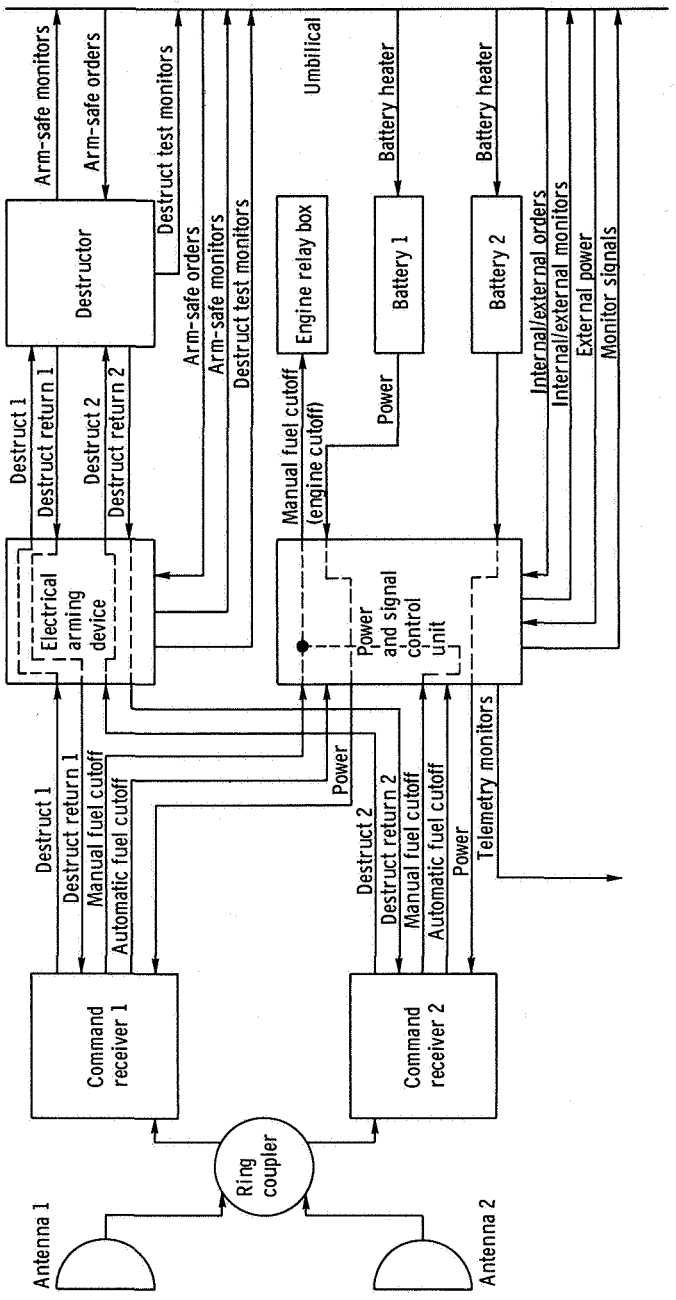

Figure VI-59. - Block diagram of Atlas vehicle destruct subsystem, AC-17.

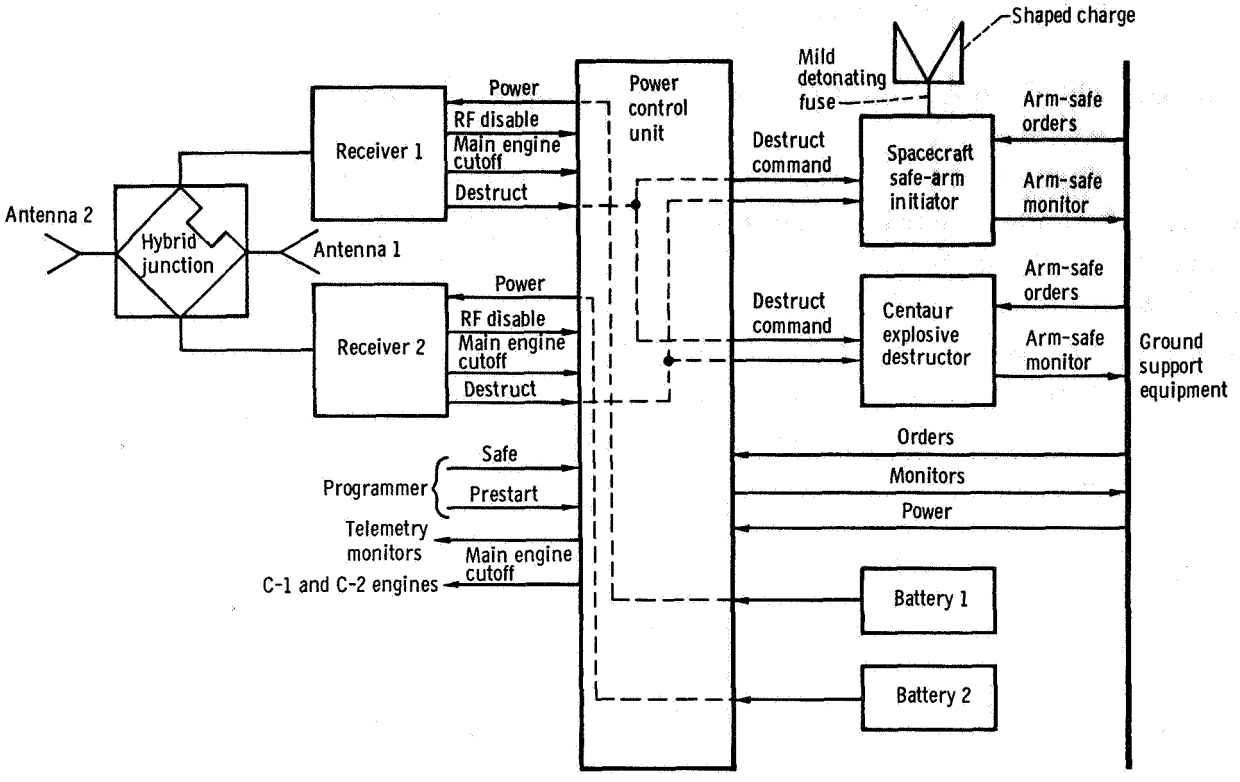

Figure VI-60. - Block diagram of Centaur vehicle destruct subsystem, AC-17.

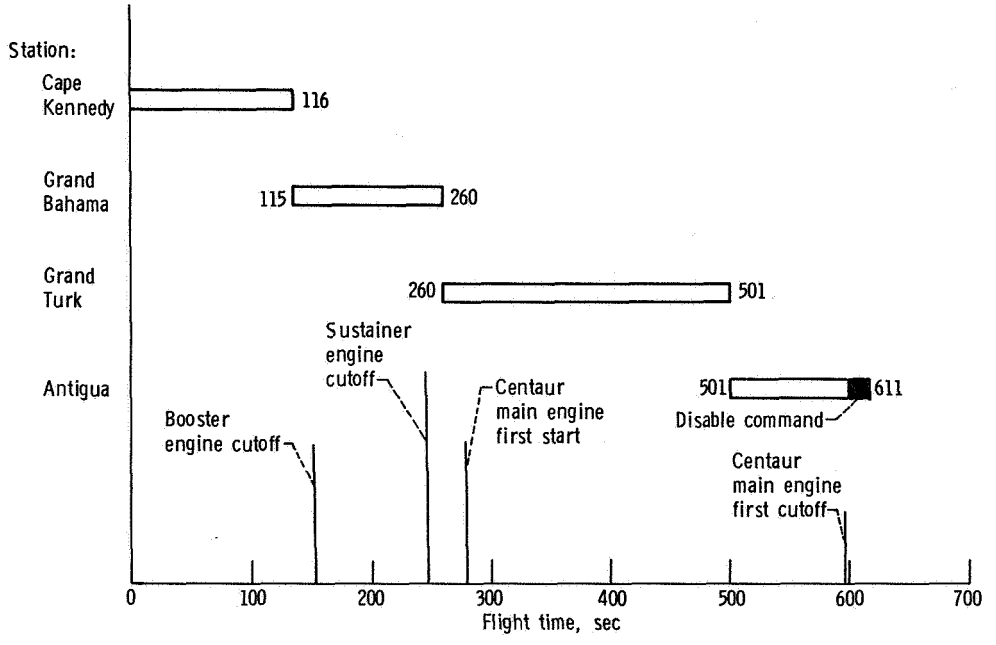

Figure VI-61. - Range safety command system transmitter coverage, AC-17.

GUIDANCE AND FLIGHT CONTROL SYSTEMS

by Dean W. Bitler, Edmund R. Ziemba, Donald F. Garman, and Corrine Rawlin

The objectives of the guidance and flight control systems are to stabilize and control the launch vehicle; steer the vehicle along the required flightpath; determine when the vehicle has reached the velocity required to place the spacecraft in the desired orbit; and provide command signals to other vehicle systems to start flight events such as jettison insulation panels, separate stages, and start main engines. An inertial guidance system is installed on the Centaur stage. Separate flight control systems are installed on the Atlas stage and on the Centaur stage.

The Atlas flight control system controls the Atlas-Centaur vehicle by gimbaling the Atlas booster, sustainer, and vernier engines to provide thrust vector control. The Centaur flight control system controls the Centaur (1) by gimbaling the main engines to provide thrust vector control while the main engines are operating or (2) by commanding various combinations of the hydrogen peroxide attitude control engines on or off during coast periods when the main engines are not operating.

Three modes of operation are used for stabilization, control, and guidance of the launch vehicle. These modes are "rate stabilization only," "rate stabilization and attitude control," and "rate stabilization and guidance control." Block diagrams of the three modes are shown in figure VI-62. The flight times during which a particular mode or a combination of modes are used are shown in figure VI-63. Figure VI-63 also shows the modes of operation of the Centaur hydrogen peroxide attitude control system which are discussed in the section Flight Control Systems that follows.

The rate-stabilization-only mode stabilizes the roll axis of the Centaur stage continuously after Atlas/Centaur separation. This mode is also used to stabilize the pitch and yaw axes of the Centaur stage for 4.0 seconds following both Centaur main engine starts. In this mode, output signals from rate gyros are used to control the vehicle. The output signal of each rate gyro is proportional to the angular rate of rotation of the vehicle about the input axis of each gyro. The output signal is then used to control gimbaling of the engine in a direction to minimize the output signal; hence, the vehicle angular rate is also minimized. Rate stabilization is also combined with position (attitude) information in the other two modes of operation.

The rate-stabilization-and-attitude-control mode is used for pitch, yaw, and roll control during the Atlas booster phase of flight and for roll control only during the Atlas sustainer phase. This mode is termed attitude control since the displacement gyros (one each for the pitch, yaw, and roll axes) provide a reference attitude to which the vehicle is to be alined. However, if the actual flightpath differs from the desired flightpath, there is no way of determining the difference and correcting the flightpath. The reference attitude is programmed to change during booster phase. These changes in reference

attitude cause the vehicle to roll to the programmed flight azimuth angle, and to pitch downward and yaw if required. Vehicle stabilization is accomplished in the same manner as in the rate-stabilization-only mode. The rate stabilization signals are algebraically summed with the attitude reference signals. These resultant signals (one signal for each axis) are then used to control and stabilize the vehicle by gimbaling the engines to minimize (null) the signal.

The rate-stabilization-and-guidance-control mode is used for the pitch and yaw axes during Atlas sustainer phase, for Centaur main engine firing, and during the coast period following main engine cutoff. In this mode, the guidance system provides the attitude and direction reference. If the resultant flightpath, as measured by the guidance system, is not the required flightpath, the guidance system issues steering signals to direct the vehicle to the required flightpath. Vehicle stabilization is accomplished in the same manner as in the rate-stabilization-only mode. The pitch and yaw rate stabilization signals are algebraically summed with the appropriate pitch and yaw steering signals from the guidance system. These resultant signals (one for pitch and one for yaw) are used to control and stabilize the vehicle.

Figure VI-64 is a simplified diagram of the interface between the guidance system and the flight control systems.

Guidance System

The Centaur guidance system is an inertial system which becomes completely independent of ground control at approximately T - 12 seconds.

System description. - The guidance system performs the following functions:

(1) Measures vehicle acceleration in fixed inertial coordinates

(2) Computes the values of actual vehicle velocity and position and computes the vehicle flightpath to attain the trajectory injection point

(3) Compares the actual position to the desired flightpath and issues steering signals

(4) Issues discrete commands

The guidance system consists of five separate units. Three of the units form a group called the "inertial measurement units." The other two units are the navigation computer unit and the signal conditioner unit. A simplified block diagram of the guidance system is shown in figure VI-65.

Inertial measurement units: The inertial measurement units measure vehicle acceleration and consist of the following three units:

(1) The inertial platform unit, which contains the platform assembly, gyros, and accelerometers

(2) The pulse rebalance, gyro torquer, and power supply unit, which contains the electronics associated with the accelerometers

(3) The platform electronics unit, which contains the electronics associated with the gyros

The platform assembly uses four gimbals which provide a three-axes coordinate system. The use of four gimbals, instead of three, allows complete rotation of all three vehicle axes about the platform without gimbal lock. Gimbal lock is a condition in which two axes coincide, causing loss of one degree of freedom. A gimbal is shown in figure VI-66. The azimuth gimbal is isolated from movements of the vehicle structure by the other three gimbals. The inertial components (three gyros and three accelerometers) are mounted on the azimuth (or inner) gimbal. A gyro and an accelerometer are mounted as a pair with their sensing axes parallel. The gyro and accelerometer pairs are also alined on three mutually perpendicular (orthogonal) axes corresponding to the three axes of the platform.

The three gyros are identical and are of the signal-degree-of-freedom, floated-gimbal, rate-integrating type. Each gyro monitors one of the three axes of the platform. These gyros are elements of control loops, the sole purpose of which is to maintain each axis fixed in inertial space. The output signal of each gyro is connected to a servoamplifier whose output controls a direct-drive torque motor which moves a gimbal of the platform assembly. By controlling each gimbal, the inner gimbal is fixed in inertial space and provides a stable known reference for the accelerometers. Since the inner gimbal is fixed in inertial space and the outer roll gimbal is attached to the vehicle, the angles between the gimbals provide a means for transforming steering signals from inertial coordinates to vehicle (body) coordinates. The transformation is accomplished by electromechanical resolvers mounted between gimbals. The resolvers produce electrical signals proportional to the sine and cosine functions of the gimbal angles. These electrical signals are used to provide an analog solution of the mathematical equations for coordinate transformation by interconnecting the resolvers in the proper manner.

The three accelerometers are identical and are of the single-axis, viscous-damped, hinged-pendulum type. The accelerometer associated with each axis measures the change in vehicle velocity along that axis by responding to acceleration. Acceleration of the vehicle causes the pendulum to move off center. The associated electronics then produce precise current pulses to recenter (rebalance) the pendulum. These rebalance pulses are either positive or negative depending on an increase or decrease in vehicle velocity. These rebalance pulses, representing changes in velocity (incremental velocity), are also routed to the navigation computer unit for computation of vehicle velocity.

Proper flight operation requires alinement and calibration of the inertial measuring units during launch countdown. The characteristic constant torque drift rate and mass unbalance along the input axis of each gyro are measured. The scale factor and zero bias offset of each accelerometer are also measured. These prelaunch-determined

values are stored in the navigation computer for use during flight. The inner gimbal of the platform is alined to the reference azimuth direction by ground-based optical equipment. This gimbal is also alined perpendicular to the local vertical by using the two accelerometers in the horizontal plane.

Navigation computer unit: The navigation computer computes velocity and other navigation and guidance parameters. It is a digital computer with a magnetic drum memory. The memory drum has a capacity of 2816 words (25 bits per word) of permanent storage, 256 words of temporary storage, and six special-purpose tracks. Permanent storage is prerecorded and cannot be altered by the computer. The temporary storage is the working storage of the computer. The six special tracks are for addressing, instruction register, multiplication, and integration.

The operation of the navigation computer is controlled by the prerecorded program. This program directs the computer to use the prelaunch equations, navigation equations, and guidance equations. The prelaunch equations establish the initial conditions for the navigation and guidance equations. Initial conditions include (1) a reference trajectory; (2) launch-site geographical position, and (3) initial values of navigation and guidance functions. Based on these initial conditions, the guidance system starts flight operation approximately 12 seconds before lift-off.

The navigation equations are used to compute vehicle velocity and actual position. Velocity is determined by algebraically summing the incremental velocity pulses from the accelerometers. An integration is then performed on the computed velocity to determine actual position. Corrections for the prelaunch-determined gyro and accelerometer constants are also made during the velocity and position computation to improve the navigation accuracy. For example, the velocity data derived from the accelerometer measurements are adjusted to compensate for the accelerometer scale factors and zero offset biases measured during the launch countdown. The direction of the velocity vector is also adjusted to compensate for the gyro constant-torque drift rates measured during the launch countdown.

The guidance equations continually compare actual position and velocity with the position and velocity required for orbital injection. Based upon this position comparison, steering signals are generated to steer the vehicle along an optimized flightpath to obtain the desired injection conditions. The guidance equations are used to generate six discrete commands: booster engine cutoff, sustainer engine cutoff backup, Centaur main engine first cutoff, main engine second cutoff, "null" the propellant utilization system, and start the B timer. The booster engine cutoff command and the sustainer engine cutoff backup command are issued when the measured vehicle acceleration equals predetermined values. The Centaur main engine cutoff commands are issued when the computed angular momentum equals that required for injection into the appropriate orbit. The command to null the propellant utilization system is issued 15 seconds before the computer-predicted Centaur main engine second cutoff command. The command to start

the B timer is issued when criteria governing positioning of Centaur second powered phase are satisfied.

During the booster phase of flight, the navigation computer provides pitch and yaw steering to the Atlas stage. AC-17 is the first flight on which the Centaur provided the entire pitch program. (Yaw steering has been provided by Centaur on previous flights.) One pitch program and one yaw program are selected, based on prelaunch upper-wind soundings, from a series of predetermined programs. These selected programs are entered and stored in the computer during launch countdown. The programs consist of discrete pitch and yaw turning rates for specified time intervals from T + 15 seconds until booster engine cutoff. These programs permit changes to be made in the flight reference trajectory during countdown to reduce anticipated aerodynamic heating and structural loading conditions on the vehicle.

The B timer starts and controls the sequence for main engine second start. When the engines are started, the resulting vehicle acceleration is sensed by the guidance system/guidance equations. When the proper acceleration level is sensed, the guidance equations automatically branch to the second-powered-phase mode of operation. This mode includes the issuance of the main engine second cutoff command. Before MECO-2, the B timer has been stopped; the second MECO command is used to restart the B timer. The B timer, in turn, issues commands to control subsequent events which include spacecraft separation. Therefore, if the engines do not start, the guidance equations are not switched to the second-powered-phase mode; and, consequently, the main engine second cutoff command is not issued, the B timer is not restarted, and the timer switches which initiate spacecraft separation are not activated.

Signal conditioner unit: The signal conditioner unit is the link between the guidance system and the vehicle telemetry system. This unit modifies and scales guidance system parameters to match the input range of the telemetry system.

System performance. - The performance of the guidance system was satisfactory. Guidance system data were evaluated for the period between T - 0 seconds and the scheduled Centaur main engine second start. The issuance of discrete commands; the operation of the guidance steering loops, gyro control loops, and accelerometer loops; and other measurements were evaluated in terms of general performance.

Discrete commands: All the guidance system discrete commands through the Centaur main engine first powered phase were issued as expected by the airborne computer, including the L1 discrete which starts the B timer and initiates the Centaur main engine second start. No subsequent discrete commands were issued because of the failure to achieve Centaur second start. Table VI-9 lists the discretes, the criterion for the issuance of each discrete, and the actual and predicted times of occurrence.

Guidance steering loops: The pitch and yaw steering signals issued by the guidance system are proportional to the components of the steering vector (desired vehicle

pointing vector) along the vehicle pitch and yaw axes. The steering signals have been converted into the angular errors between the steering vector and the vehicle roll axis (vehicle pointing vector) in the pitch and yaw planes.

Guidance steering was activated at 8 seconds prior to booster engine cutoff. At this time the pitch error was 7^{o} nose down and the yaw error was 1.7^{o} nose left. The vehicle attitude changes were required to correct for errors accumulated during the booster phase of the flight, when the guidance system is supplying the preselected pitch and yaw signals. The steering signals were less than 1^{o} in both pitch and yaw throughout the sustainer phase of flight. Guidance steering was deactivated at sustainer engine cutoff in preparation for Atlas/Centaur separation. When guidance steering was reactivated, about 4 seconds after Centaur main engine first start, the pitch error was 7^{o} nose down and the yaw channel indicated no steering error. During the Centaur first powered phase the steering signals did not exceed 3^{o} in pitch and 1.5^{o} in yaw. During coast phase the steering signals did not exceed 5^{o} in pitch and yaw. At T + 3665.1 seconds the steering signals respond to the reorientation maneuver prior to the Centaur main engine start. The steering signals were disabled during the planned engine second start sequence.

Gyro control loops and accelerometer loops: At T + 56 seconds the fourth gimbal uncaged. The inertial platform was stable throughout the Atlas and Centaur powered phases of flight, and also through the coast phase prior to Centaur second start. The platform gimbal control loops operated satisfactorily to maintain the inertial reference with maximum displacement errors of less than 15 arc-seconds (dynamic accuracy tolerance, 60 arc-sec). Normal low-frequency oscillations (2 Hz) were observed in all gyro control loops and are attributed to vehicle dynamics during powered phases. The accelerometer loops operated satisfactorily through Atlas and Centaur powered phases and Centaur coast phase with a maximum of less than 1 arc-second of pendulum displacement.

Other measurements: All the guidance system signals and measurements which were monitored during the flight were normal and indicated satisfactory operation of the system. All temperature control functions operated within range, and all system skin temperatures remained within specifications.

Flight Control Systems

System description - Atlas. - The Atlas flight control system provides the primary functions required for vehicle stabilization, control, sequencing, and execution of guidance steering signals and consists of the following major units:

(1) The displacement gyro unit, which contains three single-degree-of-freedom, floated, rate-integrating gyros and associated electronic circuitry for gain selection and signal amplification: These gyros are mounted to the vehicle structure in an orthogonal

triad configuration alining the input axis of a gyro to its respective vehicle axis of pitch, yaw, or roll. Each gyro provides an electrical output signal proportional to the integral of the time rate of change of angular displacement from the gyro reference axis.

(2) The rate gyro unit, which contains three single-degree-of-freedom, floated rate gyros and associated electronic circuitry: These gyros are mounted in the same manner as the displacement gyro unit. Each gyro provides an electrical output signal proportional to the angular rate of rotation of the vehicle about the gyro input (reference) axis.

(3) The servoamplifier unit, which contains electronic circuitry to amplify, filter, integrate, and algebraically sum combined position and rate signals with engine position feedback signals: The electrical outputs of this unit direct the hydraulic actuators which gimbal the engines to provide thrust vector control.

(4) The programmer unit, which contains an electronic timer; arm-safe switch; high-, low-, and medium-power electronic switches; and circuitry to set the roll program from launch ground equipment: The programmer issues discrete commands to other units of the Atlas flight control system and to the following systems: Atlas propulsion, Atlas pneumatic, vehicle separation, and Centaur flight control.

System performance - Atlas. - The flight control system performance was satisfactory throughout the Atlas phase of flight and compared favorably with previous flights. The corrections required to control the vehicle because of disturbances were well within the system capabilities. The vehicle dynamic responses resulting from each flight event were evaluated in terms of amplitude, frequency, and duration as observed on rate gyro data (table VI-10). In this table, the control capability is the ratio of engine gimbal angle used to the available total engine gimbal angle, in percent. The percent control capability used at the times of the flight events includes that necessary for correction of the vehicle transient disturbances and for steady-state requirements.

The programmer was started at 1.1-meter (42-in.) rise, which occurred at approximately T + 1 second. At this time the vehicle began to gimbal the engines for vehicle control. The significant vehicle transients were quickly damped and required a maximum of 12 percent of the control capability. At T + 2 seconds the roll program was initiated. Rate gyro data indicated an average clockwise roll rate varying between 0.6 and 0.7 degree per second over the 13-second period. This integrated to approximately 8.2° of roll, which compared favorably with the 8° required to change the vehicle heading from the 105° launcher azimuth to the 97° flight azimuth.

The pitch and yaw programs were initiated at T + 15 seconds. The programmed rates are shown in table VI-11. The guidance pitch program Code PP31 was selected based upon launch day upper-wind data. The measured pitch rate from T + 15 to T + 25 seconds was approximately 0.2 degree per second. From T + 25 seconds the measured rate was observed to be between -0.54 and -0.63 degree per second. These measured rates compare favorably with the programmed rates of -0.190 and -0.556 degree per

second for the two respective time periods. Comparison of the measured and programmed rates was not made after T + 35 seconds because the rates thereafter are predominately caused by aerodynamic loading. Guidance yaw program Code YP6 was also selected based upon launch day upper-wind data. The yaw rates were too small to be distinguished on rate gyro data.

Rate gyro data indicated that the period of maximum aerodynamic loading was approximately from T + 86 to T + 93 seconds. During this period a maximum of 28 percent of the control capability was required to overcome both steady-state and transient loading.

Atlas booster engine cutoff occurred at approximately T + 152 seconds. The rates imparted to the vehicle by this transient required 12 percent of the sustainer engine gimbal capability. The Atlas booster engine section was jettisoned at about 3 seconds after booster engine cutoff. The rates imparted by this disturbance were nearly damped by the time Centaur guidance was admitted.

During the Atlas booster phase of the flight, the Atlas flight control system provided the vehicle attitude reference. At approximately 8 seconds after booster engine cutoff the Centaur guidance system provided the attitude reference. A maximum of 28 percent of the total control capability was required to move the vehicle to the new reference. The maximum vehicle rate transient during this change was a pitch rate of 2.34 degrees per second peak to peak, with a duration of 6 seconds.

Insulation panels and nose fairing were jettisoned at T + 196.8 and T + 233.5 seconds, respectively. The observed vehicle rate transients due to these disturbances were damped within 2 seconds.

The maximum angular rates observed at sustainer engine cutoff and Atlas/Centaur separation occurred in the pitch plane and were less than 1 degree per second.

System description - Centaur. - The Centaur flight control system provides the primary means for vehicle stabilization and control, execution of guidance steering signals, and timed switching sequence for programmed flight events. The Centaur flight control system (fig. VI-67) consists of the following major units:

(1) The rate gyro unit, which contains three single-degree-of-freedom, floated, rate gyros with associated electronics for signal amplification gain selection and conditioning of guidance steering signals: These gyros are mounted to the vehicle in an orthogonal triad configuration alining the input axis of each gyro to its respective vehicle axis of pitch, yaw, or roll. Each gyro provides an electrical output signal proportional to the angular rate of rotation of the vehicle about the gyro input (reference) axis.

(2) The servoamplifier unit, which contains electronics to amplify, filter, integrate, and algebraically sum combined position and rate signals with engine position feedback signals: The electrical outputs of this unit issue signals to the hydraulic actuators which control the gimbaling of the engines. In addition, this unit contains the logic and

threshold circuitry to control the engines of the hydrogen peroxide attitude control system.

(3) The electromechanical sequence timer unit, which contains a 400-hertz synchronous motor to provide the time reference and actuate switches at program times: Two timer units, designated "A" and "B," are needed because of the large number of discrete commands required for this two-powered-phase mission.

(4) The auxiliary electronics unit, which contains logic, relay switches, transistor switches, power supplies, control circuitry for the electromechanical timer, circuitry for conditioning computer-generated discretes, and an arm-safe switch: The arm-safe switch electrically isolates valves and pyrotechnic devices from the control switches. The combination of the electromechanical timer units and the auxiliary electronics unit issues discretes to other units of the Centaur flight control system and to the following systems: propulsion, pneumatic, hydraulic, separation, propellant utilization, telemetry, spacecraft, and electrical.

Vehicle steering during Centaur powered flight is by thrust vector control through gimbaling of the two main engines. There are two actuators for each engine to provide pitch, yaw, and roll control. Pitch control is accomplished by moving both engines together in the pitch plane; yaw control is accomplished by moving both engines together in the yaw plane; and roll control is accomplished by moving the engines differentially in the yaw plane. Thus, the yaw actuator responds to an algebraically summed yaw/roll command. By controlling the direction of thrust of the main engines, the flight control system maintains the flight of the vehicle on a trajectory directed by the guidance system. After main engine cutoff, control of the vehicle is maintained by the flight control system through selective firing of hydrogen peroxide engines. A more complete description of the engines and the propellant supply for the attitude control system is presented in the PROPULSION SYSTEMS section of this report.

The logic circuitry, which commands the 14 hydrogen peroxide engines either on or off, is contained in the servoamplifier unit of the flight control system. Figure VI-68 shows the alphanumeric designations of the engines and their locations on the aft end of the vehicle. Algebraically summed position and rate signals are the inputs to the logic circuitry. The logic circuitry provides five modes of operation designated "all off," "separate on," "A and P separate on," "V half on," and "S half on." These modes of operation are used during different periods of the flight and are controlled by the electromechanical sequence timer unit. A summary of the modes of operation is presented in table VI-12. In this table "threshold" designates the vehicle rate in degrees per second that has to be exceeded before the engines are commanded "on."

System performance - Centaur. - The Centaur flight control system performance was satisfactory. Vehicle stabilization and control were maintained until the time that main engine second start was to occur. All events sequenced by the timers, up to the time the B timer should have been restarted by the main engine second cutoff command,

were executed at the required times. No planned events (one of which was spacecraft separation) were commanded after MECO-2. The following evaluation is presented in paragraphs related to time sequenced portions of the flight. For typical time periods of guidance/flight control modes of operation, refer to figure VI-63. Vehicle dynamic responses for selected flight events are tabulated in table VI-10.

Sustainer engine cutoff (SECO) to Centaur main engine first cutoff (MECO-1) (T + 246.2 to T + 595.8 sec): The Centaur A timer was started at sustainer engine cutoff by a command from the Atlas programmer. Appropriate commands were issued to separate the Centaur stage from the Atlas stage and to initiate the Centaur main engine first firing sequence. There were no significant vehicle transients during separation. Vehicle control was maintained during the period between sustainer engine cutoff and main engine start by gimbaling the main engines as they were discharging boost pump turbine exhaust and chilldown flow. Prestart and start operations resulted in a vehicle attitude deviation of 4^{o} in pitch and 1.5^{o} in yaw. These errors were corrected when guidance steering was admitted approximately 4 seconds after main engine start. The control capability used to control this disturbance was a maximum of 8 percent. Steering corrections remained under 1.5^{o} during the first powered phase. Rate gyro data indicated an unusual 37-hertz oscillation in pitch, yaw, and roll for a period ranging from approximately T + 471 to T + 548 seconds. The highest rates during this time were observed in the pitch plane. The pitch rate data also contained a lower frequency (0.22 Hz) oscillation. The maximum peak-to-peak pitch rate observed was approximately 3.16 degrees per second at the lower frequency. Investigation of this phenomenon indicated coupling between the engine flexible body dynamics and the control system and resulted in the implementation of a filter on the rate gyro output of subsequent Centaurs. The remainder of the first powered phase appeared normal as compared to previous flights. Main engine first cutoff occurred at approximately T + 595.8 seconds. Transients due to engine cutoff were damped within 4 seconds as the vehicle entered the coast phase of flight.

Main engine first cutoff (MECO-1) through main engine second start (MES-2) command (from T + 595.8 to T + 4265.1 sec): The hydrogen peroxide attitude control system was active between MECO-1 and MES-2 in the V-half-on and S-half-on modes of operation and performed satisfactorily. (These modes of operation are described in table VI-12. The AC-17 attitude control system configuration is shown in figures VI-11 and VI-12). Analyses of rate gyro histories during the V-half-on mode indicated nearly constant disturbance torques in pitch, yaw, and roll following MECO-1 and preceding MES-2 command. At MECO-1 + 76 seconds the S-half-on mode was commanded. During the S-half-on mode an expected loss of telemetry coverage occurred 322 seconds after MECO-1. The only planned event which occurred during this period was venting of the hydrogen tank. When telemetry was again acquired both the milligravity accelerometer and the guidance accelerometers indicated an increase from their previous values. This

increase corresponded to a positive axial force of approximately 4.0 newtons (0.9 lbf). The axial acceleration history of the vehicle during the S-half-on mode is shown in figure VI-69.

Associated with the increase in axial acceleration was a nose-down pitch disturbance torque. Disturbance torques in yaw and roll were not observed to change. To explain the forces which were acting on the vehicle to cause the changes observed in the data is speculative. Hydrogen tank venting forces were observed to cause little rate gyro activity, which is consistent with past flight experience. The venting was, therefore, discounted as the cause of the observed change in vehicle dynamics. A cryogenic leak in the aft bulkhead area was considered the most likely cause of the changes seen in vehicle dynamics and the changes observed in hydrogen peroxide system performance later in the flight. A hypothetical placement of an axial force on the aft bulkhead would place the vector in the throat of the C-1 engine.

The axial acceleration of the vehicle remained fairly constant for the remainder of the S-half-on mode. From approximately T + 2950 to T + 4225.1 seconds, the end of the S-half-on mode, there was a gradual increase in acceleration of approximately 0.13 g's. The disturbance torques on the vehicle appeared to remain constant during the time period for which the gradual increase in axial acceleration was observed.

At T + 4225.1 seconds the V-half-on mode was initiated and lasted for 40 seconds to assure settled propellants for main engine second start. During this period the boost pumps were commanded to start. Hydrogen peroxide did not reach the boost pumps and main engine second start did not occur (see section Hydrogen Peroxide Engine and Supply System). The vehicle continued to coast without attitude control and subsequently tumbled. Because of the design of sequenced events, it was impossible to separate the spacecraft.

TABLE VI-9. - DISCRETE COMMANDS, AC-17

Discrete command	Criterion for discrete to be issued	Actual time, T + sec	Predicted time, T + sec
Booster engine cutoff	When square of vehicle thrust acceleration is greater than 27.5 $(g's)^2$	152.0	152.8
Sustainer engine cutoff backup	When square of vehicle thrust acceleration is less than 0.7 $(g's)^2$	248.0	253.0
Centaur main engine first cutoff	When angular momentum criteria for parking orbit is satisfied	595.8	588.2
B timer start (Centaur main engine second start sequence)	When positioning criteria with reference to the earth has been satisfied for the second powered phase	4262.0	4202.0
Null propellant utilization		Not issued	4312.0
Centaur main engine second cutoff	When angular momentum criteria for transfer orbit are satisfied	Not issued	4365.5
Terminate lock vent valves		Not issued	6663.5
Energize power changeover switch		Not issued	6665.5

TABLE VI-10. - VEHICLE DYNAMIC RESPONSE TO FLIGHT DISTURBANCES, AC-17

Event	Time[a], sec	Measurement	Rate gyro peak-to-peak amplitude, deg/sec	Transient frequency, Hz	Transient duration, sec	Required control capability, percent
Lift-off	T + 0	Pitch	1.08	12.5	(b)	(c)
		Yaw	1.07	10.0	(d)	(c)
		Roll	.63	9.1	(b)	(c)
1.1-Meter (42-in.) rise	Between T + 0.94 and T + 1	Pitch	1.62	7.8	1.5	12
		Yaw	.89	6.7	6.0	2
		Roll	2.72	.8	1.5	2
Region of maximum aerodynamic loading	T + 91 T + 98 T + 91	Pitch	1.44	0.4	T + 86 to T + 93	28
		Yaw	1.69	.39		24
		Roll	1.63	.5		24
Booster engine cutoff	T + 152.1	Pitch	2.78	5.0	3.0	8
		Yaw	1.60	5.0	1.2	12
		Roll	2.26	1.25	3.0	12
Booster engine jettison	T + 155.2	Pitch	[e]1.98	5.0	5.0	(f)
			2.16	.72	5.0	(f)
		Yaw	3.03	6.25	5.0	(f)
			4.27	.91	10.0	(f)
		Roll	[g]2.90	5.0	5.0	(f)
			2.90	.72	5.0	(f)
Admit guidance	T + 160.1	Pitch	2.34	0.33	6.0	28
		Yaw	.36	5.5	5.0	24
		Roll	1.18	.78	9.0	8
Insulation panel jettison	T + 196.8	Pitch	2.52	20	1.0	(h)
		Yaw	1.25	14.3	.7	8
		Roll	1.45	20	.8	(h)
Nose fairing jettison	T + 233.5	Pitch	6.02	25	2.0	(h)
		Yaw	1.96	30	1.0	(h)
		Roll	1.99	35	1.0	(h)
Sustainer engine cutoff	T + 245.6	Pitch	0.90	40 and 0.73	1.5	---
		Yaw	.36	20	(i)	---
		Roll	.91	.83	.6	---
Atlas/Centaur separation	T + 248.1	Pitch	0.99	30	0.7	---
		Yaw	(i)	------	---	---
		Roll	.73 (spike)	40	(i)	---
Main engine first start	T + 258.9	Pitch	2.52	0.32	3	8
		Yaw	.713	.50	3	8
		Roll	2.18	.455	2.3	8
Admit guidance	T + 262.9	Pitch	2.70	0.15	9	8
		Yaw	.54	5	2	8
		Roll	.36	40	2	8
Main engine first cutoff	T + 595.9	Pitch	5.21	30	1	12
		Yaw	3.21	30	.7	12
		Roll	1.90	30	4	12

[a]Time of transient as seen on rate gyro data.
[b]Increase to T + 1 sec.
[c]Autopilot not yet active.
[d]Similar oscillation continues to T + 1 sec.
[e]Spike of 5.39 deg/sec at 1.4 Hz.
[f]Sustainer engine control inactive during booster engine jettison.
[g]Spike of 6.66 deg/sec at 5.0 Hz.
[h]Noisy data.
[i]Too small to measure.

TABLE VI-11. - PROGRAMMED PITCH AND YAW RATES, AC-17

Time from lift-off, sec	Pitch program code PP31, deg/sec	Yaw program code YP6, deg/sec
0 to 15	0	0
15 to 25	-.190	-.153
25 to 45	-.556	-.029
45 to 50	-.712	+.126
50 to 60	-.750	-.002
60 to 75	-.740	+.101
75 to 79	-.720	+.059
79 to 97	-.752	-.042
87 to 103	-.630	-.030
103 to 130	-.390	0
130 to Booster engine cutoff	-.230	0

TABLE VI-12. - DESCRIPTION OF ATTITUDE CONTROL SYSTEM MODES OF OPERATION, AC-17

[Thrust; A engines, 15.6 N (3.5 lbf); P engines, 26.7 N (6.0 lbf); S engines, 13.3 N (3.0 lbf); V engines, 222.4 N (50.0 lbf).]

Mode	Flight period	Description
All off	Powered phases	This mode prevents operation of all attitude control engines regardless of error signals.
Separate on[a]	Main engine second cutoff (MECO-2) + 570 seconds to MECO-2 + 2300 seconds	When in separate-on mode, a maximum of two A and two V engines and one P engine fire. These engines fire only when appropriate error signals pass their respective thresholds. A engines: When 0.2-deg/sec threshold is exceeded, suitable A engines fire to control in yaw and roll. A1/A4 and A2/A3 combinations are inhibited. P engines: When 0.2-deg/sec threshold is exceeded, suitable P engine fires to control in pitch. P1/P2 combination is inhibited. S engines: Off. V engines: When 0.3-deg/sec threshold is exceeded, suitable engines fire (as backup for higher rates). V1/V3 and V2/V4 combinations are inhibited.
A and P separate on[a]	Main engine second start (MES-2) + 5 seconds to MES-2 + 197 seconds	This mode is the same as separate-on, except V engines are inhibited. During this mode, alinement and retromaneuver are accomplished.
V half on	1. MECO-1 to MECO-1 + 76 seconds 2. MES-2 - 40 seconds to MES-2 3. MECO-2 to MECO-2 + 5 seconds 4. MECO-2 + 197 to MECO-2 + 246 seconds	A engines: When 0.2-deg/sec threshold is exceeded, suitable A engines fire to control in roll only. P engines: Off. S engines: Off. V engines: When 0.2-deg/sec threshold is exceeded, a minimum of two and a maximum of three V engines fire to control in pitch and yaw. When there are no error signals, V2/V4 combination fires continuously. This continuous firing serves two purposes: to settle propellants, in flight periods 1, 2, and 3; to provide lateral and added longitudinal separation between Centaur and spacecraft, in flight period 4.
S half on	1. MECO-1 + 76 seconds to MES-2 - 40 seconds 2. MECO-2 + 246 seconds to MECO-2 + 570 seconds	A engines: When 0.2-deg/sec threshold is exceeded, suitable A engines fire to control in roll only. P engines: Off. S engines: When 0.2-deg/sec threshold is exceeded, a minimum of two and a maximum of three S engines fire to control in pitch and yaw. When there are no error signals, S2/S4 combination fires continuously for propellant retention purposes. V engines: When 0.3-deg/sec threshold is exceeded, a minimum of one and a maximum of three V engines fire to control in pitch and yaw. When a V engine fires, the corresponding S engine is commanded off. This mode is used to retain settled propellants, in flight period 1; and to provide lateral and added longitudinal separation between Centaur and spacecraft at a low peroxide consumption rate, in flight period 2.
Separately commanded	1. MES-1 + 290 seconds to MES-1 + 292.5 seconds 2. MES-1 + 290 seconds to MES-1 + 300 seconds	V1/V3 combination on. A and P engines on; S1 and S3 engines on. Engines were commanded on to thermal condition them for long coast.

[a]This mode was available; however, it was not used because of the failure.

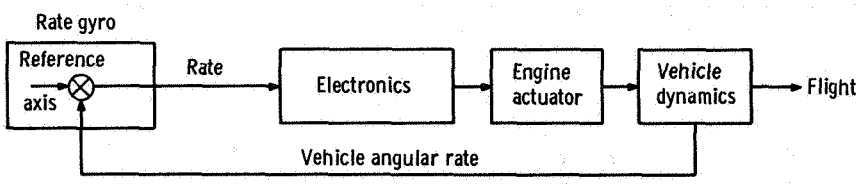

(a) Rate-stabilization-only mode.

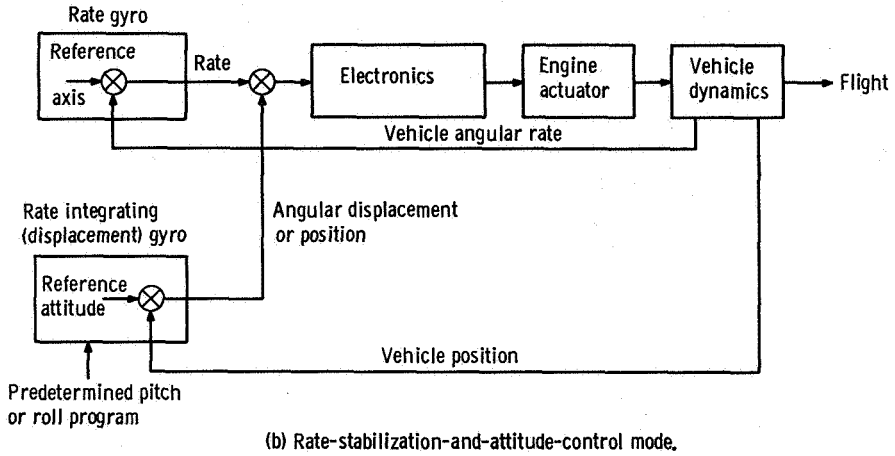

(b) Rate-stabilization-and-attitude-control mode.

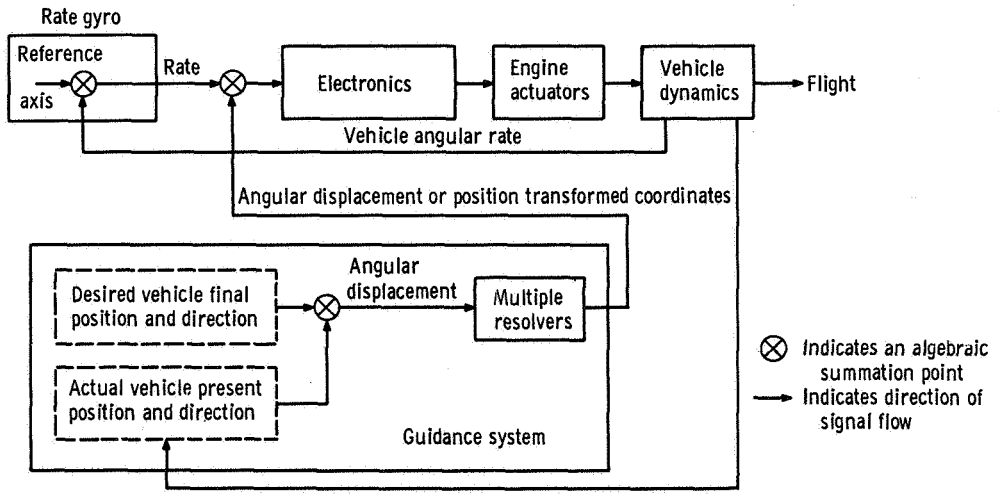

(c) Rate-stabilization-and-guidance-control mode.

Figure VI-62. - Guidance and flight control modes of operation, AC-17.

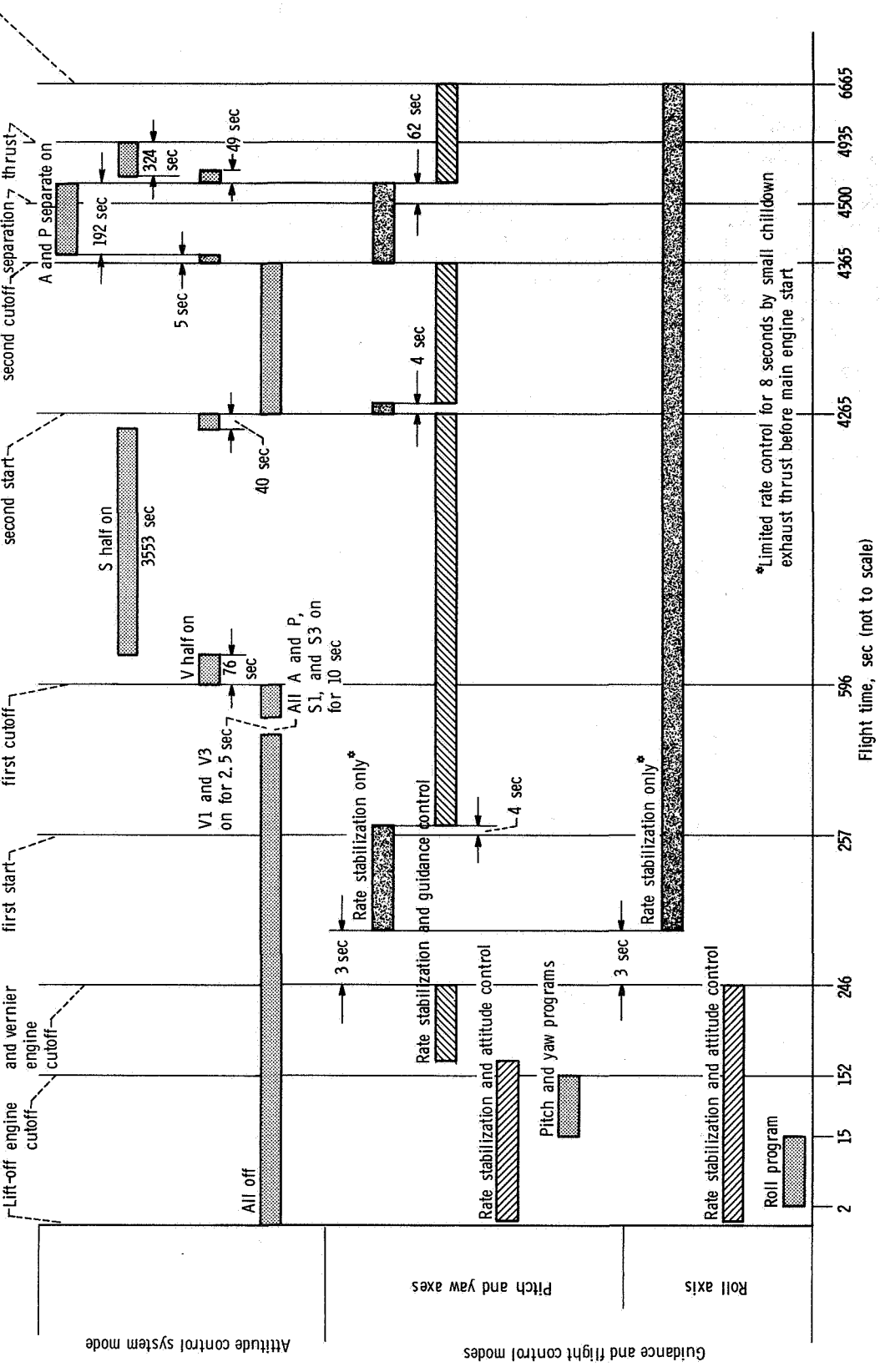

Figure VI-63. - Planned time periods of guidance and flight control modes and attitude control system mode of operation, AC-17. Times shown are for reference only.

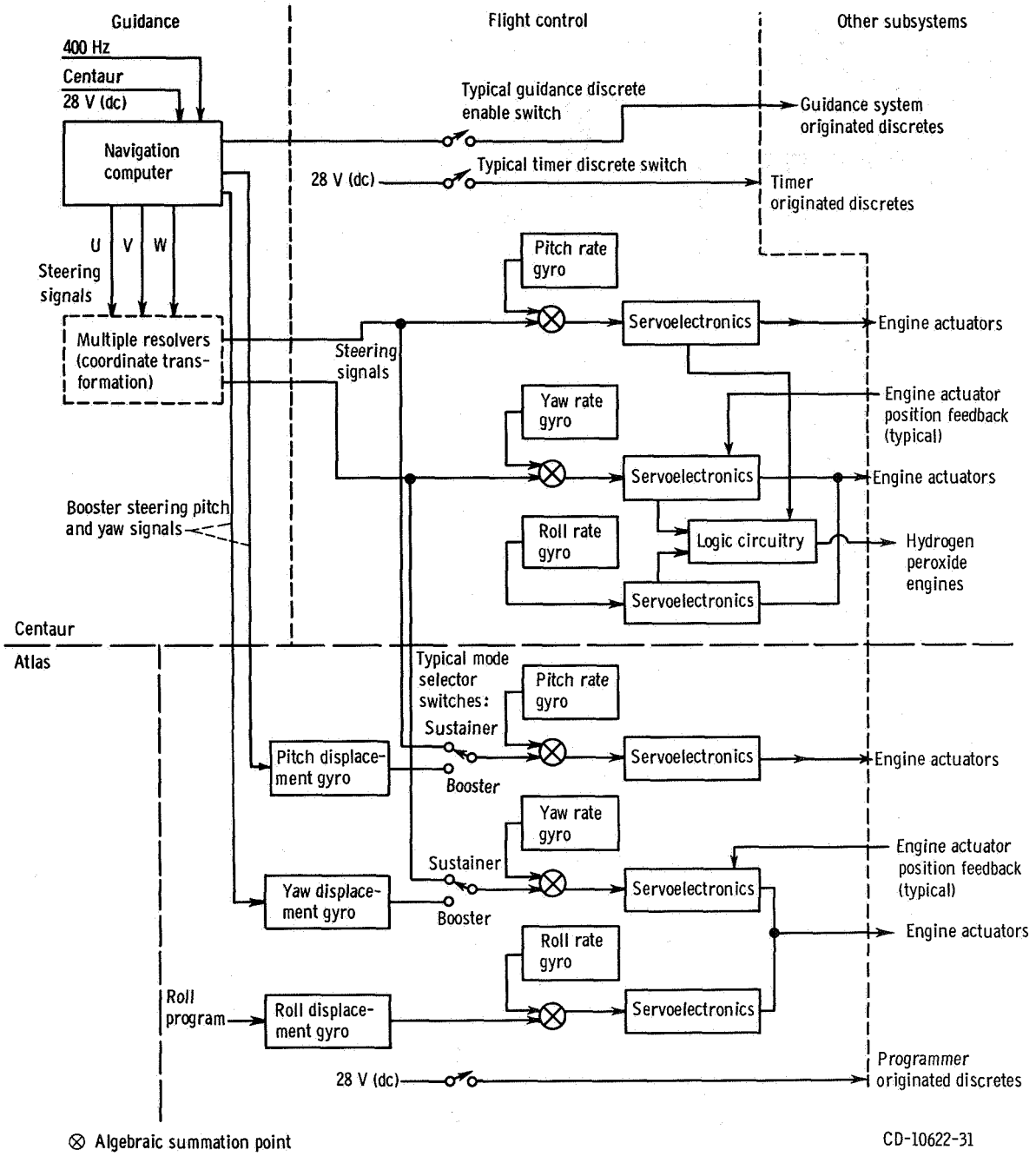

Figure VI-64. - Simplified guidance and flight control systems interface, AC-17.

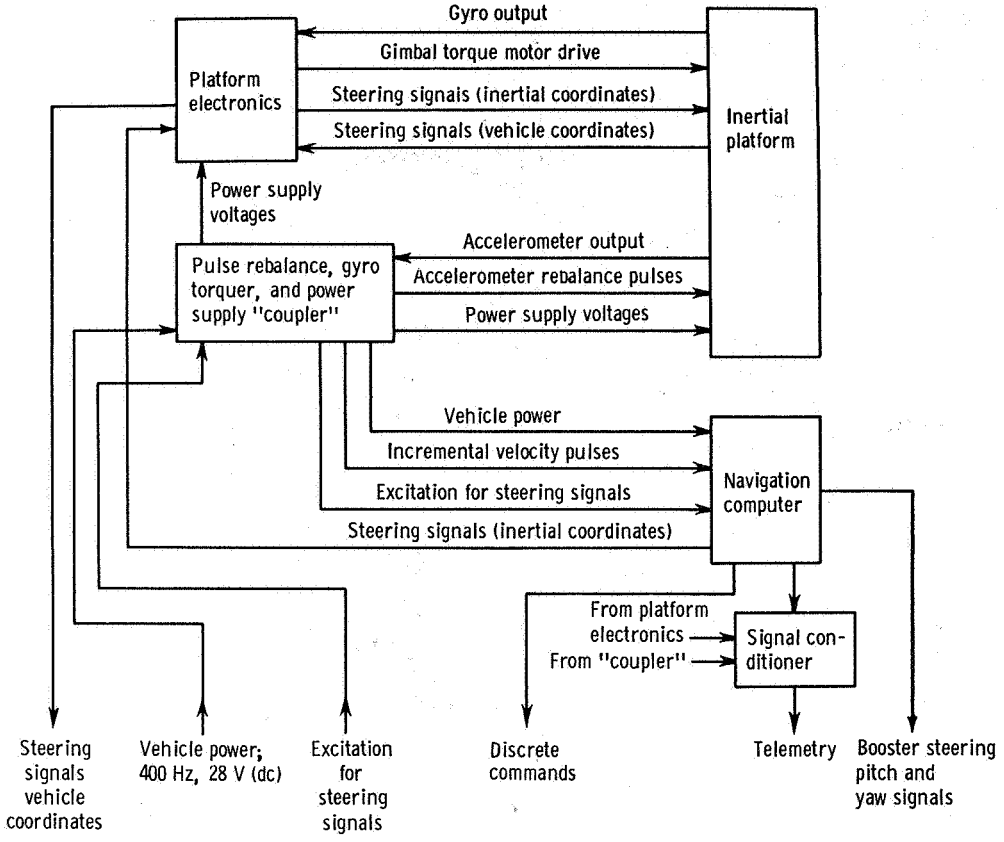

Figure VI-65. - Simplified block diagram of Centaur guidance system, AC-17.

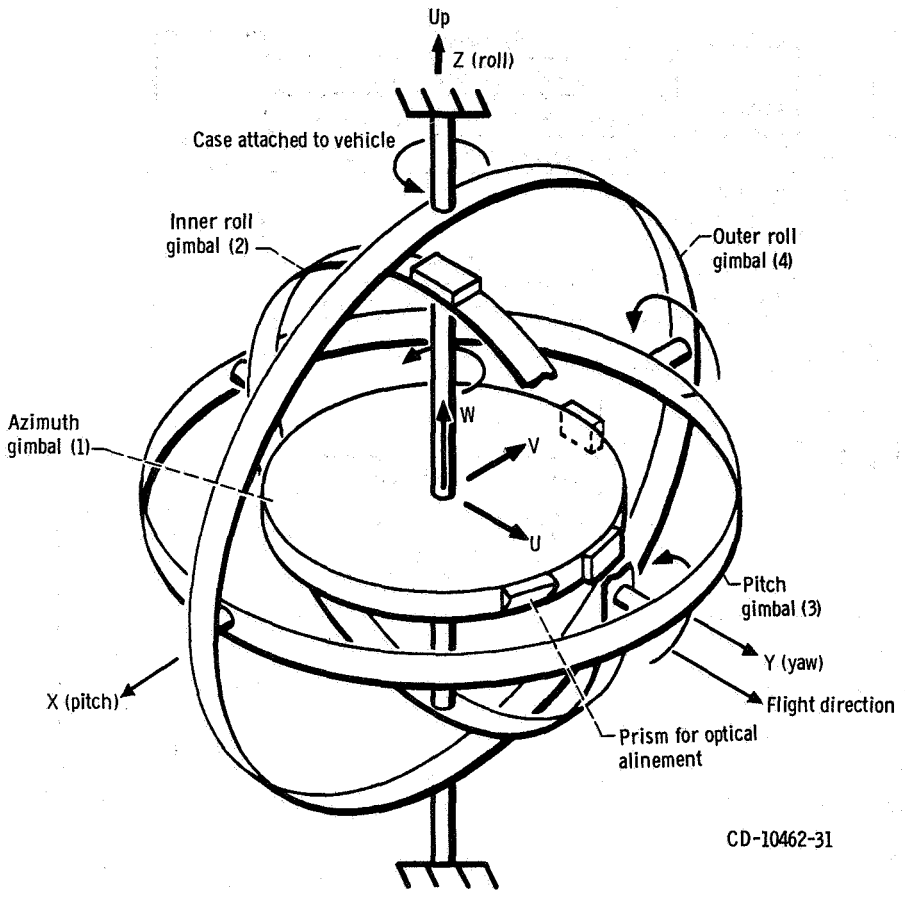

Figure VI-66. - Gimbal diagram, AC-17. Launch orientation: inertial platform coordinates, U, V, and W; vehicle coordinates, X, Y, and Z.

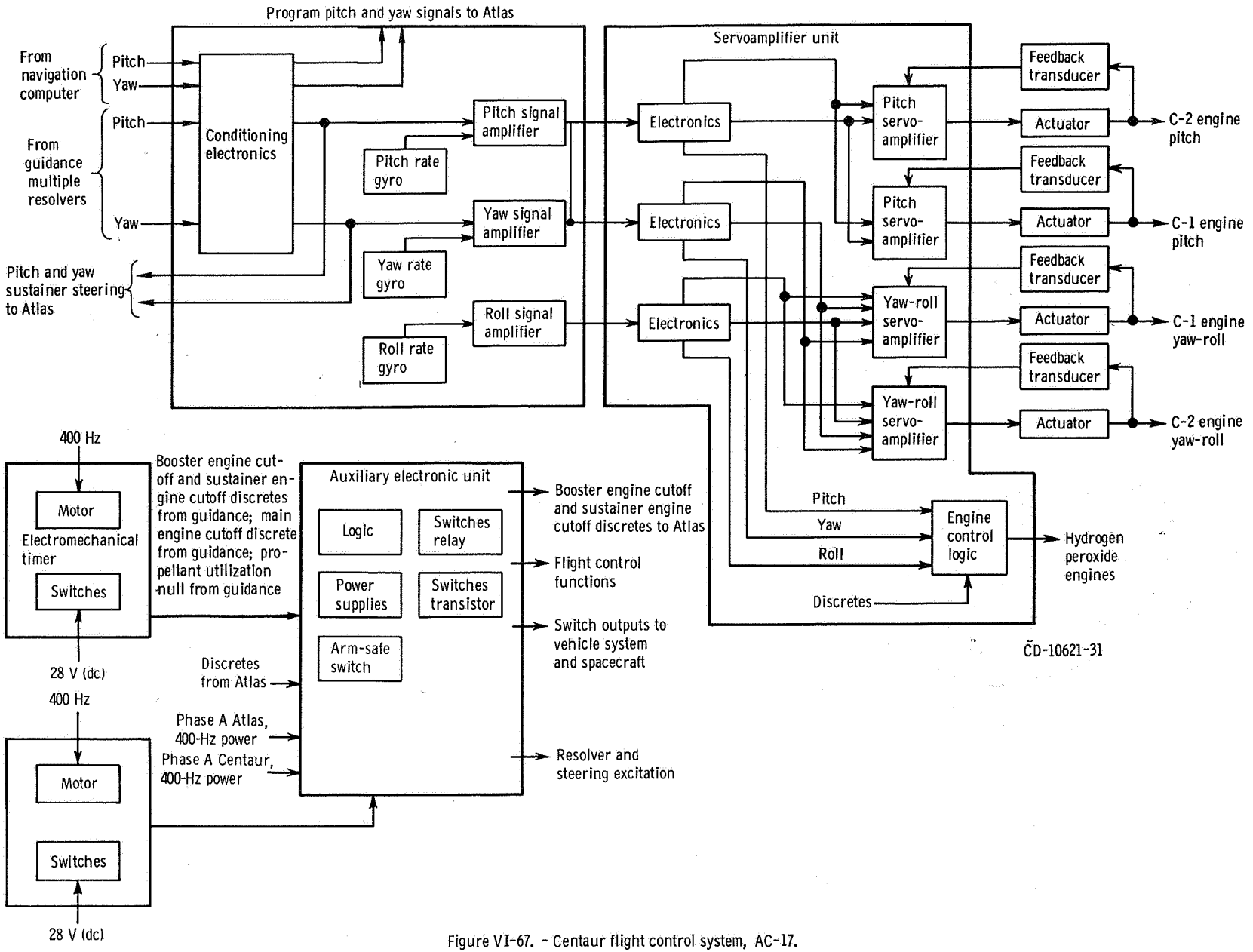

Figure VI-67. - Centaur flight control system, AC-17.

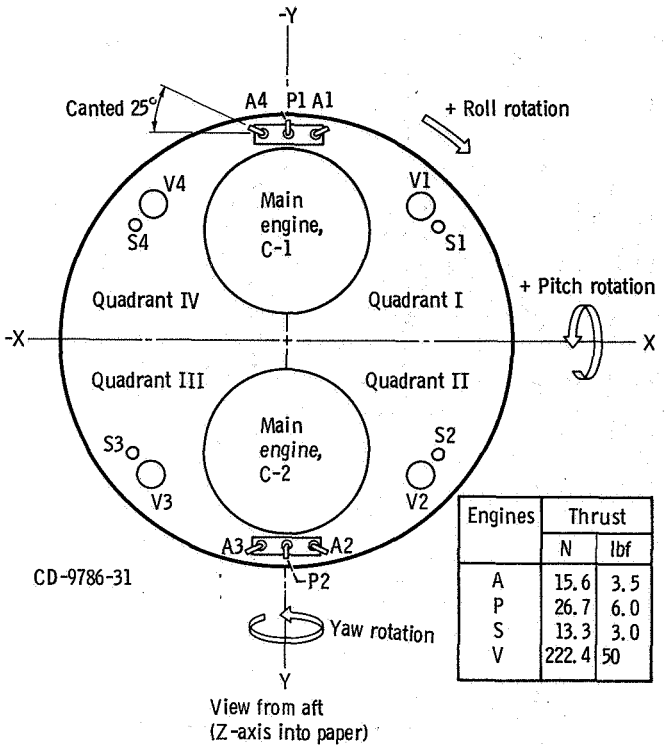

Engines	Thrust	
	N	lbf
A	15.6	3.5
P	26.7	6.0
S	13.3	3.0
V	222.4	50

Figure VI-68. - Attitude engines alphanumeric designations and locations, AC-17. *Signs of axes are convention for flight control system.*

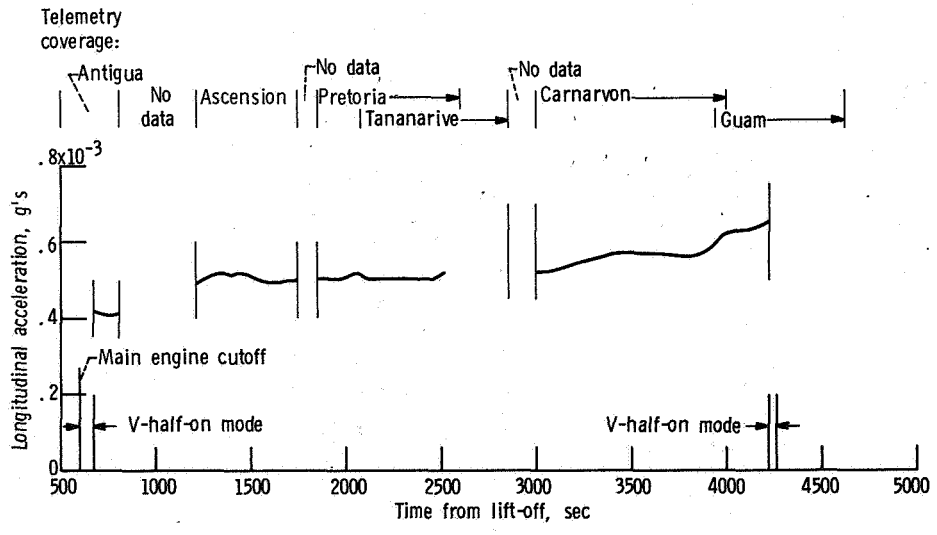

Figure VI-69. - Axial acceleration history during coast S-half-on mode, AC-17.

VII. CONCLUDING REMARKS

The Atlas-Centaur performed satisfactorily to place the Centaur/ATS-D into the desired parking orbit. After an orbital coast of 61 minutes, the Centaur main engine second start sequence was initiated. However, the main engines failed to restart and consequently the mission objective was not achieved.

Results of a comprehensive investigation and test program, conducted at General Dynamics' Convair Aerospace Division and at Lewis Research Center, attributed the failure to the freezing of hydrogen peroxide in a common supply line to the propellant boost pumps. It is concluded that the most probable cause of the freezing was a cryogenic (liquid oxygen) leaking onto the hydrogen peroxide supply line.

Lewis Research Center,
National Aeronautics and Space Administration,
Cleveland, Ohio, November 29, 1971,
491-02.

APPENDIX - OTHER FAILURE MODES INVESTIGATED TO DETERMINE CAUSE OF AC-17 FAILURE

by Donald B. Zelten

In addition to the probable cause of failure stated in the main text, several other failure modes were investigated:

(1) Empty boost pump bottle at boost pump second start: Hydrogen peroxide is supplied to the V engines from the attitude control bottle until the bottle is depleted. Then the V engines are supplied from the boost pump bottle through the manifold line (fig. VI-11). The cluster engines are always supplied from the boost pump bottle. At T + 4225.1 seconds, the V engines began firing in the V-half-on mode and continued until main engine second start at T + 4265.1 seconds. In this mode, the A engines also fire for roll control. Boost pump second start was commanded at T + 4237.1 seconds. From this time until main engine second start, the flight data show that the A engines were firing normally and, therefore, receiving hydrogen peroxide from the boost pump bottle. In addition, as mentioned previously, measurement CP756T verified depletion of the attitude control bottle and flow from the boost pump bottle approximately 8 seconds after boost pump start at T + 4245.1 seconds. This flow was required to supply the V engine, which the flight data showed to be operating normally up to main engine second start. Therefore, it was concluded that the boost pump bottle was not empty at boost pump start.

(2) Plugging of boost pump hydrogen peroxide lines with foreign contaminants: Extreme care is taken prior to launch in maintaining system cleanliness. The boost pumps also operated normally during the first-powered-phase period. Therefore, the contaminant would have to completely block the lines some time after main engine second cutoff. The probability of this happening is extremely low.

(3) Plugging of boost pump hydrogen peroxide lines due to freezing of residual peroxide downstream of boost pump feed valve: Boost pump start is initiated by opening the boost pump feed valve, which allows hydrogen peroxide to flow to the boost pump catalyst beds where it is decomposed and the hot decomposition gas drives the boost pump turbine (fig. VI-11). Prior to AC-17 flight it was believed that after the boost pump first start the residual peroxide in the lines downstream of the boost pump feed valve would be rapidly evacuated since the turbine exhaust is exposed to the vacuum of space. However, flight data as well as post-flight testing showed that some of the liquid remains in the lines for a considerable time after boost pump first cutoff. It was hypothesized that some of this residual peroxide could freeze due to evaporative cooling and thereby plug the lines. Thermal analysis and post-flight testing confirmed that the unheated fittings could reach temperatures below the highest freezing temperature of hydrogen peroxide, which is 262 K (12° F). However, it was also verified by testing that hydrogen peroxide

will generally supercool and will not freeze until its temperature drops below about 233 K (-40° F). It was impossible to freeze the lines during complete flight configuration system tests conducted in a space environment and simulating the AC-17 flight sequence. Partial plugging was observed in some "worst case" tests in which all the line heaters were deactivated, but even under these severe conditions complete plugging in both boost pump supply lines as indicated on AC-17 could not be duplicated.

(4) Line heater failure and resulting frozen hydrogen peroxide line: If several line heaters failed during the flight, it most probably could have been detected by a noticeable change in the telemetered battery current. The sensitivity of the current measurement was such that one or possibly two heaters could have failed without being detected. In order to obstruct flow to both boost pumps, failure would have to occur in one or both of the common lines, P/N 55-24160-10 and -14 (fig. VI-11). Thermal analysis and testing showed that if both common line heaters failed, sufficient frozen hydrogen peroxide would not form to completely block the lines.

(5) Hydrogen peroxide common line frozen due to thermal contact with liquid-oxygen-tank radiation shield: In the normal installation the lines are offset from the liquid-oxygen-tank radiation shield. Thermal shorting of the tube to the radiation shield was considered as a potential failure mode. Tests simulating this condition were performed but it was not possible to freeze the hydrogen peroxide and block the flow.

(6) Small leak in the boost pump feed valve resulting in a frozen plug of hydrogen peroxide: The downstream side of the valve is exposed to a near vacuum and it was hypothesized that a small leak across the valve seat could conceivably freeze due to evaporative cooling and block flow through the valve. This failure mode was tested by using a valve with a built-in leak, but freezing did not take place.

(7) Failure of boost pump feed valve to open at boost pump second start: Boost pump start is normally initiated by energizing the normally closed boost pump feed valve. This allows the hydrogen peroxide to flow to the catalyst beds, where it is decomposed; the decomposition products are used to drive the boost pump turbines. Failure of the valve to open would readily explain the flight failure. The valve is solenoid operated. The current trace to a solenoid operated valve has a very distinct signature at the time of poppet movement, when the solenoid is being energized (see fig. A-1). This signature consists of a dip in the current trace and is caused by the effects of back electromotive force (EMF). If the poppet is restrained or fails to move for any reason, this typical signature will not appear. The AC-17 battery current trace clearly shows the signature and therefore verifies that the valve did open.

(8) Failure of both boost pump catalyst beds at boost pump second start: It is possible for a catalyst bed to fail to decompose hydrogen peroxide if the bed is contaminated or if the bed and the hydrogen peroxide are excessively cold. System cleanliness is strictly maintained; and since the catalysts operated normally during the boost pump first run, it is extremely unlikely that both of them could become contaminated during the

coast period of flight when the system was inactive. Thermal analysis plus flight data verified that the catalyst beds and the hydrogen peroxide supply were not abnormally cold. In addition, line measurements CP344T and CP345T did not show any indication of flow in the lines at boost pump start. Therefore, it is concluded that the catalyst beds were not a cause of the failure.

(9) External hydrogen peroxide leak from one or more of the common line fittings: A small leak from a common line (P/N 55-24160-10 and -14) fitting would form a thin film over the external surface of the tube in the milligravity condition that existed during the coast period. In the vacuum environment of space this thin film would freeze due to evaporative cooling and could produce conditions that would freeze the residual or stagnant hydrogen peroxide inside the tubes. Theoretical analysis showed that this failure mode is possible. In post-flight testing of a leaking system the hydrogen peroxide did not freeze sufficiently to block flow when an absolute pressure of 210 N/cm^2 (305 psi) was applied. This failure mode is considered improbable because a hydrogen peroxide leak rate large enough to produce the disturbing torque detected on the vehicle during the coast phase would have resulted in hydrogen peroxide depletion. (Refer to the section Hydrogen Peroxide Engine and Supply System for details on the disturbing torque.)

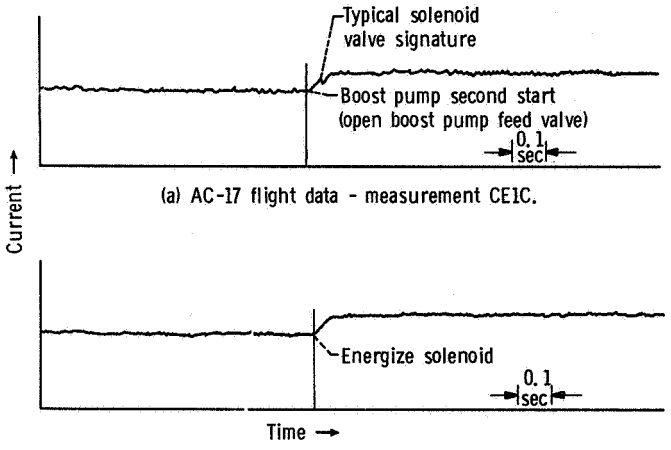

(a) AC-17 flight data - measurement CE1C.

(b) Typical data with poppet held in place.

Figure A-1. - Battery current as function of time, AC-17.

REFERENCE

1. Gerus, Theodore F.; Housley, John A.; and Kusic, George: Atlas-Centaur-Surveyor Longitudinal Dynamics Tests. NASA TM X-1459, 1967.

*U.S. GOVERNMENT PRINTING OFFICE: 1972 735-028/1056 1-3

NATIONAL AERONAUTICS AND SPACE ADMISTRATION
WASHINGTON, D.C. 20546

OFFICIAL BUSINESS
PENALTY FOR PRIVATE USE $300

FIRST CLASS MAIL

POSTAGE AND FEES PAID
NATIONAL AERONAUTICS AND
SPACE ADMINISTRATION

U.S.MAIL

POSTMASTER: If Undeliverable (Section 158 Postal Manual) Do Not Return

"The aeronautical and space activities of the United States shall be conducted so as to contribute . . . to the expansion of human knowledge of phenomena in the atmosphere and space. The Administration shall provide for the widest practicable and appropriate dissemination of information concerning its activities and the results thereof."

—NATIONAL AERONAUTICS AND SPACE ACT OF 1958

NASA SCIENTIFIC AND TECHNICAL PUBLICATIONS

TECHNICAL REPORTS: Scientific and technical information considered important, complete, and a lasting contribution to existing knowledge.

TECHNICAL NOTES: Information less broad in scope but nevertheless of importance as a contribution to existing knowledge.

TECHNICAL MEMORANDUMS: Information receiving limited distribution because of preliminary data, security classification, or other reasons.

CONTRACTOR REPORTS: Scientific and technical information generated under a NASA contract or grant and considered an important contribution to existing knowledge.

TECHNICAL TRANSLATIONS: Information published in a foreign language considered to merit NASA distribution in English.

SPECIAL PUBLICATIONS: Information derived from or of value to NASA activities. Publications include conference proceedings, monographs, data compilations, handbooks, sourcebooks, and special bibliographies.

TECHNOLOGY UTILIZATION PUBLICATIONS: Information on technology used by NASA that may be of particular interest in commercial and other non-aerospace applications. Publications include Tech Briefs, Technology Utilization Reports and Technology Surveys.

Details on the availability of these publications may be obtained from:

SCIENTIFIC AND TECHNICAL INFORMATION OFFICE

NATIONAL AERONAUTICS AND SPACE ADMINISTRATION

Washington, D.C. 20546